University of Alberta

DESIGN AND CHARACTERIZATION OF CAPACITIVE MICROMACHINED ULTRASONIC TRANSDUCERS USING FINITE ELEMENT MODELING

by

Bradley John Kirchmayer

A thesis submitted to the Faculty of Graduate Studies and Research in partial fulfillment of the requirements for the degree of Master in Science.

Department of Mechanical Engineering

Edmonton, Alberta

Spring 2006

Library and Archives Canada

Published Heritage Branch

395 Wellington Street
Ottawa ON K1A 0N4
Canada

Bibliothèque et Archives Canada

Direction du Patrimoine de l'édition

395, rue Wellington
Ottawa ON K1A 0N4
Canada

Your file Votre référence
ISBN: 0-494-13835-1
Our file Notre référence
ISBN: 0-494-13835-1

NOTICE:
The author has granted a non-exclusive license allowing Library and Archives Canada to reproduce, publish, archive, preserve, conserve, communicate to the public by telecommunication or on the Internet, loan, distribute and sell theses worldwide, for commercial or non-commercial purposes, in microform, paper, electronic and/or any other formats.

The author retains copyright ownership and moral rights in this thesis. Neither the thesis nor substantial extracts from it may be printed or otherwise reproduced without the author's permission.

AVIS:
L'auteur a accordé une licence non exclusive permettant à la Bibliothèque et Archives Canada de reproduire, publier, archiver, sauvegarder, conserver, transmettre au public par télécommunication ou par l'Internet, prêter, distribuer et vendre des thèses partout dans le monde, à des fins commerciales ou autres, sur support microforme, papier, électronique et/ou autres formats.

L'auteur conserve la propriété du droit d'auteur et des droits moraux qui protège cette thèse. Ni la thèse ni des extraits substantiels de celle-ci ne doivent être imprimés ou autrement reproduits sans son autorisation.

In compliance with the Canadian Privacy Act some supporting forms may have been removed from this thesis.

While these forms may be included in the document page count, their removal does not represent any loss of content from the thesis.

Conformément à la loi canadienne sur la protection de la vie privée, quelques formulaires secondaires ont été enlevés de cette thèse.

Bien que ces formulaires aient inclus dans la pagination, il n'y aura aucun contenu manquant.

Canada

DEDICATION

This thesis is dedicated to my loving parents, Bernard and Wendy Kirchmayer. I am forever indebted to you for all of your wonderful support and encouragement.

ABSTRACT

Capacitive Micromachined Ultrasonic Transducers (CMUTs) have been investigated using finite element models. A 2D axisymmetric model and a reduced order model illustrate the relationship between collapse voltage and electrode radius. A 3D solid model and a reduced order model calculate the resonant frequency of prestressed CMUT membranes.

The reduced order model is determined optimal due to its ability to calculate collapse voltage and resonant frequency with minimal computing time. A parametric study utilizing the optimum model illustrates that membrane radius and thickness are the most significant CMUT design parameters. Other significant parameters include the air permittivity, residual stress and membrane's modulus of elasticity, Poisson's ratio, and density.

The parameters are used to design CMUTs for a specific collapse voltage or resonant frequency. Using a design process, CMUTs can be designed within 10% of the specified values for resonant frequencies between 0.7-47.9 MHz and collapse voltages up to 3000V.

ACKNOWLEDGEMENTS

I want to thank my advisors, Dr. Walied Moussa and Dr. David Checkel for their guidance and motivation. I would also like to thank my readers, Dr. Roger Toogood and Dr. Jim McMullin for their insightful comments and constructive criticisms.

I wish to thank ATCO Gas for allowing me to pursue this opportunity while providing a flexible working environment. Special thanks are reserved for my supervisor, Jim Nygren and manager, Greg Schmidt who saw the value of continuing my formal education.

And last but not least I would like to thank my girlfriend, Tara Duffy for all the understanding and patience she has shown throughout the preparation of this thesis.

TABLE OF CONTENTS

1	**Introduction to Capacitive Micromachined Ultrasonic Transducers**	**1**
	1.1 Introduction	1
2	**Previously Reported CMUT Modeling**	**6**
	2.1 Introduction	6
	2.2 CMUT Fabrication	7
	2.3 Early Analytical Models	9
	2.3.1 Calculating Static Deflection	9
	2.3.2 Calculating Dynamic Response	11
	2.4 Conclusions	13
3	**Finite Element Modeling of a CMUT**	**14**
	3.1 Introduction	14
	3.2 CMUT Operating Parameters	14
	3.3 Previous Finite Element Modeling	15
	3.4 CMUT Finite Element Models	18
	3.4.1 2D Axisymmetric Model	18
	3.4.2 3D Solid Model	21
	3.4.3 Reduced Order Model	25
	3.5 Results	27
	3.5.1 2D Modeling Results	27
	3.5.2 3D Solid Modeling Results	28
	3.5.3 Reduced Order Modeling Results	30
	3.6 Conclusions	31
4	**Refined FEA Modeling and Parametric Study of a CMUT**	**33**
	4.1 Introduction	33
	4.2 Refined FEA Models	33
	4.2.1 Collapse Voltage Modeling	34
	4.2.2 Resonant Frequency Modeling	36
	4.3 Parametric Study Results	38

4.3.1 Collapse Voltage..... 40
4.3.2 Resonant Frequency..... 45
4.4 Conclusions..... 50
5 Designing CMUTs for Specific Applications **52**
5.1 Introduction..... 52
5.2 Impedance Modeling..... 52
5.3 CMUT Variable Design Parameters..... 57
5.3.1 RF and CV Relationships for Membrane Radius..... 57
5.3.2 RF and CV Relationships for Membrane Thickness..... 60
5.4 CMUT Design Procedures..... 63
5.4.1 Parametric Multiplication Factors..... 63
5.4.2 RF and CV Design..... 65
5.4.3 CMUT Design Examples..... 68
5.5 Conclusions..... 72
6 Summary of Significant Results **74**
6.1 Introduction..... 74
6.2 Finite Element Modeling..... 74
6.2.1 2D Axisymmetric Model..... 75
6.2.2 3D Solid Model..... 76
6.2.3 Reduced Order Model..... 76
6.3 Parametric Study..... 78
6.3.1 Insignificant Parameters..... 78
6.3.2 Significant Parameters..... 79
6.3.3 Designer Input Parameters..... 80
6.4 Modeling Process..... 80
6.4.1 Modeling with Membrane Radius, Thickness and Multiplication Factors..... 81
6.4.2 Step-By-Step Modeling for Collapse Voltage and Resonant Frequency..... 82
6.4.3 Mechanical Impedance Modeling with FEA..... 83
6.5 Proposed Future Work..... 84

A Mathematical Modeling of CMUTs **86**

A.1 Mason's Derivation of the Dynamic Response of a CMUT..... 86

A.2 Electrostatic Force Derivation..... 92

B Finite Element Modeling Code **95**

B.1 2D Axisymmetric Model Code..... 95

B.2 3D Solid Model Code..... 97

B.3 Reduced Order Model Code..... 101

C Calculating Average Membrane Displacement **110**

D CMUT Design Examples **114**

D.1 Design Example #1..... 114

D.2 Design Example #2..... 116

D.3 Design Example #3..... 118

References **120**

LIST OF TABLES

3.1 Material Properties of CMUT Models..... 18

3.2 Geometric Parameters for 2D Model..... 19

3.3 3D Model Geometry..... 21

4.1 CMUT Parametric Study Variables..... 39

4.2 Parameters Producing Small Changes in Collapse Voltage..... 41

4.3 Parameters Producing Small Changes in Resonant Frequency..... 46

5.1 Control CMUT Model Input Variables..... 58

5.2 Summary of Equations 5.14 and 5.15 Accuracy Ranges..... 62

C.1 Average Membrane Displacement Calculated Using Master Nodes and Radial Areas..... 111

C.2 Radial Percentage Averaging..... 113

LIST OF FIGURES

1.1 CMUT Array, Element, and Cross-Section..... 2
1.2 Transmitter Element Ultrasound Generation..... 3
1.3 Receiver Element Ultrasound Detection..... 3

2.1 CMUT Fabrication Steps..... 7
2.2 Spring-Mass-Capacitor System..... 9

3.1 Cross-Sectional View of 2D CMUT Model..... 19
3.2 Half Expansion of a Displaced CMUT Membrane..... 21
3.3 Side View of a Three Quarter Expansion..... 21
3.4 Quarter Section Volume Division..... 22
3.5 Mapped Mesh of 3D Solid Model..... 22
3.6 Residual Stress Induced in Membrane Using Thermal Properties..... 24
3.7 2D Axisymmetric Model – Collapse Voltage for Varying R_E..... 27
3.8 3D Solid Model – Resonant Frequency Shift with 2% Change in R_M.. 29
3.9 Reduced Order Model – Resonant Frequency Shift with 2% Change in R_M..... 30

4.1 Change in Collapse Voltage due to Varying Electrode Radius..... 35
4.2 Comparison of 3D Solid Model with Analytical Model..... 37
4.3 Comparison of Reduced Order Model with Analytical Model..... 37
4.4 Change in CV Due to 10% Variation in Membrane Radius..... 42
4.5 Change in CV Due to 10% Variation in Membrane Thickness..... 42
4.6 Change in CV Due to 10% Variation in Membrane Elasticity..... 43
4.7 Change in CV Due to 10% Variation in Air Permittivity..... 43
4.8 Change in CV Due to Variation in Residual Stress..... 44
4.9 Change in RF Due to 10% Variation in Membrane Radius..... 47
4.10 Change in RF Due to 10% Variation in Membrane Thickness..... 47

4.11 Change in RF Due to 10% Variation in Membrane Elasticity..... 48
4.12 Change in RF Due to 10% Variation in Air Density..... 48
4.13 Change in RF Due to Variation in Residual Stress..... 49

5.1 Absolute Mechanical Impedance for Analytical and FEA Models..... 56
5.2 RF and CV as a Function of Membrane Radius..... 58
5.3 RF and CV as a Function of Modified Aspect Ratio..... 59
5.4 RF vs AR_{Mod} for Various Membrane Thicknesses..... 60
5.5 CV vs AR_{Mod} for Various Membrane Thicknesses..... 61
5.6 CMUT Design Process Flow Chart..... 67
5.7 Geometric Configuration of a 49 CMUT Element Sensor Array..... 70

A.1 Parallel Plate Capacitor Design of a CMUT..... 92
A.2 Circuit Approximation of a Parallel Plate CMUT..... 92

C.1 Calculating Average Displacement Radial Distances..... 112

NOMENCLATURE

Symbol	Name
α_M	Membrane Coefficient of Expansion
AR_{Mod}	Modified Aspect Ratio
CV	Collapse Voltage
d_o	Capacitor Plate Separation
δ_T	Change in Geometric Dimensions
E	Young's Modulus of Elasticity (denoted by subscript)
ε_o	Electric Permittivity Constant
F	Force (type denoted with subscripts)
FM	Full Metallization of Top Electrode
HM	Half Metallization of Top Electrode
j	Imaginary Constant
κ	Dielectric Constant (component denoted by subscript)
m	Mass
P	Pressure (type denoted by subscript)
R, r	Radius (component denoted by subscript)
RF	Resonant Frequency
ρ	Density (component denoted by subscript)
S	Membrane Area
σ	Residual Stress (type denoted by subscript)
T	Temperature

t.....Thickness (component denoted by subscript)

υ.....Poisson's Ratio (component denoted by subscript)

V.....Voltage (type denoted by subscript)

v.....Velocity (type denoted by subscript)

ω.....Frequency in Radians

x.....Membrane Displacement

Z_M.....Mechanical Impedance of the CMUT Membrane

Subscript	**Description**
A	Air Gap
AC	Alternating Current
avg	Average
Cap	Capacitor
DC	Direct Current
E	Top Electrode
I	Insulator
M	Membrane

CHAPTER 1

INTRODUCTION TO CAPACITIVE MICROMACHINED ULTRASONIC TRANSDUCERS

1.1 Introduction

Ultrasonic sensing has developed into a highly effective process for Non-Destructive Evaluation (NDE), medical imaging, and gas sensing. Currently the most prevalent choices for ultrasonic transducers are piezoelectric crystals and composites. Although piezoelectric transducers have been utilized in all of the above mentioned applications, problems associated with their material properties have limited their capabilities. In certain applications these limitations have resulted in impedance mismatch, high-temperature instability, and various manufacturing difficulties.

A relatively new and promising alternative to piezoelectric transducers, are Capacitive Micromachined Ultrasonic Transducers (CMUTs). CMUTs consist of numerous elements arranged in an array that either transmit or receive ultrasonic waves. Each CMUT element consists of a metal electrode embedded on top of a very thin silicon nitride membrane. The membrane is supported by silicon substrate walls, which suspend the membrane above the bottom electrode (silicon bulk). Figure 1.1 depicts a typical CMUT array, element, and element cross-section. When an electric potential is placed across the two membranes, Coulomb forces are induced that cause the membrane to deflect.

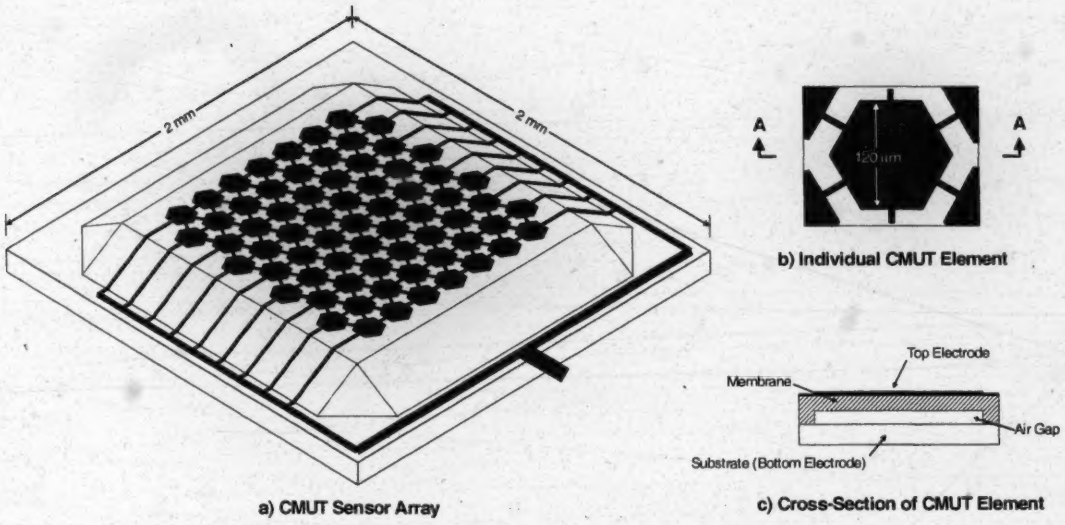

Figure 1.1: CMUT Array, Element, and Cross-Section

For transmitter CMUTs a DC bias voltage and driving AC voltage are utilized to vibrate the membrane at the AC voltage frequency. The membrane vibration produces ultrasonic waves that are emitted into the medium. Conversely, receiver CMUTs consist of DC biased membranes that are deflected when the ultrasound waves interact with them. The deflection of the membrane produces a change in voltage between the CMUT electrodes. This electric potential will oscillate with the same frequency as the transmitted ultrasonic waves and can be easily detected using a voltmeter. Figures 1.2 and 1.3 illustrate transmitter and receiver CMUT elements.

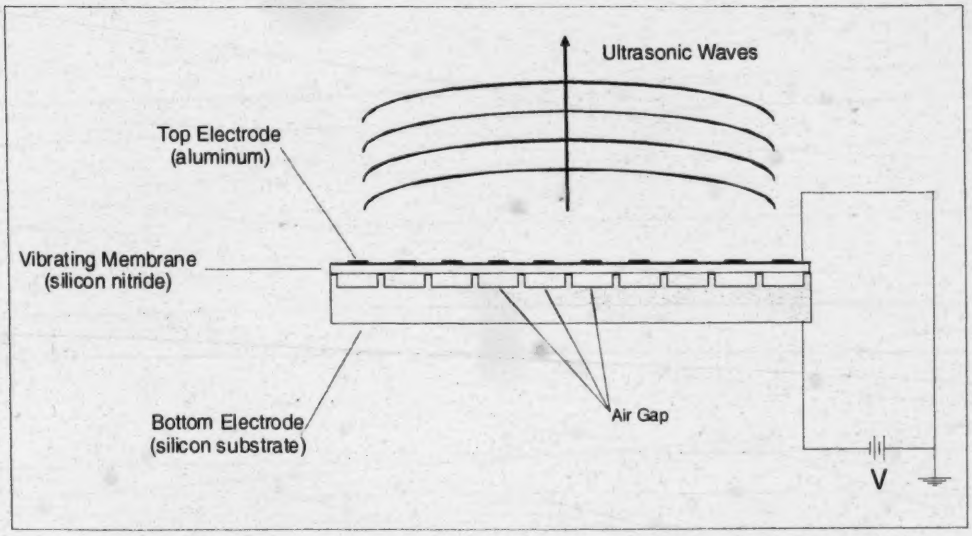

Figure 1.2 Transmitter Element Ultrasound Generation

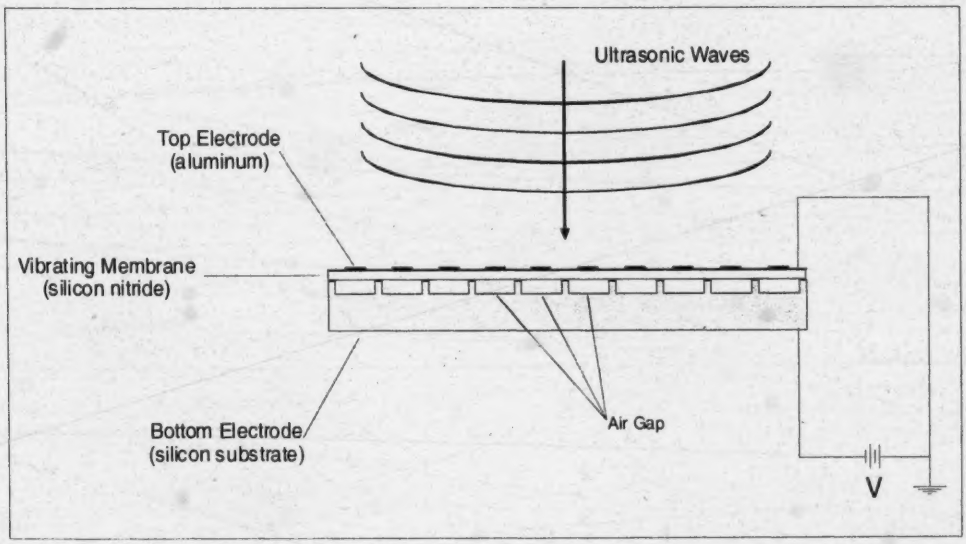

Figure 1.3 Receiver Element Ultrasound Detection

The popularity of CMUTs can be attributed to previously reported work that has produced devices capable of overcoming many of the problems associated with

piezoelectric devices. Impedance problems were solved by the CMUT's small membrane mass, which enables ultrasound generation in air and gases, without the use of matching layers. CMUTs also allow for higher operating temperatures than the piezoelectric transducers. At increased operating temperatures piezoelectric ceramics tend to depole which reduces the piezoelectric effect and forces created. The more common ceramics will depole at relatively low temperatures (<100°C) severely hindering the transducer's ability to generate ultrasonic waves. The electrostatic force that drives CMUTs is not temperature dependent and the CMUT materials can withstand reasonably higher temperatures. Finally, CMUT fabrication technology is derived from the microchip industry, so they are fairly easy and inexpensive to replicate.

Although microfabrication advances and the economies of scale allow for the inexpensive production of large batches of similar CMUT arrays, the cost of prototyping a single array for specific applications can still be quite high. To reduce research and prototyping costs in the design of CMUTs, many researchers have developed models capable of accurately depicting CMUT behavior. In Chapter 2, the previously reported models and fabrication techniques are discussed. The early mathematical models are presented and their limitations listed. Problems associated with the analytical models have led many researchers to develop finite element analysis (FEA) models.

Chapter 3 expands upon finite element modeling as a useful tool in CMUT design. Three FEA models are developed to illustrate two important CMUT operating parameters: the collapse voltage and resonant frequency. Accuracy of the finite element models is verified by comparing the results with previously reported results. Advantages and disadvantages of each model are also discussed.

In Chapter 4 the finite element models from Chapter 3 are refined and revisited. The models are compared against one another to determine an optimum model for future CMUT design. Criteria for the optimum model include accuracy, computing time, ease of use, and solution capabilities. A parametric study is performed using the optimized model to illustrate the importance of each CMUT parameter. The characterization as either a significant or insignificant parameter is dependent upon their influence of the collapse voltage and resonant frequency.

In Chapter 5 the most significant parameters are employed in a process that allows a CMUT to be designed for a specific operating parameter. Significant parameters that are completely variable are deemed user defined variables and formulas are presented to design with these parameters. Other significant parameters that are not fully variable are accounted for using correcting multiplication factors. The design process is outlined in a step-by-step flow chart and three design examples are presented to illustrate the process and its accuracy.

Chapter 6 is a summary of the significant results presented in this dissertation. The importance of the individual modeling steps is outlined and the accuracy and advantages of finite element modeling is reiterated. Also discussed in Chapter 6 are proposals for future research in finite element impedance modeling and microfabrication of a working CMUT array.

CHAPTER 2

PREVIOUSLY REPORTED CMUT MODELING

2.1 Introduction

The same research that has led to improvements in CMUT design has also illustrated the importance of accurate modeling. Initial costs to build prototype CMUTs can be high, therefore by producing accurate models, numerous CMUT configurations can be studied for a comparably cheaper cost. Much of the previous research has involved building models that can accurately represent a single manufactured design. These models were then utilized to investigate different CMUT designs.

In previous research, to verify the model accuracy specific CMUT configurations needed to be fabricated and tested. Many different techniques have been used to create CMUTs and much of the ongoing research is based upon advancing the microfabrication technology. Fabrication techniques have been presented in [2], [6] and [7].

Most of the analytical models are derived from the governing mathematical theory that has been presented in [1], [2], and [3]. While these simplified analytical models showed good accuracy for certain CMUT designs, they could not account for complex geometric conditions, such as a half metallization top electrode. To overcome these limitations, more complex finite element models were created. These models have been presented and verified using theoretical and experimental results in [3], [4], and [8].

2.2 CMUT Fabrication

There are numerous materials and fabrication techniques that can be utilized to manufacture CMUTs. Much of the fabrication technology has been extracted from the semiconductor industry. This paper assumed that CMUTs would be fabricated with the commonly found technique illustrated in Figure 2.1 and referenced by Ladabaum et al. [2].

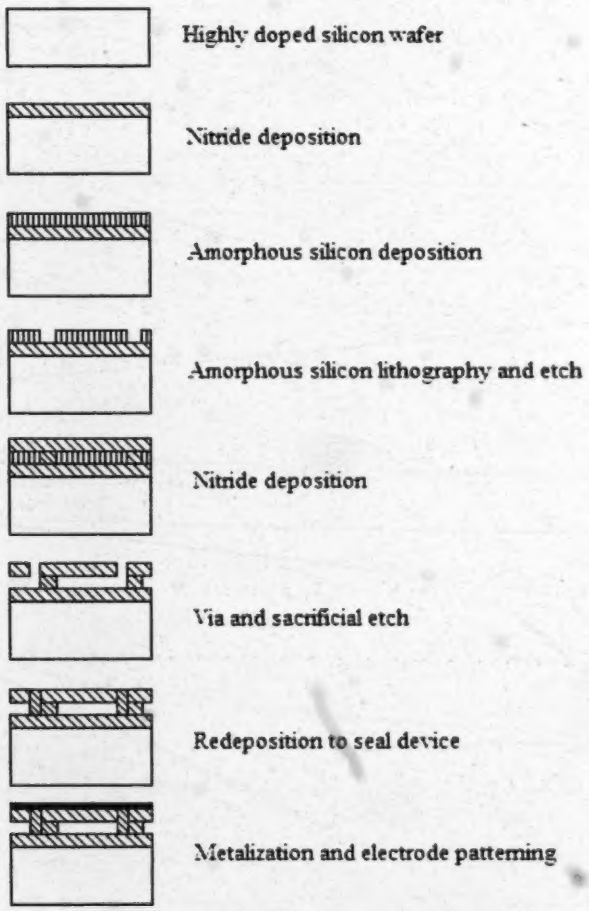

Figure 2.1: CMUT Fabrication Steps

This process begins with a highly doped silicon wafer that will serve as the bottom electrode. The silicon is typically doped with a 4-h phosphorous gas phase drive to achieve the required electrical conductivity. A thin insulating layer of silicon nitride is then deposited on the wafer using a low-pressure chemical-vapor deposition (LPCVD) process.

The sacrificial layer, comprised of amorphous silicon, is then deposited and dry-etched into hexagonally shaped islands. These islands will define the effective gap between the two electrodes, and thus form the geometric limits for membrane deflection.

Next another thin layer of silicon nitride is deposited via an LPCVD process. This layer will become the membrane for the CMUT, and thus, the mechanical impedence and electrostatic forces for the element are dependent upon the thickness and material properties of the silicon nitride. At this time a residual stress can be introduced to the membrane by controlling the silane and ammonia ratio during the LPCVD process.

Vias are then dry-etched into the silicon nitride membrane and the amorphous silicon islands are removed by way of sacrificial etching. The sacrificial etching utilizes potassium hydroxide and water (KOH) at 75 °C, which will dissolve the amorphous silicon but will leave the silicon nitride insulating layer and membrane intact. The vias are then sealed with either silicon nitride, or low-temperature oxide (LTO) depsosition.

Finally, the top electrode is produced by sputtering a metal on top of the membrane and dry-etching to produce a pattern. A variety of metals can be used as the top electrode, with aluminum and gold listed amongst the most common choices. The metal deposition, along with lithographically defined trenches, will define the bonding connections between the top and bottom electrodes.

2.3 Early Analytical and Finite Element Models

Much of the past work on CMUTs has involved the derivation of analytical models to define both emitting and receiving transducers. The mathematical theory presented was developed to define the static deflection due to the bias DC voltage and the dynamic response due to the driving AC voltage. The models were able to couple the electrostatic and structural domains of the transducers using equivalent circuit analysis. When the simplified analytical models could not account for the complex geometries being investigated, researchers turned to finite element analysis to create the more sophisticated models.

2.3.1 Calculating Static Deflection

An early mathematical model to describe the static deflection of a CMUT membrane due to the bias DC voltage is presented in [2]. This model utilized a first order analysis of a CMUT that was approximated as a spring-mass-capacitor system, as shown in Figure 2.2.

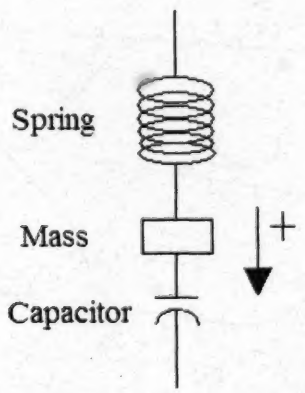

Figure 2.2: Spring – Mass – Capacitor System

With this assumption the mass represents the mass of the membrane and top electrode, the spring represents the stiffness of the membrane, and the capacitor represents the top (metal) and bottom (substrate) electrodes. The capacitor applies an electrostatic force that causes the membrane to deflect inward, while the stiffness of the membrane counteracts this effect, attempting to restore the membrane to its original location. From [2] the force of the capacitor and the force of the spring can be defined as follows:

$$F_{capacitor} = \frac{\varepsilon_o S V^2}{2(d_o - x)^2} \tag{2.1}$$

$$F_{spring} = -k_M x \tag{2.2}$$

Where ε_o is the electric permittivity, S is the area of the capacitor plates, x is the displacement of the mass, d_o is the separation of the capacitor plates and k_M is the membrane's spring constant.

By applying only a DC bias voltage and assuming the system has reached a steady-state, the governing equations can be written as:

$$F_{capacitor} + F_{spring} = F_{mass} \tag{2.3}$$

$$m\frac{d^2x(t)}{dt^2} - \frac{\varepsilon_o S[V(t)]^2}{2[d_o - x(t)]^2} + k_M x(t) = 0 \tag{2.4}$$

And reduced to:

$$\frac{\varepsilon_o S V_{DC}^2}{2(d_o - x)^2} = k_M x \tag{2.5}$$

From an inspection of equation 2.5 it can be argued that the membrane spring constant, k_M, and static deflection, x, assume a uniform membrane displacement which is not an accurate representation of the CMUT behavior. As the membrane center is pulled towards the bottom electrode the outer edges will remain in place resulting in a arching of the membrane. Using the mathematical theory presented above, it is difficult to account for the complex capacitive and restoring spring forces that are a result of the curvilinear shape of a deflected membrane.

Conversely, finite element analysis can easily account for the deflected membrane, thus many researchers have begun utilizing it to calculate the static deflections of CMUT elements. In [3] a thermal-structural model was used to approximate the electrostatic-structural domain of a CMUT. The model was used to calculate the static deflections for CMUTs with complex electrode patterning. In [4] a directly coupled electrostatic-structural model was used to calculate the static deflections caused by the bias DC voltage. The results published in these papers were utilized to verify the accuracy of the finite element models developed for this thesis.

2.3.2 Calculating the Dynamic Response

The dynamic response of a CMUT element has been mathematically modeled in both [2] and [5]. Both models approximate the hexagonal elements as circular to simplify the solution. The earlier model presented in [5] approximated the CMUT as a membrane with only tension subjected to a uniform pressure. The later model presented in [2] approximated the CMUT as a membrane with tension and stiffness. This model

will revert back to the membrane with tension if the membrane thickness or stiffness disappears.

The theory to define the CMUT element as a membrane with tension and stiffness is derived from Mason, [1]. The governing equation for this CMUT model is defined as:

$$\frac{(E_M + \sigma_M)t_M^3}{12(1-\upsilon_M^2)}\nabla^4 x(r) - \sigma_1 \nabla^2 x(r) - P_{Cap} - \omega^2 \rho_M t_M x(r) = 0 \qquad (2.6)$$

Where E_M is the membrane's modulus of elasticity, σ_M is the membrane tension, υ_M is the membrane's Poisson ratio, t_M is the membrane thickness, ρ_M is the membrane density, σ_1 is the surface tension ($\sigma_M * t_M$), P_{Cap} is the pressure of the capacitive forces, ω is the harmonic frequency, and $x(r)$ is the displacement as a function of membrane radius. Using equation 2.6, a definition for displacement for specific radial distances, r, can be derived (the full derivation can be found in Appendix A):

$$x(r) = \frac{P_{Cap}}{\omega^2 \rho_M t_M}\left[\frac{k_2 I_1(k_2 r_M)J_0(k_1 r) + k_1 J_1(k_1 r_M)I_0(k_2 r)}{k_2 I_1(k_2 r_M)J_0(k_1 r_M) + k_1 J_1(k_1 r_M)I_0(k_2 r_M)} - 1\right] \qquad (2.7)$$

Where J_n and I_n are Bessel and modified Bessel functions of the n^{th} order, respectively and k_1 and k_2 can be defined as:

$$k_1 = \sqrt{\frac{\sqrt{d^2 + 4c\omega^2} - d}{2c}} \qquad (2.8) \quad \text{and} \quad k_2 = \sqrt{\frac{\sqrt{d^2 + 4c\omega^2} + d}{2c}} \qquad (2.9)$$

With c and d defined as:

$$c = \frac{(E_M + \sigma_M)t_M^2}{12\rho_M(1-\upsilon_M^2)} \qquad (2.10) \quad \text{and} \quad d = \frac{\sigma_M}{\rho_M} \qquad (2.11)$$

The membrane displacement can be plotted against frequency to illustrate the resonant frequency. In [2] the displacement was utilized to calculate the mechanical impedance. The mechanical impedance was input into an equivalent circuit model

derived from Mason's principle of electromechanical converting systems. The results of the impedance models published in these papers were used to verify the harmonic responses of the CMUT models developed for this dissertation.

2.4 Conclusions

Previous research has demonstrated the value of modeling capacitive micromachined ultrasonic transducers. Both the analytical and finite element models have shown good accuracy and have been verified using fabricated CMUTs for specific configurations. Finite element analysis is quickly replacing the mathematical modeling due to its enhanced ability to model complex geometric configurations. FEA models shown in [3] and [4] have already surpassed the capabilities of the analytical models with respect to static response of a CMUT biased by a DC voltage.

Research for this thesis has expanded the role of finite element modeling to calculate the CMUT operating responses. Various finite element models capable of both static and dynamic analysis were created and are examined in the proceeding sections. The accuracy of these models will be verified by comparing their results with the results of the analytical and finite element models discussed in this section.

CHAPTER 3

FINITE ELEMENT MODELING OF A CMUT

The following chapter has been formatted in article form and published in the ANSYS Solutions Winter 2005 Magazine. The article is titled "Finite Element Modeling of Capacitive Micromachined Ultrasonic Transducers" and can be found on pages 16-19.

3.1 Introduction

Finite element analysis (FEA) is proving to be a virtually indispensable tool in all Micro Electro Mechanical Systems (MEMS) development including CMUT design. The following chapter shows the value of finite element modeling in determining two critical CMUT operating factors: the collapse voltage and the resonant frequency.

To investigate the operating parameters, three different finite element models were created. The models were chosen based on their ability to calculate either the collapse voltage or the resonant frequency. Results from the models are compared with previously published findings and the advantages and disadvantages of each model are outlined. When compared to the published FEA and analytical models, the 3 finite element models illustrate the appropriate responses and a high level of accuracy.

3.2 CMUT Operating Parameters

The performance of a CMUT can be directly related to the collapse voltage and the resonant frequency. Both factors rely upon the CMUT's geometric configuration and

material properties. Depending upon the sensing application either the collapse voltage or the resonant frequency will govern the CMUT's operation.

The electric potential between the two electrodes can be increased to the point where the electrostatic force overcomes the membrane's restoring spring force. When this happens the attraction between the electrodes will cause the membrane to collapse unto the bottom electrode. This electric potential is called the collapse voltage or pull-in voltage. It will govern the maximum applied voltage for a working CMUT.

As reported in [2], for a CMUT to emit ultrasound waves in air, the impedance caused by the CMUT's membrane must be properly matched to the impedance of the surrounding air. To produce the required membrane amplitudes for accurate impedance matching and receiver detection, the membrane must be operated at its resonant frequency. For water immersion transmitters this is not required because the impedance of the membrane's non-resonant motion is closely matched to that of the surrounding water.

3.3 Previous Finite Element Modeling

Most of the research previously done on CMUT's has involved the creation of simplified models to demonstrate the complex behavior of the silicon nitride membrane. Various methods, such as finite element analysis (FEA), and equivalent circuit modeling, have been used to portray the collapse voltage and operating frequency of CMUT's. These models have also been used to develop relationships between the membrane geometry and the operating parameters. The relationships allow the CMUT geometry to be optimized for a particular operating parameter.

In both [3] and [4], an FEA software package called ANSYS was used to create a finite element model capable of depicting CMUT collapse voltage. Both papers examined the relationship between collapse voltage and top electrode parameters for an unstressed silicon nitride membrane.

In [3] a two dimensional (2D) axisymmetric model was subjected to a thermal-structural analysis and the collapse voltage was calculated for varying electrode size. The FEA software version used for this model did not directly support electro-magnetic field solutions, so a thermal-structural analysis was used and an analogy was made to relate the solution to the electrostatic-structural domain. The ANSYS model illustrated that the electrode radius could be reduced to one half the size of the membrane radius without greatly altering the collapse voltage. Decreasing the electrode radius to less than half though, led to very large increase in the collapse voltage.

The finite element model created in [4] utilized a newer version of ANSYS with an electrostatic-structural analysis to examine the collapse voltage. This paper also employed a 2D axisymmetric model but utilized an electrostatic-structural solving program to couple the electrostatic force of the electrodes with the structural restoring force of the membrane. Also presented in this paper were results for a variety of electrode geometric parameters, including radius, thickness, material type, and position.

Unfortunately, different membrane geometries were used in [3] and [4], making it difficult to compare the two modeling techniques. Therefore, one of the goals for this chapter was to develop a 2D axisymmetric CMUT model using the electrostatic-structural technique presented in [4] for the membrane geometry introduced in [3]. The collapse voltage for varying electrode radius could then be calculated and compared with

results obtained from the thermal-structural analogy used in [3]. The model description and results are documented in the latter section of this chapter.

The effect of operating frequency has been widely examined by many researchers in the past. In [2], [6], and [7], impedance models were used to illustrate the response of a silicon nitride membrane over a particular frequency range. By graphing the mechanical impedance over a frequency range the resonant frequency can be obtained.

The impedance model developed by X. Jin et al. in [6] verified the strong relationship between membrane geometry and resonant frequency. It was shown that increasing or decreasing the membrane radius by 2% caused a 3.5% shift in resonant frequency. Changing the membrane thickness by 5% also caused a 3.5% shift in resonant frequency.

To the author's knowledge, there has been no work done to model the resonant frequency of a prestressed CMUT membrane using FEA software capable of electrostatic-structural analysis. Therefore, another goal of this paper was to model the resonant frequency of a prestressed membrane with similar geometric parameters to those found in [6]. Two different methods were used to model the membrane and the results were compared with those previously published. The first method involved three dimensional (3D) solid modeling coupled with an electrostatic-structural transducer element (TRANS126 in the ANSYS software), while the second method utilized a reduced order element (ROM144 in ANSYS) to create a reduced order model of a CMUT. The modeling and results are outlined in the following sections.

3.4 CMUT Finite Element Models

Three separate models were created using ANSYS v.7 to illustrate CMUT behavior. The first was a 2D axisymmetric model used to investigate the collapse voltage. The second was a 3D solid model coupled with a transducer element used to demonstrate the resonant frequency of a prestressed membrane. The third was a reduced order model that also depicted the resonant frequency of a prestressed membrane.

All three CMUT models utilized identical materials as taken from [4], and listed in Table 3.1. The ANSYS line code for the models can be found in Appendix B.

Table 3.1: Material Properties of CMUT Models

	Si_3N_4 (membrane)	Air (gap)	Si (bottom electrode)	Al (top electrode)
Young's Modulus, E (Pa)	3.20E+11	N/A	1.69E+11	6.76E+10
Density, ρ (kg/m^3)	3270	N/A	2332	2700
Poisson's Ratio, ν	0.263	N/A	N/A	0.3555
Dielectric Constant, κ	7.6	1.04	11.8	N/A

3.4.1 2D Axisymmetric Model

As first illustrated in [4] and repeated here, ANSYS was used to model an unstressed circular CMUT element. The circular geometry was chosen for two reasons. First, the circular shape is an accurate approximation for the manufactured hexagonally shaped elements, and second, this geometry allows for a 2D axisymmetric solution, reducing the required computing time. Figure 3.1 depicts the geometry of the axisymmetric model.

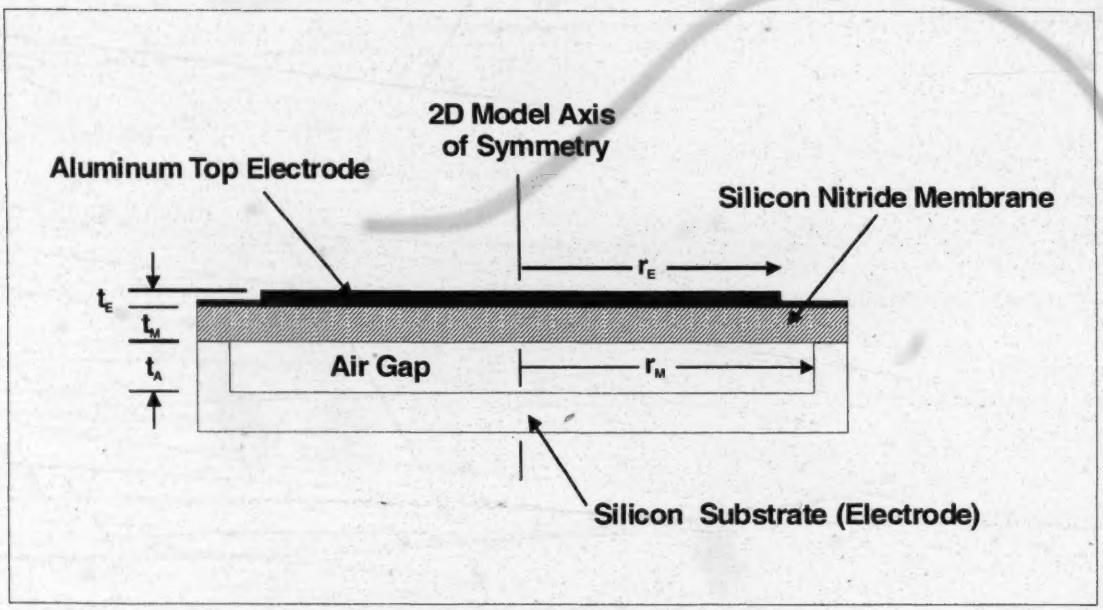

Figure 3.1: Cross-Sectional View of 2D CMUT Model

The model consisted of a silicon substrate base, a silicon nitride membrane, an air gap, and a metal electrode. Since the purpose of this analysis was to verify the relationship between the electrode radius, r_E, and the collapse voltage, all other geometric parameters were held constant. These included the membrane thickness, t_M, membrane radius, r_M, air gap thickness, t_A, and electrode thickness, t_E. The thin insulating layer found in most CMUTs was assumed to have negligible effects, thus it was left out of the model. Table 3.2 below lists the values for the geometric parameters.

Table 3.2: Geometric Parameters for 2D Model

Parameter	r_M	t_M	t_A	t_E	r_E
Dimension (μm)	25.0	0.6	1.0	0.1	Variable 2-25

The 2D model's membrane and top electrode were created using 8-noded structural plane elements with two degrees of freedom (DOF) at each node consisting of x and y displacements. The air gap was modeled using an 8-noded electrostatic plane element with one DOF at each node consisting of electric potential. Boundary conditions for the membrane included no horizontal displacement along the centerline of the model and the outer edge of the membrane, as well as no horizontal or vertical displacement of the silicon substrate.

To simulate the potential difference across the element, the substrate was grounded and the applied voltage was loaded on the metal electrode. Competing electrostatic and structural physics environments were used to simulate the static membrane deflection observed when the electrode was biased by the direct current (DC) voltage. A built-in electrostatic-structural solver (ESSOLV) transferred nodal coordinates between the two environments to obtain an iterative solution that converged to within 5% change in either structural displacement or electrical field strength. The collapse voltage was found when the solution could not converge, causing the membrane displacement to exceed the structural limitations of the model.

Figure 3.2 shows a half expansion of the 2D axisymmetric membrane. The membrane was biased with a voltage less than the collapse voltage, thus it was displaced but it did not collapse. Figure 3.3 shows the side view of the same membrane with a three quarter expansion.

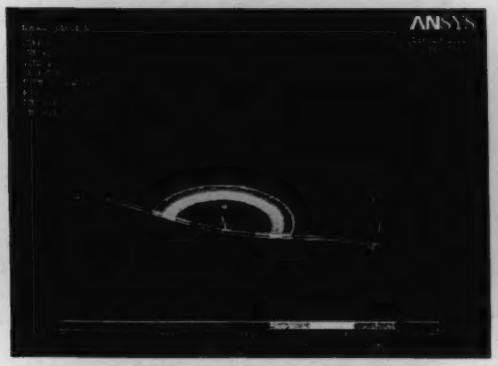

Figure 3.2: Half Expansion of a Displaced CMUT Membrane

Figure 3.3: Side View of a Three Quarter Expansion

3.4.2 3D Solid Model

The 3D solid model was created to investigate the relationship between membrane geometry and resonant frequency. In the 3D model the CMUT membrane was again approximated to be circular. For this model a residual prestress of 60 MPa tension (product of LPCVD fabrication) was applied to the silicon nitride membrane. The membrane was also biased by a DC voltage. The geometry of the model, listed in Table 3.3, is the same geometry as the CMUTs presented in [6]. Therefore, the resonant frequencies obtained by the 3D model can be verified with the results from [6].

Table 3.3: 3D Model Geometry

Parameter	Membrane Radius, r_M	Electrode Radius, r_E	Membrane Thickness, t_M	Electrode Thickness, t_E	Air Gap Thickness, t_A
Dimension (μm)	50.0	50.0	1.0	0.2	1.0

The 3D model reduces the CMUT to its membrane, electrodes, and air gap. To model the membrane and electrode, 20-noded structural brick elements (SOLID45 and SOLID95, respectively) were used. The air gap was modeled with a transducer element (TRANS126) that converts energy between the electrostatic and structural domains. Each node of the transducer has 2 DOF relating to displacement and electric potential. Since the bottom electrode consists of the silicon substrate, which is assumed to have no displacement, it was simply modeled by the bottom nodes of the transducer elements.

In order to generate elements with acceptable angles and aspect ratios, mapped meshing with manual sizing was used. The FEA software used could not apply mapped meshing to circular geometries, thus the membrane and electrode were quartered and the individual volumes were glued together, so that mapped meshing was possible. Figures 3.4 and 3.5 display the quarter section volume division and the meshed model with an intermediate element size.

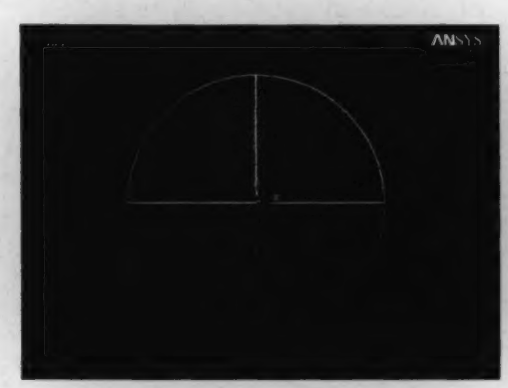

Figure 3.4: Quarter Section Volume Division

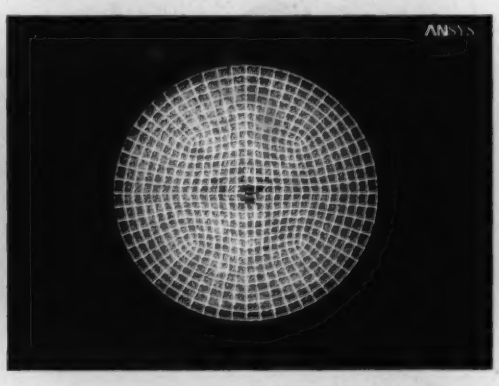

Figure 3.5: Mapped Mesh of 3D Solid Model

The membrane element was selected so that a residual stress could be applied through the use of the element's thermal properties. When the membrane is subjected to a temperature change, ΔT, the element's deflection, δ_T (change in geometric dimensions), will change in proportion to the membrane's thermal coefficient of expansion, α_M, and overall length, L.

$$\delta_T = \alpha_M (\Delta T) L \tag{3.1}$$

By applying the appropriate boundary conditions the membrane edges can be constrained, which acts as force to counteract the temperature strain. If the membrane cannot expand and contract due to the temperature change then the net deflection is equal to zero and a thermal stress, $\sigma_{thermal}$, is introduced.

$$\sigma_{thermal} = -E_M \alpha_M \Delta T \tag{3.2}$$

Where:
$$\Delta T = T_{uniform} - T_{reference} \tag{3.3}$$

If the reference temperature is set to zero than the uniform temperature that must be applied to the membrane elements in order to produce the residual stress, $\sigma_{thermal}$, is equal to:

$$T_{uniform} = \frac{\sigma_{thermal}(1 - \upsilon_M)}{E_M \alpha_M} \tag{3.4}$$

The $(1 - \upsilon_M)$ term, where υ_M is Poisson's ratio, accounts for the multi-axial loading of the membrane. Figure 3.6 illustrates a 60 MPa tension stress induced in the silicon nitride membrane. Although the electrode elements cannot model thermal effects, some residual stress is induced due to the displacement required to match the contracting membrane.

Figure 3.6: Residual Stress Induced in Membrane using Thermal Properties

Once the residual stress was modeled the static deflection due to a bias DC voltage, V_{DC}, was calculated. A voltage was applied to each end of the transducer elements which were connected to the bottom surface nodes of the membrane and the nodes representing the silicon substrate. When the DC voltage was applied, the transducer elements calculated the electrostatic capacitor force which in turn pulled the electrodes towards each other. The membrane's structural stiffness tried to counteract the displacement and eventually a steady-state deflection for the bias V_{DC} was observed.

Using a prestressing command (PSTRES) in the FEA software, the membrane deflection caused by the V_{DC} bias and residual prestress was reused as the starting point for static, modal, harmonic, and transient solutions. To model the resonant frequency of the CMUT a residual stress of 60 MPa (tension) and a bias voltage of 30 V_{DC} were utilized. From the static solution a partial block lanczos solver calculated the first 5 modal frequencies. Finally, a harmonic analysis was solved for a 1 Volt alternating current (AC) load applied over a range that encompassed the first resonant (modal) frequency.

3.4.3 Reduced Order Model

The third FEA model developed for this paper utilized a reduced order element (ROM144 in ANSYS) to create a reduced order model of the electrostatic-structural domain. As the name suggests a reduced order model is a simplified model that uses master nodes to reduce to the overall size of the model's database. By developing the governing relationships for certain master nodes the FEA software can replace the numerous elements in a 2D or 3D model with a single reduced order element. The typical reduced order element will have a fraction of the nodes of the full model, thus the computational time required for analysis is greatly reduced. In this model the entire 3D CMUT model, comprised of over 5000 nodes, was reduced to one element consisting of 30 nodes. The 30 nodes had degrees of freedom relating to voltage, displacement, and current, thus the element was ideal for electrostatic-structural analysis.

While reduced order modeling is a very useful tool for CMUT modeling, creating the elements does require a more complex and time consuming process. Following are the FEA software procedures used to create the reduced order element (ROM144) and to solve for the resonant frequency of a CMUT membrane. In order to validate the CMUT model, the geometric parameters used were the same as previously used with the 3D solid model.

The first step in creating the reduced order element is to generate a 3D model defining the membrane, electrodes, air gap, and air above the top electrode. This was done using similar techniques as found in the above 3D solid modeling. The membrane and electrode were again modeled with 20-noded structural brick elements. A residual stress was placed on the membrane using the thermal properties. Instead of using a

transducer element to couple the model though, the air gap and air above the top electrode were modeled using 20-noded electrostatic brick elements. Competing electrostatic and structural physics environments were then utilized to couple the system. This was similar to the 2D axisymmetric model employed in section 3.4.1.

Once the 3D model and physics environments were created, a generation-pass was used to build the reduced order element. In a generation pass the master nodes are defined and static loads are applied in the structural domain. The FEA software calculates the displacement of the master nodes and therefore develops force-displacement relationships for the structural domain of the CMUT. The modal frequencies of the system are also calculated and certain modes are chosen to govern the model. For the CMUT, the center of the membrane was chosen as the master node and the first modal (resonant) frequency was chosen as the governing parameter. When enough data has been collected to properly define the structural response of the system, the reduced order element is created.

The reduced order element can then be used for electrostatic-structural analysis. This is defined as the use-pass for a reduced order model. To validate the model a use-pass was completed that consisted of a harmonic analysis for a 60 MPa pre-stressed membrane with a $30V_{DC}$ bias and a $1V_{AC}$ driving voltage. Similar to the 3D model, a pre-stressing command (PSTRES) was utilized to obtain the static deflection. The pre-stressed CMUT membrane was then subjected to a harmonic analysis for a set frequency range.

3.5 Results

The three FEA models presented in this chapter were validated using results from reference literature. The collapse voltage results for the 2D axisymmetric model were verified with the thermal-structural analogous solutions presented in [3]. The resonant frequencies modeled by the 3D solid model and the reduced order model were verified using the impedance model found in [6]. This section also lists the advantages and disadvantages of the various modeling methods.

3.5.1 2D Modeling Results

The 2D axisymmetric model was used to calculate the collapse voltage for varying electrode radius. The results of this analysis are plotted in Figure 3.7.

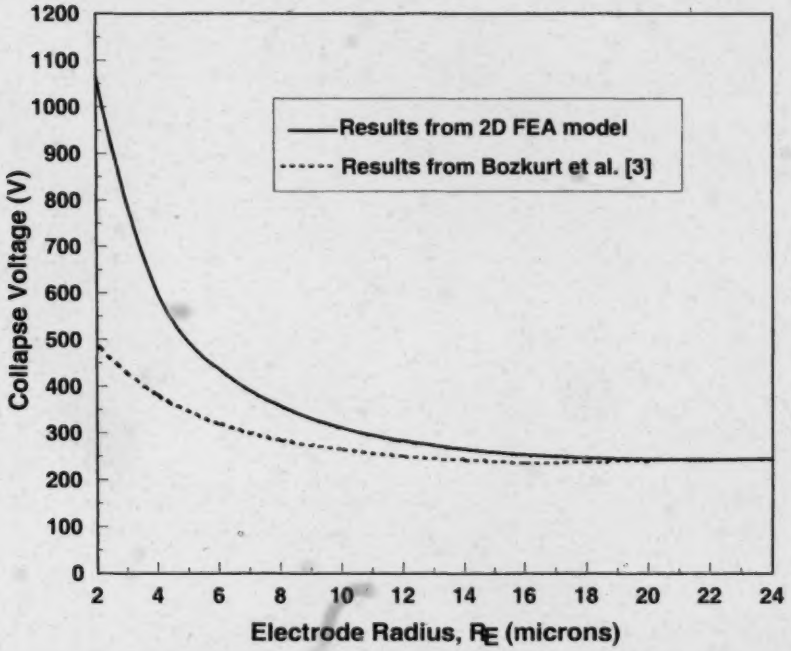

Figure 3.7: 2D Axisymmetric Model - Collapse Voltage for Varying R_E

Comparing the results with those obtained by Bozkurt et al. [3], it is seen that both models demonstrate similar behavior for electrode radii greater than or equal to half the membrane radius. The collapse voltage results for electrode radii greater than and equal to half the membrane radius are within 15% of results previously reported. As the electrode radius gets smaller though the values obtained here and the values obtained in [3] begin to diverge. At an electrode radius of 2 microns the results from the electrostatic-structural analysis are almost double those of the thermal-structural analogy.

Due to inaccuracies in both models the actual collapse voltage for small electrode radius is likely between the two values. For instance, the electrostatic-structural solver program uses weak coupling and thus may not have included the full capacitor force of the electrodes. Conversely the thermal-structural analysis did not include the stiffness of the top electrode and thermal forces are typically more linear than capacitive forces. In [3] it was proven that the optimum electrode radius was equal to half of the membrane radius, thus the 2D axisymmetric model can be used to calculate the collapse voltage for this optimized CMUT membrane.

Advantages of the 2D axisymmetric model include its ability to calculate static deflection and collapse voltage. It also includes the dielectric effects of the membrane and the 2D model reduces computational time. Disadvantages include the weak coupling nature, and the inability to perform a harmonic or modal analysis.

3.5.2 3D Solid Modeling Results

The 3D solid model was used to calculate the resonant frequency for a 30 V_{DC} biased CMUT membrane with a 60 MPa residual stress and a radius and thickness of 50

microns and 1 micron, respectively. By varying the radius by 2%, a shift in resonant frequency was observed, as shown in Figure 3.8. While the resonant frequencies can be observed, the nodal displacement occurring at these values are physically unrealizable and should be ignored. The reason the displacements are so inaccurate lies in the fact that there is no damping introduced in the model and if the model was run at its true resonant frequency the displacement would approach infinity.

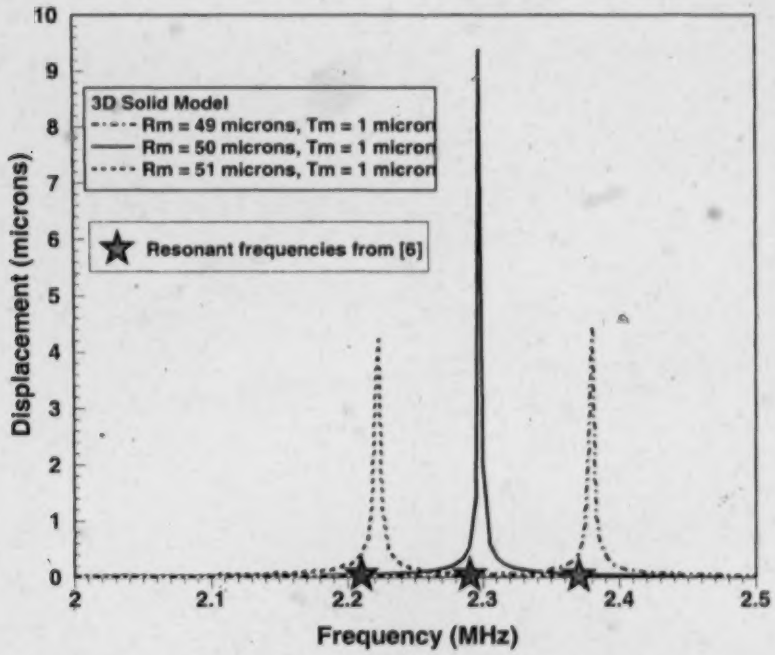

Figure 3.8: 3D Solid Model - Resonant Frequency Shift with 2% Change in R_M

By comparing the results obtained with those presented by X. Jin et al. [6], the 3D model was verified to accurately represent the resonant frequency of a CMUT. Advantages of this model include the strong coupling nature of the transducer element, the ability to model the static deflection due to a bias DC voltage, and the ability to model

residual stress caused by fabrication. The main disadvantage of the 3D solid model is the large amount of computational time required for the harmonic analysis.

3.5.3 Reduced Order Modeling Results

The reduced order model was also used to calculate the resonant frequency for a 30 V_{DC} biased CMUT membrane with a 60 MPa residual stress. Results for the analysis are shown in Figure 3.9.

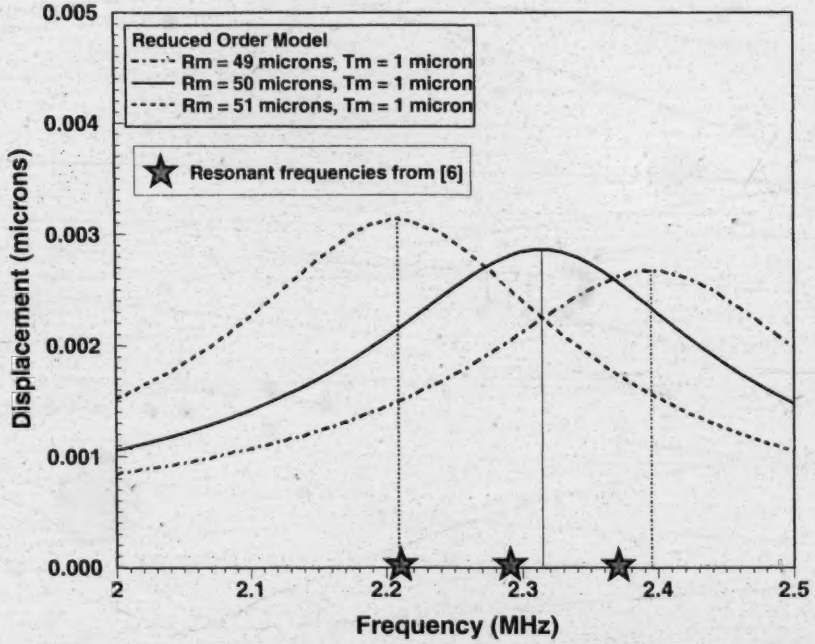

Figure 3.9: Reduced Order Model - Resonant Frequency Shift with 2% Change in R_M

The results obtained appear to be in good agreement with those published in [6]. Although the reduced order model's frequencies appear to be slightly higher, a smaller

element size will enhance the accuracy, at the cost of increased computational time during the generation-pass. Since the membrane was modeled with air above it and below it there was sufficient damping in the system to represent the true deflection of the membrane. Thus, the nodal amplitudes displayed in the above graphs are considered to be accurate.

Reduced order modeling has many advantages not seen with other modeling techniques. The reduced order elements can model static, modal, harmonic, and transient responses, while including the residual stress caused by fabrication. It has very quick computational time for the use-pass and has the potential to calculate the collapse voltage. Disadvantages include the complex and lengthy element generating process, and the lack of literature regarding the new FEA element. The latter of these two is due to the relatively new status of the reduced order element (ROM144) and thus should improve over time.

3.6 Conclusions

This chapter presented three finite element models developed using FEA software (ANSYS v.7), that were used to model the collapse voltage and resonant frequency of CMUTs.

A 2D axisymmetric model was used to calculate the relationship between collapse voltage and electrode radius for a CMUT membrane with a radius of 25μm and thickness of 0.6μm. The collapse voltage agreement with previously reported findings was within 15% for electrode radius greater than or equal to half the membrane radius. As the electrode radius decreased to less than half of the membrane radius, large discrepancies

arose between the model presented here and the model presented in [3]. An assumption was made that both models had problems modeling the complex electrostatic-structural relationships for small electrode radius and thus the collapse voltage likely resided between the two values.

Two separate models, a 3D solid model and a reduced order model, were used to calculate the resonant frequency of a CMUT. A membrane with a radius of 50 microns, and a thickness of 1 micron, was induced with a residual stress of 60 MPa (tension) and biased at 30 VDC. The membrane's resonant frequency was then calculated and compared with past literature. The 3D solid model and reduced order model produced resonant frequencies of 2.29 MHz and 2.32 MHz, respectively. The models were also verified by adjusting the membrane geometry and calculating the shift in frequency. The results for both models corresponded well with previously published observations.

CHAPTER 4

REFINED FEA MODLEING AND PARAMETRIC STUDY OF A CMUT

4.1 Introduction

In this chapter, the finite element models presented in Chapter 3 were refined for increased accuracy, and revisited. The objective of this process was to compare the capabilities of the finite element models to determine which one was best suited to model CMUT behavior. The most appropriate model was then utilized for a thorough parametric study. The parametric study illustrated changes in collapse voltage and resonant frequency due to 10% variations in a CMUT's geometric and material properties, as well as changes in the membrane's residual stress over a 200 MPa range.

4.2 Refined FEA Models

The collapse voltage modeling was revisited using the 2D axisymmetric model and the reduced order model. Both models utilized a refined mesh and were subjected to the same modeling parameters as those used to verify the 2D model in Chapter 3. The material properties and geometric parameters are documented in Table 3.1 and Table 3.2, respectively.

The resonant frequency modeling was revisited by refining both the 3D solid model and the reduced order model. As in Chapter 3, the results were compared to those published in [6] that were obtained using equivalent circuit modeling. Material

properties and geometric parameters for the resonant frequency modeling are documented in Table 3.1 and Table 3.3, respectively.

4.2.1 Collapse Voltage Modeling

As discussed in Chapter 3, the relationship between electrode radius and collapse voltage was used to verify the accuracy of the 2D axisymmetric model for electrode radii between full and half membrane radius. In order to verify the 2D model with the finite element model presented in [3], the CMUT membrane was modeled with no residual stress. For this chapter the 2D model with a refined mesh was reused to verify the collapse voltage results obtained with the reduced order model with a refined mesh.

Refining the mesh increases the number of elements used in both models. Increasing the number of elements will produce more accurate elements but results in longer computing times. An optimum mesh size can be observed by comparing the model convergence for varying the number of element with the computing time required for the models. For the collapse voltage modeling a user defined maximum computing time of 1 hour was specified.

Similar to the 2D model, the reduced order model employs structural and electrostatic Physics environments to solve for the collapse voltage. Both models were used to calculate the change in collapse voltage due to varying the electrode radius. This is an important study because, as shown in [3], it is beneficial to build CMUTs with half metallization of the top electrode. While analytical models cannot account for a half metallized top electrode, the finite element models can easily portray this as seen in Figure 4.1.

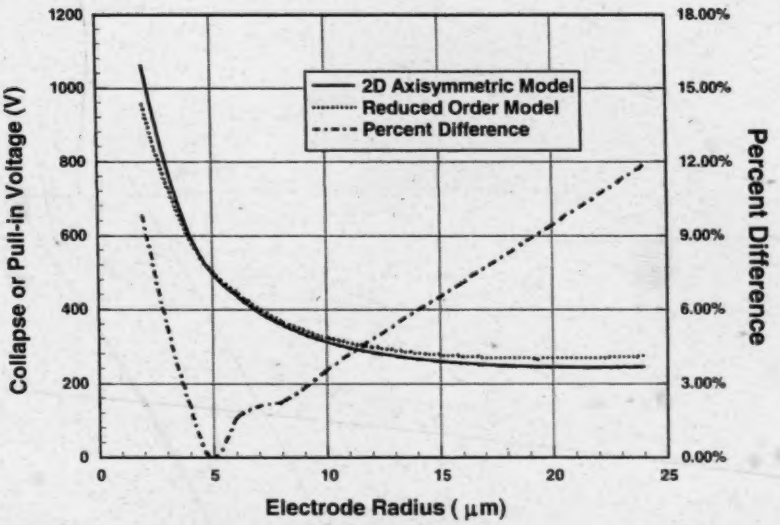

Figure 4.1: Change in Collapse Voltage due to varying Electrode Radius

As reported in Chapter 3 the 2D model was verified by comparing its results with the results obtained by a finite element model presented in [3]. Presuming that the 2D axisymmetric model is an accurate representation, the reduced order model can be compared against it.

Figure 4.1 illustrates that the reduced order model results closely follow the 2D axisymmetric results. The largest difference of 12% is found for a fully metallized electrode. When the top electrode is reduced to half metallization the percent differences drops to 5%. To allow for a safety factor, CMUTs should typically be operated at DC bias voltages of less than half of the collapse voltage. This safety factor makes the small percent difference between the models insignificant.

It has been shown that both models can accurately depict the collapse voltage for an unstressed CMUT membrane, but the reduced order models does have some advantages over the 2D axisymmetric model. The reduced order model can account for a

membrane residual stress, while the 2D axisymmetric model cannot. The reduced order model can also solve for a harmonic solution, while the 2D model can only be used for static solutions.

4.2.2 Resonant Frequency Modeling

Also presented in Chapter 3 were two finite element models capable of modeling the resonant frequency of a CMUT complete with membrane residual stress. The models included the aforementioned reduced order model and a 3D solid model. They were verified using the results obtained from an analytical model that was presented in [6]. The two models were refined for accuracy by increasing the number of elements and reinvestigated for this chapter.

As in Chapter 3, the refined models utilized a fully metallized top electrode and a 60 MPa membrane residual prestress. A 30 VDC bias voltage was also applied and the geometric parameters (see Table 2.3) matched the parameters of the analytical model found in [6]. For this chapter the membrane's radius of 50 μm was once again varied +/- 2% and the shift in resonant frequency was observed. All other parameters were held constant.

Displacement results for the 3D solid model and reduced order model were graphed to illustrate the first resonant frequency. The shift in resonant frequency due to a 2% variation in membrane radius was used to verify the models. Comparisons of the 3D solid model and the reduced order model with the analytical model are displayed in Figures 4.2 and 4.3, respectively.

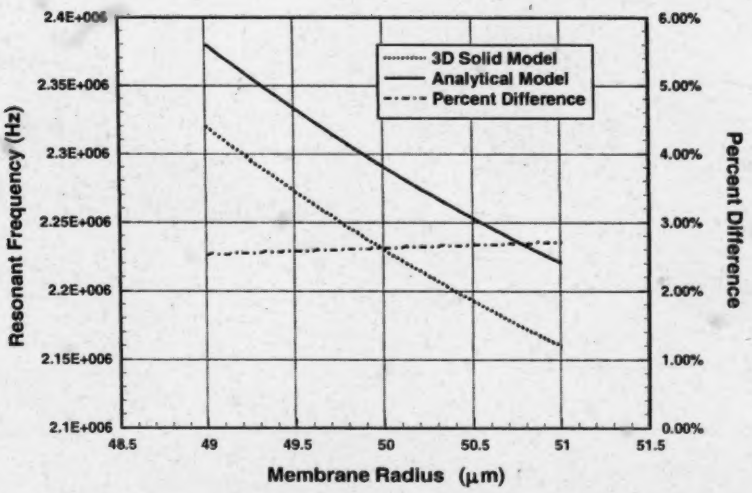

Figure 4.2: Comparison of 3D Solid Model with Analytical Model

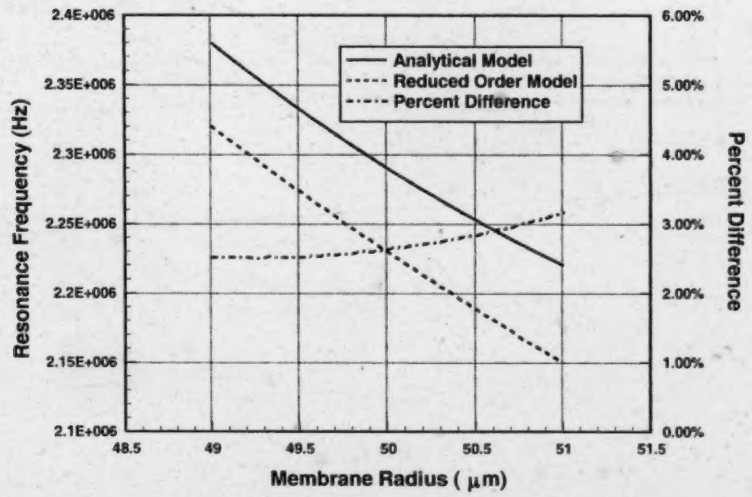

Figure 4.3: Comparison of Reduced Order Model with Analytical Model

Both finite element models demonstrate very high accuracy when compared with the analytical model. While there is a small 2-3% difference, it remains relatively consistent throughout the variation of the membrane radius. This difference may be

related to different material properties values, but nonetheless it is small enough to neglect. The 3D solid model, reduced order model, and analytical model all illustrate a similar trend of a 5% decrease in resonant frequency due to a 2% increase in membrane radius.

Both finite element models produced the same resonance results but the reduced order model has a couple of advantages over the 3D solid model. The first is a greatly reduced number of elements which significantly reduces the computing time. The refined 3D model consisted of 19281 elements and required 15:50 hours to complete the resonant frequency modeling. The reduced order model was created by reducing 16864 3D solid elements down to 1 electrostatic-structural element. This enabled the resonant frequency modeling to be completed in 0:45 hours. Another advantage the reduced order model had was the ability to quickly calculate the collapse voltage using the same model that was created to study the resonant frequency. While the 3D solid model can calculate the collapse voltage it requires a large amount of computing time, thus the reduced order model is better suited for this application.

4.3 Parametric Study Results

From the above results, it is apparent that the reduced order model is the most complete modeling tool to investigate the collapse voltage and resonant frequency of CMUTs. The analytical, 2D axisymmetric, and 3D solid models will produce accurate results, but the reduced order model has significant advantages over these models.

For instance, the analytical model cannot account for complex geometries, such as a half metallized top electrode. Since the reduced order model is based on 3D elements it

is capable of modeling these complex geometric patterns. The reduced order model can also induce a membrane prestress and perform harmonic analysis to solve for the resonant frequency; these are two capabilities the 2D model does not possess. Due to its reduced number of nodes, it will also solve electrostatic-structural problems much faster than the 3D solid model, thereby minimizing the required computing time. For these reasons the reduced order model was chosen for the parametric study.

Table 4.1: CMUT Parametric Study Variables

Geometric Parameter	Value (μm)	Variation
Membrane Radius	50	+/- 10%
Membrane Thickness	1	+/- 10%
Electrode Radius	50 and 25	+/- 10%
Electrode Thickness	0.2	+/- 10%
Air Gap Thickness	1.4	+/- 10%
Material Property Parameter	**Value**	**Variation**
Membrane Elasticity	320 GPa	+/- 10%
Membrane Poisson Ratio	0.263	+/- 10%
Membrane Density	3270 kg/m^3	+/- 10%
Electrode Elasticity	67.6 GPa	+/- 10%
Electrode Poisson Ratio	0.3555	+/- 10%
Electrode Density	2700 kg/m^3	+/- 10%
Other Parameters	**Value**	**Variation**
Air Gap Dieletric Strength	1	+/- 10%
Membrane Residual Stress	60 MPa (Tension)	0 – 200 MPa (Tension)

In the parametric study a standard CMUT was modeled, then each parameter was varied +/- 10% and the changes in collapse voltage and resonant frequency were observed. Changes were also observed for variations in residual stress over a 200 MPa range. The standard model considered was the 50 μm membrane radius, fully metallized CMUT from the aforementioned resonant frequency modeling. Using the reduced order model this design resulted in a collapse voltage and resonant frequency of 266 V and 2.23 MHz, respectively. The parameters that were varied independently of each other are listed in Table 3.1. Half metallization CMUTs were also included in the parametric investigation. The half metallization standard model produced a collapse voltage and resonant frequency of 292 V and 2.15 MHz, respectively. This is roughly a 10% higher collapse voltage and 4% lower resonant frequency than the full metallization CMUT.

4.3.1 Collapse Voltage

CMUT membrane deflection is a result of competing electrostatic and structural forces. The collapse voltage can be defined as the point where the electrostatic force increases faster than the structural restoring force. From this force description, it is evident that the collapse voltage will be affected by parameters that govern the structural stiffness and the electrostatic field.

Many of the parameters do not significantly influence the stiffness or electrostatic field; therefore varying these parameters produces only small changes in the collapse voltage. The manufacturing tolerances for these parameters can be reduced because imperfections will not have a large affect on the CMUT's characteristics. Parameters that produce a 1% or smaller change in collapse voltage are listed in Table 4.2.

Table 4.2: Parameters Producing Small Changes in Collapse Voltage

Variable Parameter	Percent Change due to 10% Variation	
	Full Metallization	*Half Metallization*
Elect. Thickness	1.1 %	0.3 %
Elect. Elasticity	0.8 %	0.3 %
Elect. Poisson Ratio	0.3 %	0.0 %
Elect. Density	0 %	0 %
Mem. Poisson Ratio	0.8 %	0.7 %
Mem. Density	0 %	0 %

The results illustrate that 10% variations in the top electrode's geometric and material parameters will not significantly affect the collapse voltage. Therefore a less refined manufacturing tolerance can be utilized for the metallization process. This is beneficial because the 0.2 μm thick metal electrode is the CMUT's smallest component and a refined tolerance would be difficult to achieve.

It should also be noted that the collapse voltage is a static solution and subsequently, it is not affected by varying the CMUT density. The density will alter the resonant frequency though, so it cannot be completely ignored.

Parameters that will produce a significant change in the collapse voltage are the membrane thickness, the membrane radius, the membrane modulus of elasticity, the air permittivity, and the residual stress. The collapse voltage results for variations in these parameters are illustrated in Figures 4.4-4.8.

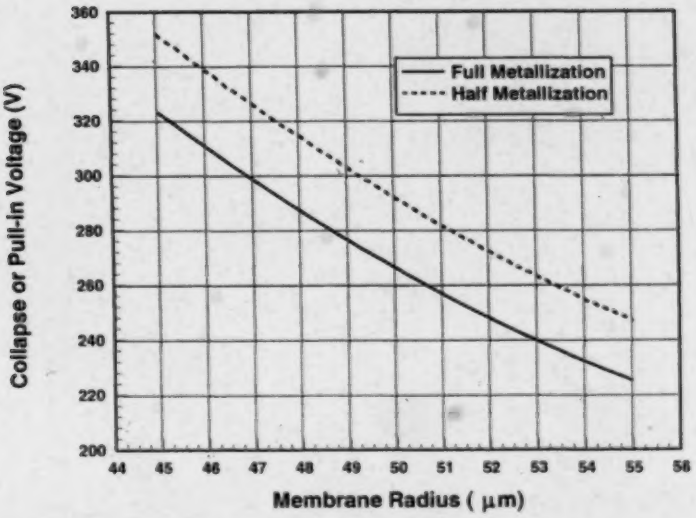

Figure 4.4: Change in Collapse Voltage due to 10% Variation in Membrane Radius

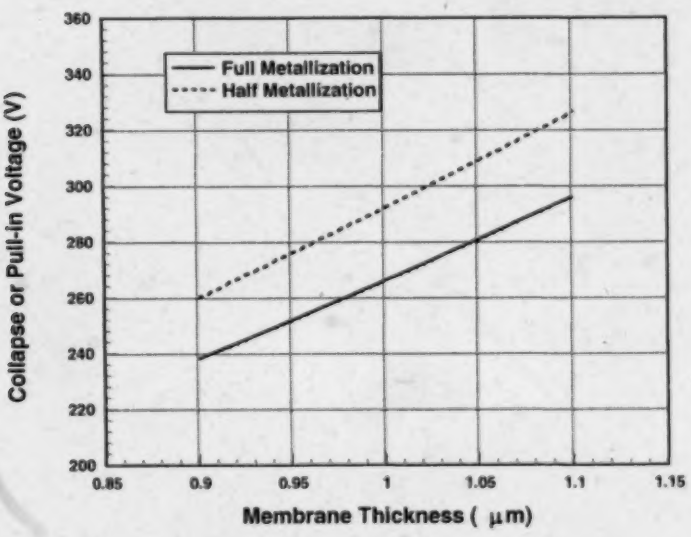

Figure 4.5: Change in Collapse Voltage due to 10% Variation in Membrane Thickness

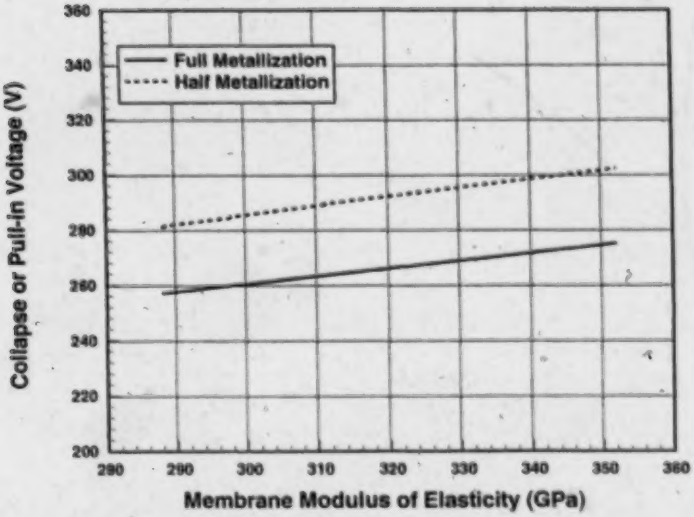

Figure 4.6: Change in Collapse Voltage due to 10% Variation in Membrane Elasticity

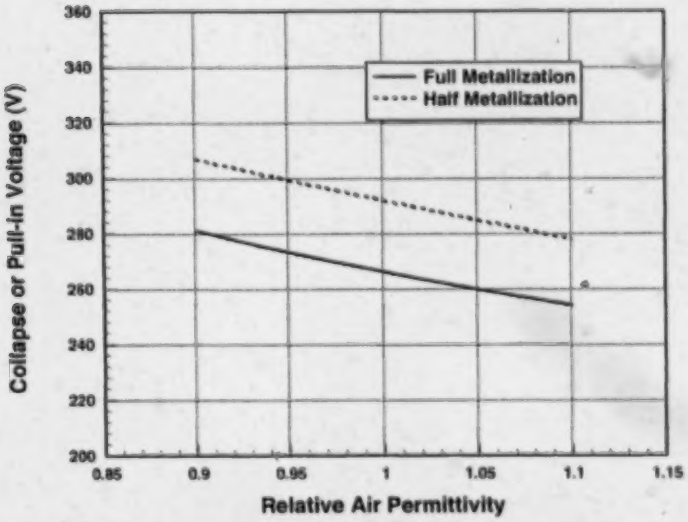

Figure 4.7: Change in Collapse Voltage due to 10% Variation in Air Permittivity

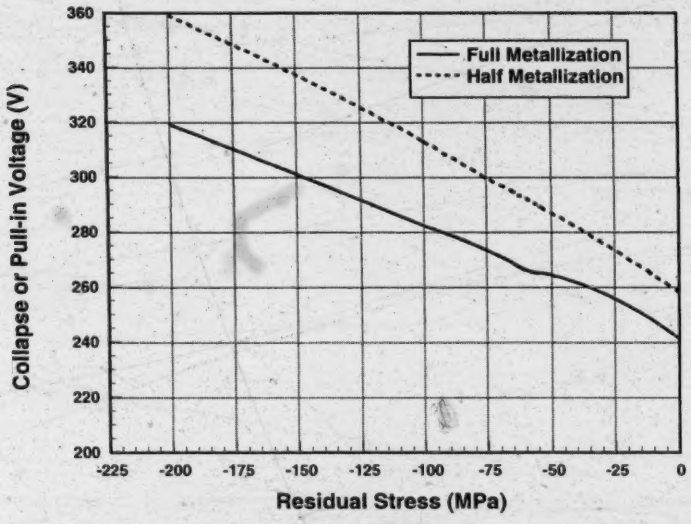

Figure 4.8: Change in Collapse Voltage due to Variation in Residual Stress

The graphs illustrate that varying the membrane's geometric parameters will produce the greatest change in collapse voltage. Although a 10% variation in membrane radius produces the largest collapse voltage change, the highest manufacturing tolerances are required for the membrane thickness. This is because a 10% variation in the thickness is equal to 0.1 μm, while for the radius a 10% variation is 5 μm. This results in 11% and 0.4% shift in collapse voltage due to 0.1 μm variations in the membrane's thickness and radius, respectively. The membrane's modulus of elasticity is also an important parameter that can vary widely, therefore accurate material data is required for CMUT fabrication.

The air dielectric strength (relative permittivity) will vary depending on the operating or sensing medium. Thus, a complete understanding of the CMUT's operating environment is essential for accurate design models. Residual stress is another parameter that can greatly affect the collapse voltage. The residual stress is directly related to

manufacturing and will vary depending on fabricating temperatures and processes. While residual stress can be designed for by altering the fabrication process, it requires a high level of control over all manufacturing aspects to produce accurate results.

Another important relation observed is that the half metallization model varies at the same rate as the full metallization model. Throughout the parametric study the half metallization model consistently shows a 10% higher collapse voltage than the full metallization model. This provides solid verification for the half metallization reduced order model.

4.3.2 Resonant Frequency

When an AC voltage is applied to the CMUT it will cause the membrane to vibrate at the voltage harmonic frequency. The membrane deflections will be greatest at the resonant or natural frequencies. The simplest expression for resonant frequency equates the frequency to the square root of the stiffness divided by the mass. CMUT stiffness and mass are two variables that are dependent upon the CMUT's geometric and material parameters. Increasing the stiffness to mass ratio will raise the resonant frequency, while decreasing this ratio will lower the resonant frequency.

Similar to the collapse voltage, many of the parameters studied do not significantly influence the stiffness or mass; therefore they have little affect on the resonant frequency. Once again the manufacturing tolerances for these parameters can be reduced, as long as the parameters do not affect the collapse voltage. Parameters that produce a 1% or smaller change in resonant frequency are listed in Table 4.3.

Table 4.3: Parameters Producing Small Changes in Resonant Frequency

Variable Parameter	Percent Change due to 10% Variation	
	Full Metallization	*Half Metallization*
Elect. Thickness	0.5 %	0.5 %
Elect. Elasticity	0.9 %	0.5 %
Elect. Poisson Ratio	0.3 %	0.0 %
Elect. Density	0.0 %	0.0 %
Mem. Poisson Ratio	0.5 %	0.5 %
Air Permittivity	0 %	0 %

These results verify the earlier conclusion that the top electrode's parameters do not greatly affect the CMUT performance, thus the tolerances for the metallization process can be reduced. The only electrode parameter that should be strictly controlled is whether the CMUT will employ a half metallization or full metallization design.

Parameters that will produce a significant change in the resonant frequency are the membrane radius, the membrane thickness, the membrane modulus of elasticity, the membrane density, and the residual stress. Results for varying these parameters are plotted in Figures 4.9-4.13.

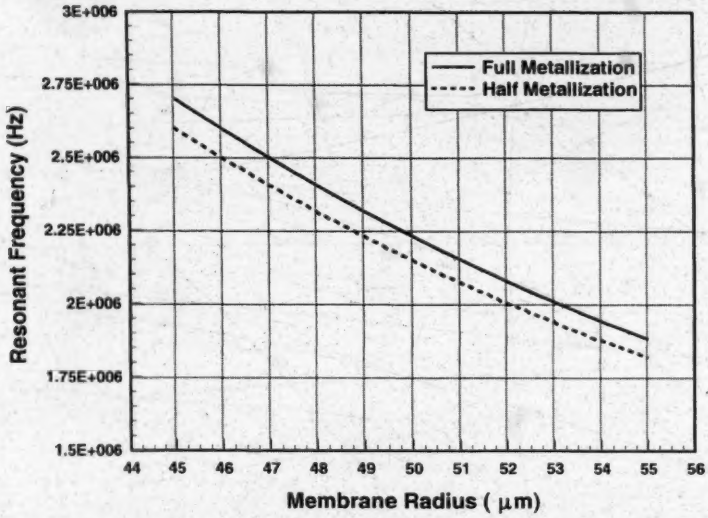

Figure 4.9: Shift in Resonant Frequency due to 10% Variation in Membrane Radius

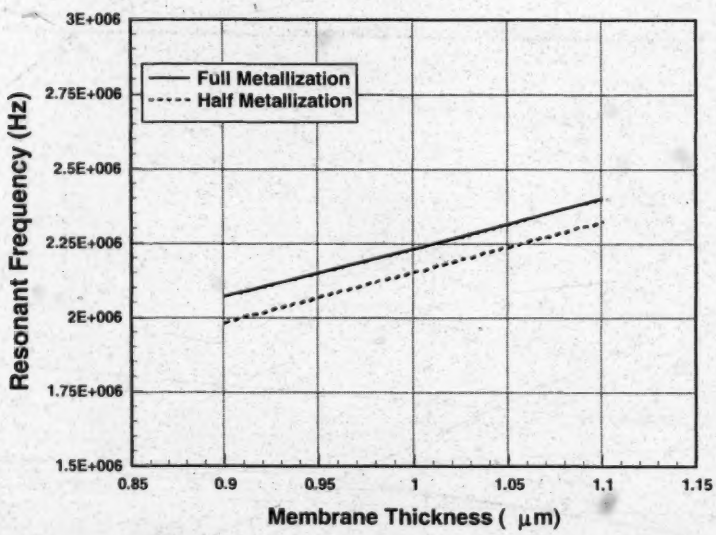

Figure 4.10: Shift in Resonant Frequency due to 10% Variation in Membrane Thickness

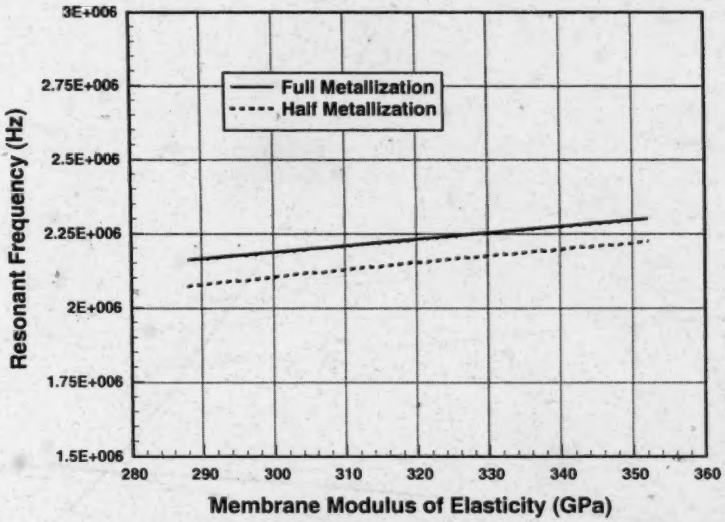

Figure 4.11: Shift in Resonant Frequency due to 10% Variation in Membrane Elasticity

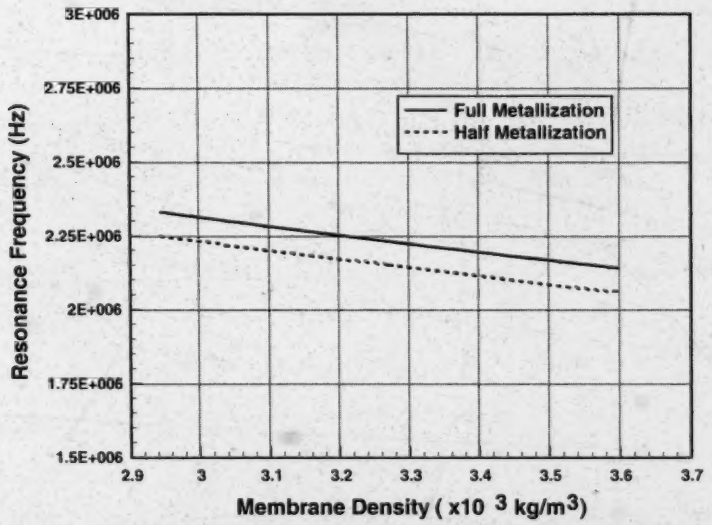

Figure 4.12: Shift in Resonant Frequency due to 10% Variation in Membrane Density

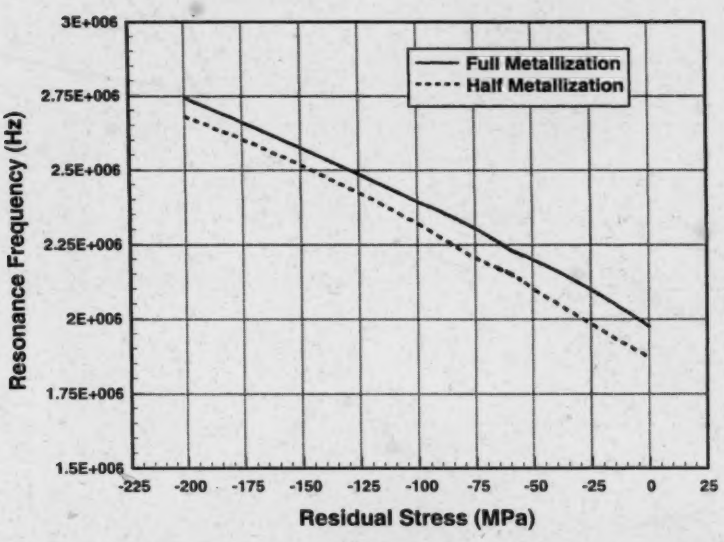

Figure 4.13: Shift in Resonant Frequency due to Variation in Residual Stress

The results illustrate that the resonant frequency is mostly affected by the membrane's geometric parameters. While the largest shifts in resonant frequency are obtained by varying the radius, the highest fabricating tolerances are once again required for the membrane thickness. A 0.1 μm variation in the membrane's thickness will result in a 7.5% shift in resonant frequency compared to a 0.4% shift due to a 0.1 μm change in membrane radius. 10% variations in the membrane's modulus of elasticity and density will also shift the resonant frequency roughly 3% and 4%, respectively.

Residual stress will also have an effect on the resonant frequency, which is similar to the effect produced on the collapse voltage. By increasing the tensile residual stress (shown as a negative value) both the collapse voltage and resonant frequency will increase. This is a common trend for all CMUT parameters, where variations that result in increases in collapse voltages will also result in increases in the resonant frequency.

The relation between the half metallization model and full metallization model can also be observed for the resonant frequency. The parametric study illustrates a consistent 4% lower resonant frequency for the half metallization model when compared to the full metallization model.

4.4 Conclusions

This paper revisited three finite element models presented in Chapter 3 that could be used to model the collapse voltage and resonant frequency of CMUTs. They included a 2D axisymmetric model, a 3D solid model, and a reduced order model. The models were compared with each other and past analytical models to determine which model was best suited to investigate CMUT behavior. The reduced order model was established as the most complete model, and was utilized in a parametric study.

The parametric study began with a CMUT consisting of a 1 μm thick membrane with a radius of 50 μm, induced with a residual stress of 60 MPa (tension). A 0.2 μm thick aluminum electrode and 1.4 μm air gap were connected above and below the membrane, respectively. Models for a full metallization top electrode and a half metallization top electrode were investigated. The full metallization model produced a CMUT with a collapse voltage of 266 V and a resonant frequency of 2.23 MHz, while the half metallization model had a collapse voltage and resonant frequency of 292 V and 2.15 MHz, respectively.

The parameters of the reduced order model were varied by 10% to study the changes in collapse voltage and resonant frequency. It was discovered that altering the membrane's geometric parameters produced the greatest changes. Reducing the radius

by 10% resulted in a collapse voltage of 323 V and a resonant frequency of 2.70 MHz; increases of roughly 20% for the full metallization model. Similar 20% increases were observed for the half metallization model. The membrane thickness was discovered to be the most crucial parameter from a fabrication aspect. Varying the thickness by only 0.1 μm caused a 10% change in collapse voltage and 7.5% change in resonant frequency. Therefore, very small manufacturing tolerances must be utilized during the membrane fabrication. Other parameters that produced significant changes were the membrane modulus of elasticity, membrane density (resonant frequency only), air permittivity (collapse voltage only), and the residual stress.

Varying the top electrode's parameters by 10% resulted in very little influence on the CMUT's behavior, thus fabricating tolerances for the metallization process can be increased. However, varying the top electrode's radius by large amounts without changing the membrane radius will produce noticeable results, such as in the half metallization model.

The half metallization reduced order model is capable of accurately representing the collapse voltage and resonant frequency behavior of a prestressed CMUT. Throughout the parametric study the half metallization model consistently demonstrated a 10% high collapse voltage and a 4% lower resonant frequency when compared with the fully metallization model.

CHAPTER 5

DESIGNING CMUTs FOR SPECIFIC APPLICATIONS

5.1 Introduction

In the previous chapters it was shown that finite element analysis could be used to accurately model CMUT's. The FEA models were used to perform a parametric study that offered a glimpse into designing CMUTs for specific operating parameters, such as resonant frequency and collapse voltage. In this chapter the results of the parametric study were expanded upon to develop a design process capable of modeling CMUTs for a user defined resonant frequency or collapse voltage.

The first step involved calculating the mechanical impedance of the FEA model and comparing this with the previously published analytical model. Following this, a design process was established that utilizes user defined parameters that can be easily changed to obtain a wide range of results. The design process also accounts for other parametric variations that are more difficult for a designer to modify. In the last section of the chapter, three CMUT examples were investigated using the resonant frequency and collapse voltage design process

5.2 Impedance Modeling

One of the most important aspects of CMUT design is the accurate modeling of the membrane's mechanical impedance. The mechanical impedance of a CMUT can be defined as the pressure applied to the membrane divided by the resultant velocity of the

membrane. For optimized ultrasound generation and sensing the mechanical impedance of the CMUT should be properly tailored to the mechanical impedance of the sensing medium.

Previous analytical models utilized the mathematical theory presented in Mason [1] for a diaphragm with tension and stiffness. As shown in Mason [1] and in Appendix A, the mechanical impedance of a CMUT membrane subjected to a uniform pressure, P, can be defined as:

$$Z_M = j\omega\rho_M t_M \left[\frac{r_M k_1 k_2 \left(k_2 I_1(k_2 r_M) J_0(k_1 r_M) + k_1 J_1(k_1 r_M) I_0(k_2 r_M)\right)}{r_M k_1 k_2 \left(k_2 I_1(k_2 r_M) J_0(k_1 r_M) + k_1 J_1(k_1 r_M) I_0(k_2 r_M)\right) - 2(k_1^2 + k_2^2) I_1(k_2 r_M) J_1(k_1 r_M)} \right] \quad (5.1)$$

Where J_n and I_n are Bessel and modified Bessel functions of the n^{th} order, respectively and k_1 and k_2 can be defined as:

$$k_1 = \sqrt{\frac{\sqrt{d^2 + 4c\omega^2} - d}{2c}} \quad (5.2) \qquad \text{and} \qquad k_2 = \sqrt{\frac{\sqrt{d^2 + 4c\omega^2} + d}{2c}} \quad (5.3)$$

With c and d defined as:

$$c = \frac{(E_M + \sigma_M) t_M^2}{12\rho_M (1 - \upsilon_M^2)} \quad (5.4) \qquad \text{and} \qquad d = \frac{\sigma_M}{\rho_M} \quad (5.5)$$

The mechanical impedance for the finite element CMUT model can be calculated by first obtaining the average membrane displacement due to an applied electrostatic pressure. For the reduced order model, master nodes can be defined at evenly spaced radial distances to obtain a displacement curve for the membrane at any given frequency. The average displacement, u_{avg}, can be calculated by multiplying the master node displacements by the radial areas, summing these values, and dividing the sum by the total area of the membrane. This is shown in Appendix C for various CMUT geometries.

The radial distance for the average displacement of various CMUT geometries can be approximated at 68% of the membrane's radius. Thus, for a membrane radius of 50 μm the average displacement will be found at a radial distance of 34 μm from the membrane's centre. Using the reduced order model, a master node positioned at this radial distance will give the average displacement for the CMUT membrane. The average displacement can then be utilized to calculate the lumped average velocity, v_{avg}, as defined in equation 5.6:

$$v_{avg} = j\omega x_{avg} \tag{5.6}$$

The electrostatic force applied to the CMUT membrane is directly related to the capacitive nature of the finite element model. Approximating the model as a parallel plate system, it can be shown that the capacitance of the CMUT is dependent upon the geometric and material parameters as written in equation 5.7:

$$C_{CMUT} = \frac{\kappa_M \kappa_A \varepsilon_0 S}{\kappa_A t_M + \kappa_A t_I + \kappa_M t_A} \tag{5.7}$$

Using the principle of virtual work, the electrostatic force can be calculated by differentiating the potential energy of the capacitor with respect to the position of mass (displacement of membrane). Assuming a constant membrane and insulator thickness, the displacement of the membrane is related only to the change in air gap thickness, t_A. Differentiating the energy with respect to change in air gap thickness gives:

$$F_{Cap} = \frac{\kappa_M^2 \kappa_A \varepsilon_0 S V^2}{2\left(\kappa_A t_M + \kappa_A t_I + \kappa_M t_A\right)^2} \tag{5.8}$$

Where:
$$V = V_{DC} + V_{AC}\sin(\omega t) \tag{5.9}$$

As shown in the previous literature and in Appendix A, by making $V_{DC} >> V_{AC}$, the dominant time varying electrostatic pressure can be defined as:

$$P_{Cap} = \frac{\kappa_M^2 \kappa_A \varepsilon_0 V_{DC} V_{AC}}{\left(\kappa_A t_M + \kappa_A t_I + \kappa_M t_A\right)^2} \tag{5.10}$$

The reduced order CMUT model presented in Chapter 3 utilizes the bottom of the membrane as its top electrode and assumes no insulator thickness. For this model t_M and t_I will equal zero reducing equation 5.10 to equation 5.11, seen below:

$$P_{Cap}' = \frac{\kappa_A \varepsilon_0 V_{DC} V_{AC}}{t_A^2} \tag{5.11}$$

Thus, the mechanical impedance of the reduced order model can be calculated using the displacement of the master node located at 68% of the membrane's radial distance and equation 5.12:

$$Z_M = \frac{P_{Cap}'}{v_{avg}} = j\frac{P_{Cap}'}{\omega x_{avg}} \tag{5.12}$$

Figure 5.1 compares the mechanical impedance of the reduced order finite element model with the mechanical impedance obtained of the analytical models described in Chapter 1. The CMUT modeled consisted of a 100 MPa prestressed membrane with a radius of 50 μm and a thickness of 1 μm, biased with a 50 V_{DC} voltage. It also included a 1 μm air gap thickness and a fully metalized top electrode with a 0.1 μm thickness. All material properties were held consistent with those found in Chapter 3.

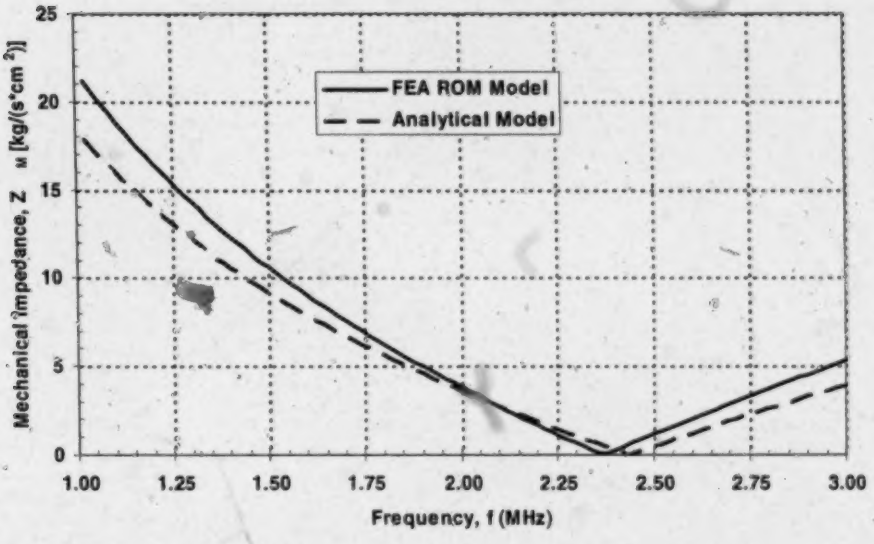

Figure 5.1: Absolute Mechanical Impedance for Analytical and FEA Models

Both models demonstrate a similar resonant frequency of approximately 2.35 MHz, which can be seen graphically as the lowest value of the mechanical impedance. While the mechanical impedance calculated using the FEA model is lower than that of the analytical model, they are in the same order of magnitude so the results can be considered somewhat accurate. One reason the FEA results are lower is that the bias voltage applied to the membrane will cause a static displacement, which in turn decreases the air gap thickness. This decrease in air gap thickness will increase the electrostatic pressure but it is not accounted for in P_{Cap}' as calculated using equation 5.11. The analytical model and the equations presented in this chapter do not account for the static deflection but the reduced order model utilizes it as a starting point for its harmonic analysis. More research and modeling is required to properly match the mechanical impedance of the FEA model to the mechanical impedance of the analytical model.

5.3 CMUT Variable Design Parameters

The parametric investigation presented in Chapter 4 briefly demonstrated how CMUT parameters could be modified to design sensors with specific resonant frequency of collapse voltage. Many of the parameters proved to be insignificant, while others illustrated their importance in determining the operating characteristics of CMUTs. Of the important parameters, material properties (membrane elasticity, membrane density, and air permittivity) and byproducts of the fabrication process (residual membrane stress) are difficult to change significantly. While these parameters need to be accounted for in the design process they are not considered a good choice for user defined variable design parameters. That leaves membrane radius and membrane thickness as applicable design parameters and the proceeding section investigates the relationships between these parameters and the resonant frequency (RF) and collapse voltage (CV).

5.3.1 RF and CV Relationships for Membrane Radius

The finite element reduced order model was used to investigate the relationship between membrane radius and the CMUT's resonant frequency and collapse voltage. Input parameters for the control CMUT model are listed in Table 5.1. The membrane radius of the control model was varied from 10 – 100 μm, while all other parameters were held constant. Figure 5.2 illustrates the change in RF and CV as a result of large changes in membrane radius.

Table 5.1: Control CMUT Model Input Variables

Parameter	Value	Parameter	Value
Mem. Radius, r_M	50 μm	Mem. Elasticity, E_M	320 GPa
Mem. Thickness, t_M	1.0 μm	Mem. Density, ρ_M	3270 kg/m^3
Elect. Radius, r_E	50 μm	Mem. Poisson's Ratio, υ_M	0.263
Elect. Thickness, t_E	0.1 μm	Elect. Elasticity, E_E	67.6 GPa
Air Thickness, t_A	1.0 μm	Elect. Density, ρ_E	2700 kg/m^3
Mem. Residual Stress, σ_M	100 MPa	Elect. Poisson's Ratio, υ_E	0.356
Bias Voltage, V_{DC}	50 V	Air Dielectric Strength, κ_A	1.00

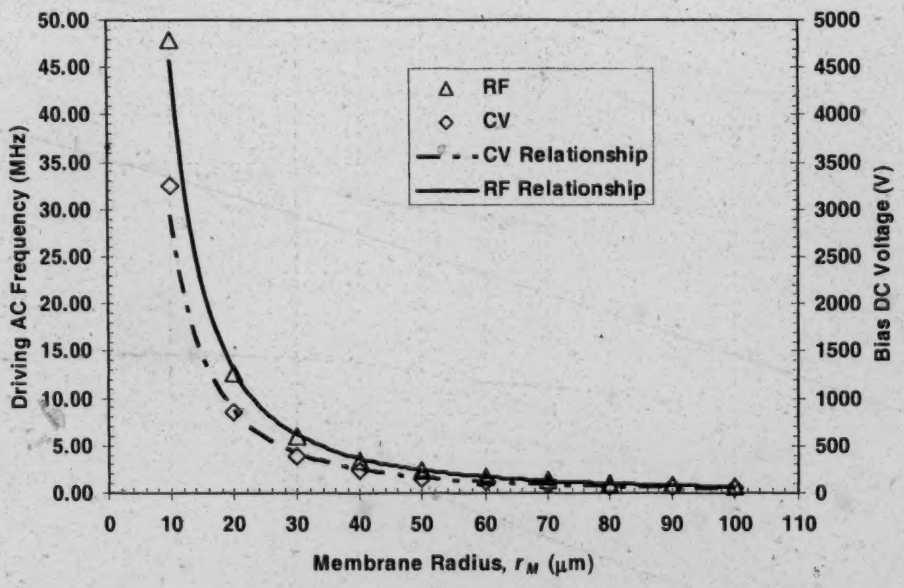

Figure 5.2: Resonant Frequency (RF) and Collapse Voltage (CV) as a function of Membrane Radius (r_M)

Figure 5.2 reveals that the relatively linear relationship illustrated in Figures 4.4 and 4.9 for a 10% variation in membrane radius will not accurately account for larger changes in membrane radius. Although the above curves could be used for CMUT design, more interesting curves are presented by plotting the RF and CV as a function of the modified aspect ratio (AR_{Mod}), as seen in Figure 5.3. The modified aspect ratio relates the membrane thickness to the membrane radius and can be defined as:

$$AR_{Mod} = \frac{t_M}{r_M^2} \tag{5.13}$$

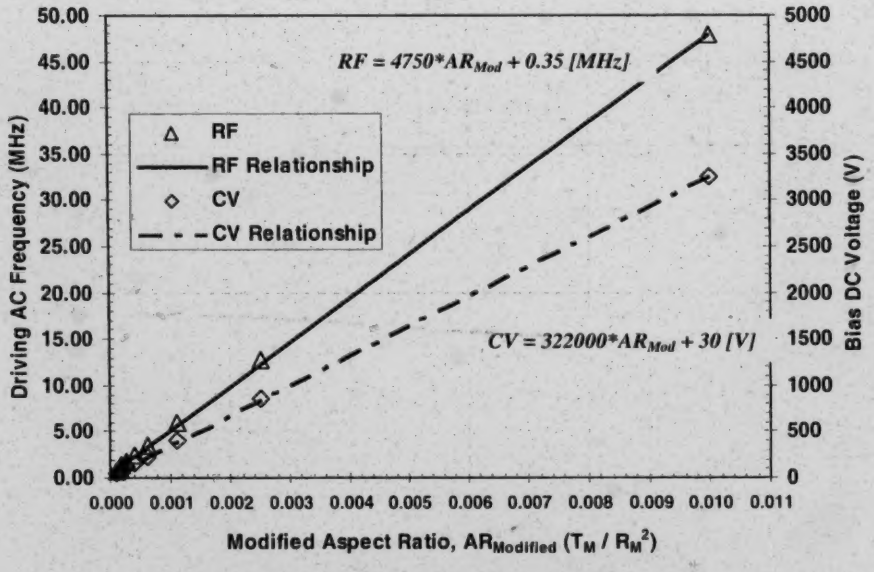

Figure 5.3: Resonant Frequency (RF) and Collapse Voltage (CV) as a function of Modified Aspect Ratio (AR_{Mod})

From Figure 5.3, linear relationships can be found to relate the modified aspect ratio to the collapse voltage (equation 5.14) and resonant frequency (equation 5.15).

Equations 5.14 and 5.15 can be used to model CMUTs for collapse voltages and resonant frequencies as high as 3300 V and 50 MHz, respectively.

$$RF = 4750 * AR_{Mod} + 0.35 \tag{5.14}$$

$$CV = 322000 * AR_{Mod} + 30 \tag{5.15}$$

5.3.2 RF and CV Relationships for Membrane Thickness

The reduced order model was also used to investigate the relationship between membrane thickness and the CMUTs resonant frequency and collapse voltage. Once again a control model was used with the parameters listed in Table 5.1. For this study the membrane thickness was varied from 0.2 - 2.0 μm, while all other parameters were held constant. Figures 5.4 and 5.5 demonstrate that the relationships defined in equations 5.14 and 5.15 are reasonably accurate for CMUT modeling of various membrane thicknesses.

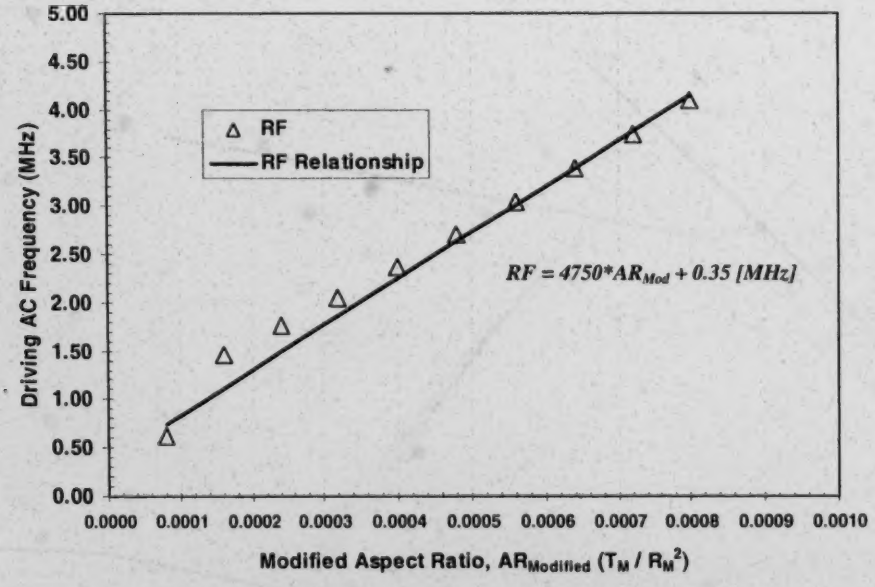

Figure 5.4: RF vs. AR_{Mod} for Various Membrane Thicknesses (t_M)

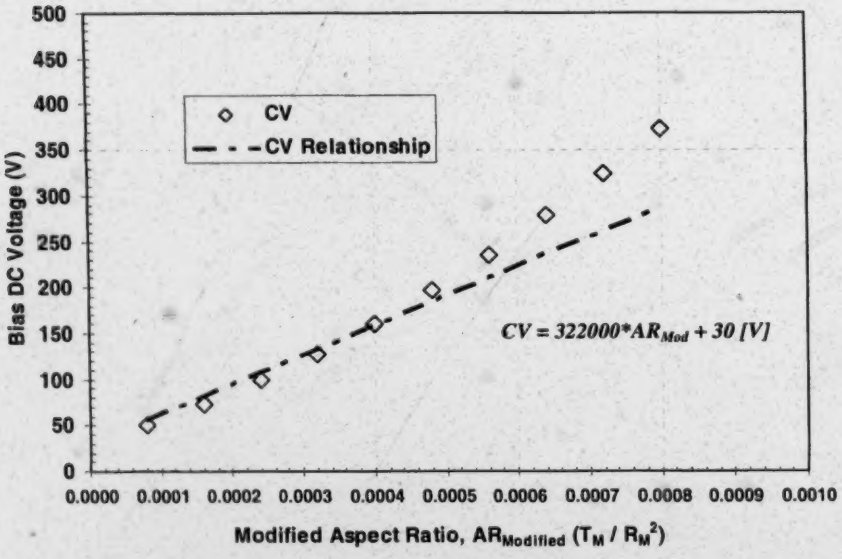

Figure 5.5: CV vs. AR_{Mod} for Various Membrane Thicknesses (t_M)

The modeling results begin to diverge from the relationships obtained from Figure 5.4 as the thickness deviates further from 1.0 μm. Equations 5.14 and 5.15 can still be used but designers should note the accuracy range limitations for various membrane thicknesses. Table 5.2 summarizes 10% and 20% accuracy ranges for the relationships when compared to the FEA modeling for various membrane thicknesses.

Table 5.2: Summary of Equations 5.14 and 5.15 Accuracy Ranges

Mem. Radius (μm)	Mem. Thickness (μm)	Modeled RF (MHz)	Equation 4.14 Accuracy Range		Modeled CV (V)	Equation 4.15 Accuracy Range	
			10%	20%		10%	20%
10	1.0	47.92	Yes	Yes	3246	Yes	Yes
20	1.0	12.74	Yes	Yes	861	Yes	Yes
30	1.0	5.92	Yes	Yes	400	Yes	Yes
40	1.0	3.50	Yes	Yes	236	Yes	Yes
50	1.0	2.37	Yes	Yes	160	Yes	Yes
60	1.0	1.74	Yes	Yes	119	Yes	Yes
70	1.0	1.35	Yes	Yes	93	Yes	Yes
80	1.0	1.08	Yes	Yes	77	Yes	Yes
90	1.0	0.87	Yes	Yes	65	Yes	Yes
100	1.0	0.67	No	No	56	No	Yes
50	0.2	0.62	No	Yes	50	No	Yes
50	0.4	1.46	No	No	73	No	Yes
50	0.6	1.76	No	Yes	99	Yes	Yes
50	0.8	2.05	Yes	Yes	128	Yes	Yes
50	1.0	2.37	Yes	Yes	160	Yes	Yes
50	1.2	2.70	Yes	Yes	196	Yes	Yes
50	1.4	3.04	Yes	Yes	236	No	Yes
50	1.6	3.39	Yes	Yes	278	No	Yes
50	1.8	3.74	Yes	Yes	324	No	Yes
50	2.0	4.10	Yes	Yes	372	No	No

5.4 CMUT Design Procedures

By using equations 5.13-5.15 and Table 5.2, the required membrane radius and thickness can be calculated for CMUTs designed for a specific resonant frequency or collapse voltage. This procedure will hold true for CMUTs that have identical modeling parameters as those specified in Table 5.1. Variations in these parameters, especially the residual stress and material properties, are very common and the resultant shift in operating parameters needs to be accounted for.

5.4.1 Parametric Multiplication Factors

Using the results of the parametric study in Chapter 4, relationships can be developed to calculate the change in resonant frequency and collapse voltage due to the change in the model parameter. For example, a 1% increase in membrane elasticity will produce a 0.314% increase in resonant frequency and a 0.338% increase in collapse voltage. Therefore, a multiplication factor can be derived that will account for the change in operating parameters due to the change in membrane elasticity:

$$RF_1 = RF_0 * ME_{RF} \qquad (5.16) \quad \text{where} \quad ME_{RF} = 1 + \frac{E_M - 320}{320} x0.314 \qquad (5.17)$$

$$CV_1 = CV_0 * ME_{CV} \qquad (5.18) \quad \text{where} \quad ME_{CV} = 1 + \frac{E_M - 320}{320} x0.338 \qquad (5.19)$$

In the above equations RF_0 and CV_0 refer to the resonant frequency and collapse voltage of a CMUT with the standard model parameters (E_M = 320 GPa). RF_1 and CV_1 refer to the modified operating parameters due to changing the membrane's modulus elasticity, E_M which has units of GPa.

The other multiplication factors that affect resonant frequency are MD_{RF} (membrane density), RS_{RF} (residual stress), and MF_{RF} (metallization factor). The metallization factor accounts for the 4% decrease in resonant frequency found for half metallization (HM) of the top electrode. When a CMUT employs full metallization (FM) of the top electrode than MF_{RF} is equal to 1. Formulas to calculate these factors as well as the full RF modification formula are listed below. In each case the altered parameter must be entered using the same units as those shown in Table 5.1 (i.e. residual stress, σ_M, must be in MPa).

$$MD_{RF} = 1 + \frac{\rho_M - 3270}{3270} x0.426 \tag{5.20}$$

$$RS_{RF} = 1 + \frac{\sigma_M - 100}{100} x0.155 \tag{5.21}$$

$$MF_{RF} = 1 \rightarrow (FM) \ldots or = 0.96 \rightarrow (HM) \tag{5.22}$$

$$RF_1 = RF_0 * ME_{RF} * MD_{RF} * RS_{RF} * MF_{RF} \tag{5.23}$$

The additional multiplication factors affecting the collapse voltage are AP_{RF} (air permittivity), RS_{RF} (residual stress), and MF_{RF} (metallization factor). The metallization factor accounts for the 10% increase in collapse voltage that occurs with half metallization of the top electrode. Formulas to calculate the collapse voltage factors as well as the CV modification formula follow below:

$$AP_{CV} = 1 + \frac{\kappa_A - 1.00}{1.00} x(-0.451) \tag{5.24}$$

$$RS_{CV} = 1 + \frac{\sigma_M - 100}{100} x0.131 \tag{5.25}$$

$$MF_{CV} = 1 \rightarrow (FM) \ldots or = 1.10 \rightarrow (HM) \tag{5.26}$$

$$CV_1 = CV_0 * ME_{CV} * AP_{CV} * RS_{CV} * MF_{CV} \tag{5.27}$$

5.4.2 RF and CV Design

To design a CMUT for a specific resonant frequency, a designer must first specify the desired RF and all model parameters with the exception of the membrane radius and thickness. The next step is to calculate all parametric multiplication factors to be used in equation 5.23. Equation 5.23 is then inverted (Equation 5.23b) to calculate the standard model resonant frequency, RF_0, where RF_1 is the user specified resonant frequency in MHz.

$$RF_0 = \frac{RF_1}{ME_{RF} * MD_{RF} * RS_{RF} * MF_{RF}} \tag{5.23b}$$

Once the standard resonant frequency is calculated it can be used in Equation 5.14b to calculate the modified aspect ratio:

$$AR_{Mod} = \frac{RF_0 - 0.35}{4750} \tag{5.14b}$$

With the modified aspect ratio defined, the designer must then decide upon model accuracy. Once this has been chosen, the membrane radius and thickness can be chosen using equation 5.13 and Table 5.2. Now that all of the parameters have been selected, a reduced order finite element model can be created and the resonant frequency of the model compared with that of the design specification.

To design a CMUT for a particular collapse voltage, similar steps to the resonant frequency design are followed. In these steps the collapse voltage multiplication factors are used as well as inverted versions of equations 5.27 and 5.15. In these formulas CV_1 is

the user specified collapse voltage and CV_0 is the standard model collapse voltage, both in units of volts.

$$CV_0 = \frac{CV_1}{ME_{CV} * AP_{CV} * RS_{CV} * MF_{CV}} \tag{5.27b}$$

$$AR_{Mod} = \frac{CV_0 - 30}{322000} \tag{5.15b}$$

Figure 5.6 is a flow chart illustrating the specific steps in CMUT resonant frequency and collapse voltage design. The proceeding section utilizes this flow chart for 3 separate CMUT design examples.

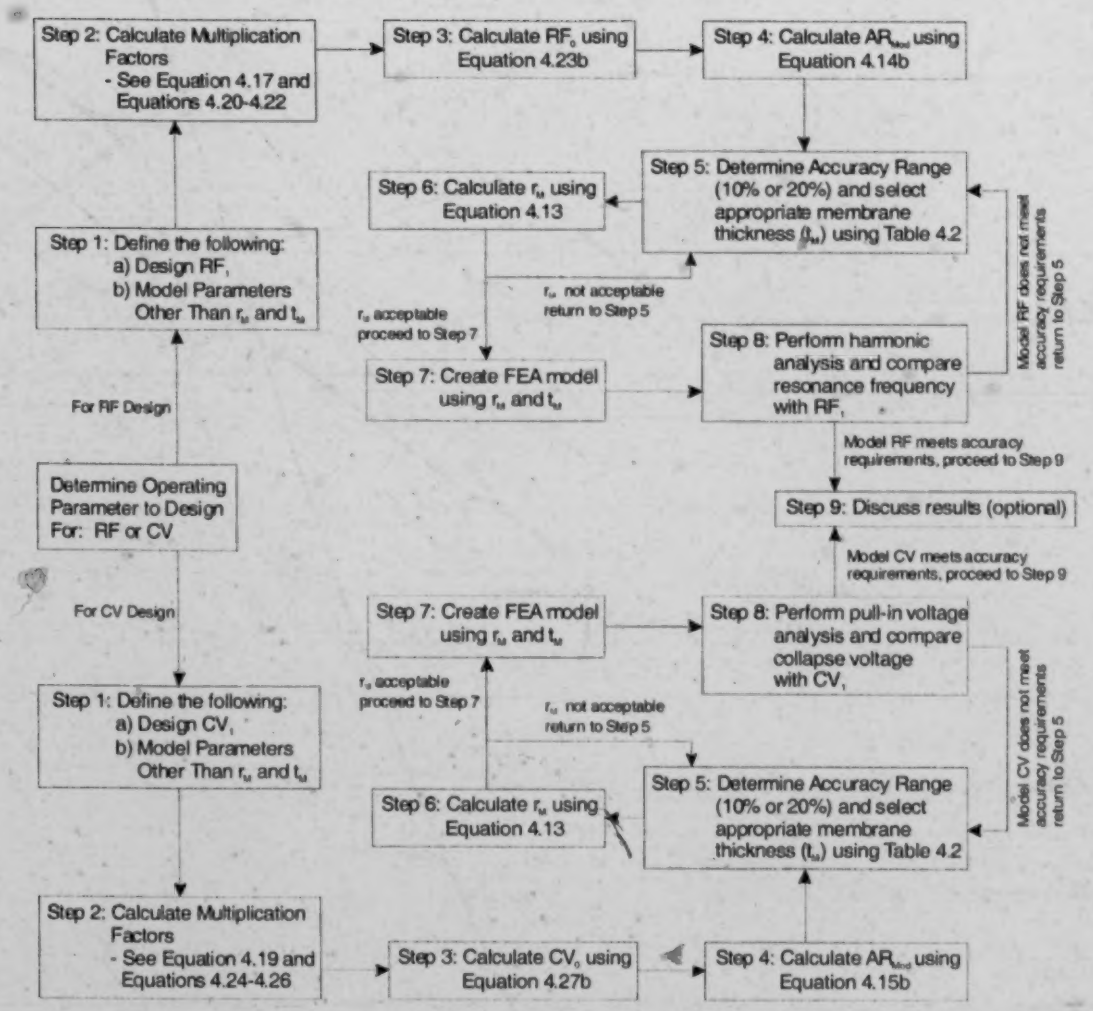
Step 2: Calculate Multiplication Factors
- See Equation 4.17 and Equations 4.20-4.22
Step 3: Calculate RF0 using Equation 4.23b
Step 4: Calculate ARMod using Equation 4.14b
Step 5: Determine Accuracy Range (10% or 20%) and select appropriate membrane thickness (tm) using Table 4.2
Step 6: Calculate rm using Equation 4.13
Step 1: Define the following:
a) Design RF,
b) Model Parameters Other Than rm and tm
rm acceptable proceed to Step 7
rm not acceptable return to Step 5
Model RF does not meet accuracy requirements return to Step 5
Step 7: Create FEA model using rm and tm
Step 8: Perform harmonic analysis and compare resonance frequency with RF,
For RF Design
Model RF meets accuracy requirements, proceed to Step 9
Determine Operating Parameter to Design For: RF or CV
Step 9: Discuss results (optional)
Model CV meets accuracy requirements, proceed to Step 9
For CV Design
Step 7: Create FEA model using rm and tm
Step 8: Perform pull-in voltage analysis and compare collapse voltage with CV,
rm acceptable proceed to Step 7
rm not acceptable return to Step 5
Step 1: Define the following:
a) Design CV,
b) Model Parameters Other Than rm and tm
Model CV does not meet accuracy requirements return to Step 5
Step 6: Calculate rm using Equation 4.13
Step 5: Determine Accuracy Range (10% or 20%) and select appropriate membrane thickness (tm) using Table 4.2
Step 2: Calculate Multiplication Factors
- See Equation 4.19 and Equations 4.24-4.26
Step 3: Calculate CV0 using Equation 4.27b
Step 4: Calculate ARCV using Equation 4.15b

Figure 5.6: CMUT Design Process Flow Chart

5.4.3 CMUT Design Examples

a) Design Example #1

Design a CMUT with a resonant frequency of 15 MHz +/- 10%. The silicon nitride from which the membrane will be fabricated has a modulus of elasticity and density of 310 GPa and 3000 kg/m^3, respectively. During fabrication a residual stress of 150 MPa will be induced in the membrane. All other material parameters are assumed to be similar to those found in Table 5.1. The fabrication shop is set up to etch 1.0 μm thick silicon nitride membranes and 0.1 μm thick fully metallized aluminum electrodes.

Results

Step 1: $RF_I = 15$ MHz

$E_M = 310$ GPa

$\rho_M = 3000$ kg/m^3

$\sigma_M = 150$ MPa

Step 2: $$ME_{RF} = 1 + \frac{310 - 320}{320} x 0.314 = 0.990$$

$$MD_{RF} = 1 + \frac{3000 - 3270}{3270} x 0.426 = 0.965$$

$$RS_{RF} = 1 + \frac{150 - 100}{100} x 0.155 = 1.078$$

$$MF_{RF} = 1 \rightarrow (FM)$$

Step 3: $$RF_0 = \frac{15MHz}{0.990 * 0.965 * 1.078 * 1.000} = 14.565MHz$$

Step 4: $$AR_{Mod} = \frac{14.565 - 0.35}{4750} = 0.00299$$

Step 5: $t_M = 1.0$ μm From Table 5.2 accuracy falls within user defined +/-10%

Step 6: $r_M = \sqrt{\frac{t_M}{AR_{Mod}}} = \sqrt{\frac{1.0}{0.00299}} = 18.3\mu m$ Table 5.2 accuracy +/-10%

Step 7: CMUT created using reduced order FEA model

Step 8: Harmonic analysis yielded a resonant frequency of 15.5 MHz which is 3.33% greater than the design resonant frequency but well within the +/-10% tolerance.

Step 9: The above process allowed for the accurate design of a CMUT with a resonant frequency of 15 MHz +/-10%. The chosen design utilizes a membrane with a thickness and radius of 1.0 μm and 18.3 μm, respectively. This design met all fabrication requirements and will result in a resonant frequency of 15.5 MHz.

b) Design Example #2

Design a CMUT with a collapse voltage greater than 250 V. The air gap will consist of a gas with a dielectric constant of 1.03. During fabrication a residual stress of 80 MPa will be induced in the membrane. The top electrode will be fabricated with full metallization. All other model parameters are assumed to be similar to those found in Table 5.1. The CMUT elements will be fabricated in an array with a minimum of 40 elements resting upon a $1mm^2$ silicon substrate. The spacing between element edges must not exceed 40 μm.

Results

This section will only review the important results but a complete step by step analysis can be found in Appendix D.2. The standard model collapse voltage, CV_0, was

calculated to be 260.3 V, giving a modified aspect ratio, AR_{Mod}, of 0.000715. Since operating bias voltages are typically much lower than the collapse voltage, a broader user defined accuracy range of 20% was chosen.

Due to the array constraints, a 7x7 matrix configuration was chosen that allows for 49 elements. With a 40 μm minimum spacing between element edges, the diameter of each element cannot exceed 97.1 μm. An element membrane radius of 45 μm was chosen, giving a membrane thickness of 1.45 μm, and element spacing of 46.25 μm.

The reduced order FEA model was created using the chosen membrane radius and thickness and the collapse voltage was calculated. The model produced a collapse voltage of 274 V, which was 10% greater than the designer specified collapse voltage. A 10% increase falls within the chosen 20% accuracy range and meets the CV > 250 V design criteria. Figure 5.7 below shows the geometric configuration of the sensor array.

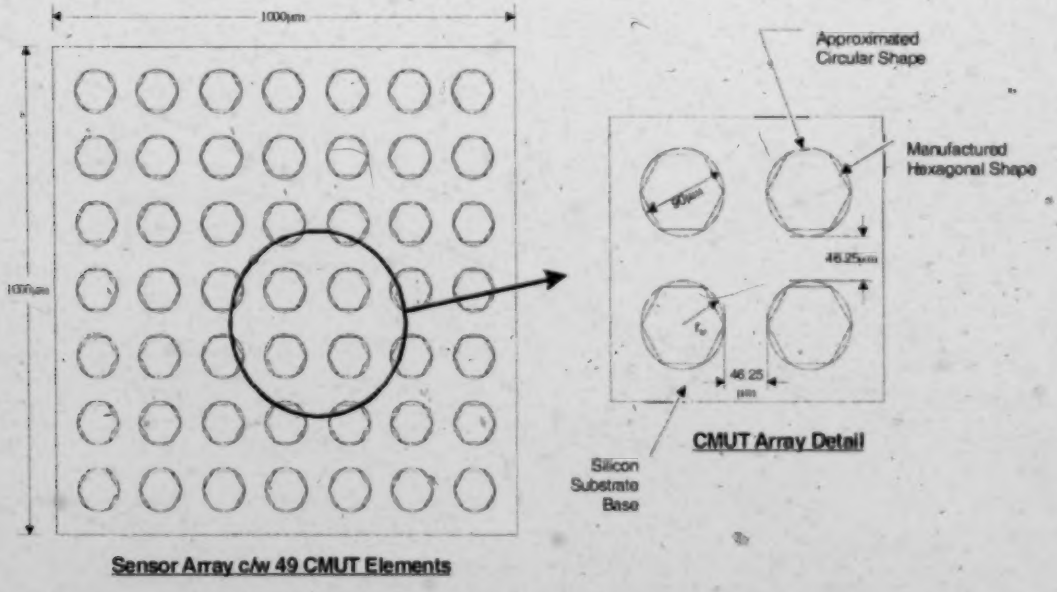

Figure 5.7: Geometric Configuration of a 49 CMUT Element Sensor Array

*c) **Design Example #3***

Design a CMUT with a resonant frequency of 2.03 MHz. During fabrication a residual stress of 60 MPa will be induced in the membrane. The top electrode will be fabricated with half metallization and will be 0.2 μm thick. All other model parameters are assumed to be similar to those found in Table 5.1.

Results

As with Example #2, this section will only review the important results but a complete step by step analysis can be found in Appendix D.3. An important note is that the electrode thickness has been increased to 0.2 μm, but the effect of this is considered to be negligible, thus it was not considered in the design process. The standard model resonant frequency, RF_0, was calculated to be 2.25 MHz, giving a modified aspect ratio, AR_{Mod}, of 0.0004. A user defined accuracy range of 10% was chosen, thereby limiting the selection of membrane thicknesses.

To simplify the model a 1.0 μm thick membrane was chosen, resulting in a membrane radius of 50 μm. Using these parameters the reduced order FEA model was created and the resonant frequency was calculated. The model produced a resonant frequency of 2.145 MHz, which was 5.36% greater than the designer specified value. This resonant frequency does fall within the 10% accuracy range that was defined by the designer, thus the design process is validated for CMUTs with half metallization of the top electrode.

5.5 Conclusions

This chapter illustrated how a CMUT could be designed to operate at a specific resonant frequency or collapse voltage. In order to create the CMUT models a process was developed that allowed for 2 designer defined geometric parameters which could accurately account for a wide range of resonant frequencies and collapse voltages. The 2 parameters were the membrane radius and membrane thickness.

The first step in creating this process was proving that the reduced order finite element model could accurately calculate the mechanical impedance of a CMUT element. The average displacement of the CMUT membrane was observed to occur at a radial location of approximately 68% of the radius from the center. Using the average membrane velocity and the modified electrostatic pressure the mechanical impedance was calculated. The results were relatively close to those found using the analytical model. Not properly accounting for the static deflection prior to the harmonic response, is likely the reason for the inaccuracy but further research is required to verify this.

Even though the mechanical impedance was not entirely accurate, it was in the same order of magnitude so the development of a design process continued. The membrane radius and thickness were greatly varied and the change in resonant frequency and collapse voltage were observed. Plotting the resonant frequency and collapse voltage versus the modified aspect ratio (t_M/r_M^2) produced linear relationships that could be utilized in the design process. The relationships were found to be accurate to within 20% for membrane radii between 10-90 μm and membrane thicknesses between 0.2-1.8 μm.

The design process also accounted for variations in other parameters deemed important in the parametric study but cannot be easily chosen by the designer. These

included certain material properties and the residual stress, all of which are likely to vary somewhat from the standard values utilized for the standard model. A flow chart was also included to illustrate the step-by-step process of designing CMUTs for a specific resonant frequency or collapse voltage.

Finally, 3 design examples were presented that validated the use of the design process. The first example was a design of a CMUT with altered material parameters to operate at a resonant frequency of 15 MHz +/-10%. Using the design process resulted in a CMUT with a membrane radius and thickness of 18.3 μm and 1.0 μm, respectively that operated at a resonant frequency of 15.5 MHz. The second example involved designing a CMUT for a collapse voltage greater than 250 V while maintaining specific geometric constraints that allowed for a minimum 40 element array to be fabricated on a 1 mm^2 substrate. This example resulted in a 49 element array with membrane radius and thickness of 45 μm and 1.45 μm, respectively. These CMUT elements modeled a collapse voltage of 275 V, which is 10% greater than the collapse voltage specified. The final example required a CMUT with a resonant frequency of 2.03 MHz and half metallization of the top electrode. To meet these requirements a model was created with a membrane radius and thickness of 50 μm and 1.0 μm, respectively. The resultant resonant frequency was 2.145 MHz, which was within the 10% user defined accuracy and validated the design process for CMUTs with half metallization.

CHAPTER 6

SUMMARY OF SIGNIFICANT RESULTS

6.1 Introduction

Capacitive Micromachined Ultrasonic Transducers are emerging as a leading candidate for many ultrasound sensing applications. Most of the advances in CMUT design can be attributed to the development of accurate modeling techniques. The research presented in this dissertation illustrated the advantages of finite element modeling and demonstrated which modeling technique was best suited for CMUT applications. Also presented in this dissertation was a design process that facilitates CMUT design for specific collapse voltages and resonant frequencies.

6.2 Finite Element Modeling

Finite element analysis was used to create three models that calculate the collapse voltage and resonant frequency of CMUT elements. The FEA software package utilized was ANSYS v.7. To calculate the collapse voltage a 2-Dimensional axisymmetric model was developed. The resonant frequency was calculated using a 3-Dimensional solid model. A Reduced Order Model was also developed that was capable of both collapse voltage and resonant frequency calculations. The modeling accuracy was verified by comparing the FEA results with results presented in the research literature. Following an examination of the accuracy, advantages, and disadvantages of three models, an optimum model was chosen for extended CMUT modeling.

6.2.1 2D Axisymmetric Model

The 2D axisymmetric model was utilized to calculate the collapse voltage of an unstressed CMUT element consisting of an aluminum top electrode, a silicon nitride membrane, an air gap, and a silicon substrate base (bottom electrode). The geometric parameters and material properties were consistent with those presented by Bozkurt et al. [3] so that the results could be directly compared. Collapse voltages were calculated for a 25 μm radius CMUT membrane with a varying top electrode radius of 2-24 μm.

The results presented in Chapter 3 illustrate that the 2D axisymmetric model produced collapse voltages within 15% of previously reported finite element models for top electrode radii greater than or equal to half of the membrane. As the electrode radius was decreased to less than half metallization ($r_E = 0.5*r_M$) greater divergence of the results occurred. The divergence of the models was explained in large part by the coupling discrepancies between the electrostatic-structural environments of the 2D model and the thermal-structural environments of the Bozkurt et al. model.

The main advantage of the 2D model is its ability to accurately model the static deflections and collapse voltage of a CMUT element for an electrode radius between full and half metallization. Other advantages include decreased computational times due to its axisymmetric nature and the ability to model the dielectric effects of the membrane. The major disadvantage of the model is its inability to model harmonic or modal responses; thus other models are required to calculate the CMUT resonant frequency.

6.2.2 3D Solid Model

The 3D solid model coupled with an electrostatic-structural transducer element was created to calculate the resonant frequency of a prestressed CMUT element subjected to a bias DC voltage and a driving AC voltage. To verify the results with those previously reported, the geometric parameters and material properties utilized were identical to those presented by Jin et al. [6]. The resonant frequency was calculated for full metallization CMUTs with 1 μm thick membranes and membrane radii of 49, 50, and 51 μm.

In Chapter 4 the results obtained with the refined 3D model for the 3 different membrane radii were within 3% of those presented in the research literature [6]. The resonant frequency of the 50 μm radius, 1 μm thickness CMUT element was 2.23 MHz. It was observed that increasing the membrane radius by 2% resulted in a decrease of 3.5% in resonant frequency. Conversely, a 2% radius decrease resulted in a 3.5% resonant frequency increase.

Advantages of the 3D model include the abilities to model static deflections due to the bias DC voltage, residual prestress due to fabrication, and resonant frequency due to the driving AC voltage. The main disadvantage is the large amount of time required for harmonic calculations due to the number of nodes in the model.

6.2.3 Reduced Order Model

The reduced order model initially studied in Chapter 3 was refined in Chapter 4 and used to calculate the resonant frequency of a CMUT element with identical parameters to those of the 3D solid model. As with the 3D solid model the reduced order

modeling results were compared with those presented by Jin et al. [6]. The reduced order model was also used in Chapter 4 to calculate the collapse voltage of CMUT elements with similar parameters to those initially modeled with the 2D axisymmetric model.

The reduced order model compares very well with the 3D model and the analytical results presented in [6]. A resonant frequency of 2.23 MHz was observed for an element with a membrane radius of 50 μm and membrane thickness of 1 μm, as were the appropriate resonant frequency shift due to a 2% change in membrane radius. The results were within 3% of the results obtained by the analytical models. Collapse voltage results for the reduced order model also proved to be very similar to the 2D model results, especially for electrode patterning between full and half metallization. The models presented in Chapters 3 and 4 demonstrate the reduced order model can be used to accurately calculate CMUT resonant frequency and collapse voltage.

The main advantage of the reduced order model is the ability to calculate several different types of response with very little computing time. These responses include static solutions capable of collapse voltage calculations and harmonic solutions capable of resonant frequency calculations. The reduced order model can also account for residual stress induced during fabrication. A noticeable disadvantage is the complex and time consuming process required to create the model so that it can be used for the quick solutions mentioned above.

After comparing the abilities of the three FEA models, the reduced order model was chosen as the optimum model for CMUT calculations. This decision was based heavily upon the advantage of having one model instead of two to calculate both collapse voltage and resonant frequency of a CMUT element. Another consideration was the

large reduction in computing time for various types of solutions that could only be obtained using a reduced order model.

6.3 Parametric Study

The optimum model was used for a parametric study to determine the influence that each model parameter has on the collapse voltage and resonant frequency. The parametric study was performed for CMUTs with full and half metallization. Material and geometric parameters were varied +/-10% and the residual stress was varied from 0-200 MPa. Collapse voltage and resonant frequency results were analyzed to determine significant and insignificant parameters. The significant parameters were reviewed on the basis of design capabilities and the most suitable choices were defined as the designer input parameters.

6.3.1 Insignificant Parameters

In Chapter 4 it was noted that variations in many of the model parameters produced very minor changes in the collapse voltage and resonant frequency. A parameter is deemed insignificant if a 10% parametric variation shifts collapse voltage and resonant frequency by 1% or less.

The insignificant parameters in the determination of the collapse voltage and resonant frequency are the top electrode's thickness, modulus of elasticity, Poisson ratio and density, as well as the membrane's Poisson ratio. Another insignificant parameter relating to the collapse voltage is the membrane's density, while the last insignificant parameter for the resonant frequency is the air permittivity.

The results of the study reinforced the previously reported assumptions that the top electrode will have a minor impact on the collapse voltage and resonant frequency, with the exception of varying the electrode radius. This is beneficial considering that the top electrode will comprise the smallest component of the CMUT element and thus will be the most difficult area to maintain high manufacturing tolerances.

6.3.2 Significant Parameters

A parameter is deemed significant if a 10% variation in that parameter produces a change in collapse voltage or resonant frequency greater than 1%. Significant parameters in the determination of both collapse voltage and resonant frequency are the membrane's radius, thickness, modulus of elasticity and residual stress, as well as the electrode's radius. Another parameter significant to collapse voltage is the air permittivity, while membrane density was also found to be significant to the resonant frequency.

The membrane's radius and thickness were discovered to be the most significant parameters relating to the CMUTs operating conditions. Varying the radius by 10% resulted in collapse voltage and resonant frequency shifts of roughly 20%. The most crucial parameter from the fabrication aspect proved to be the membrane thickness, where a 0.1 μm variation resulted in a 10% and 7.5 % shift in collapse voltage and resonant frequency, respectively. This illustrates the requirement for manufacturing tolerances on the sub-micron level during the etching phases of CMUT manufacturing. The top electrode patterning also demonstrated a significant influence on the operating conditions, with half metallization models consistently resulting in a 10% higher collapse voltage and 4% lower resonant frequency than the full metallization models.

6.3.3 Designer Input Parameters

For a parameter to be a suitable choice as a designer input in modeling CMUTs, it must conform to two principles. First, variations in the parameters must produce noticeable changes in the operating conditions, thus only significant parameters can be considered. Second, the parameter must be completely variable from the designer's perspective, thus not all significant parameters are suitable.

The material property values are dictated by the selected materials and will change depending on availability to the designer but they do not vary enough to be considered viable input parameters. Residual stress, a byproduct of microfabrication, will also vary depending upon the fabrication techniques used. Therefore residual stress needs to be accounted for but a designer will not typically have full control in selecting a desired value. This leaves geometric parameters as the most suitable choice for designer input parameters.

The results of the parametric study indicate that the membrane radius and membrane thickness are the ideal choices for design of CMUT operating conditions. As seen in Chapter 4, variations in both parameters will produce significant changes in collapse voltage and resonant frequency. These two parameters are also fully variable from a design perspective and are only limited by the restraints of microfabrication processes.

6.4 Modeling Process

Once the design input parameters were chosen, a process was developed to model CMUTs for specific applications. The membrane's radius and thickness were varied over

large ranges to develop relationships in regards to collapse voltage and resonant frequency. Multiplication factors were also developed to account for variations in the other significant parameters. A step-by-step procedure was then outlined to model CMUTs for specific operating parameters within a predetermined accuracy bandwidth. The model was also used to calculate the mechanical impedance of the CMUT element.

6.4.1 Modeling with Membrane Radius and Thickness and Multiplication Factors

In Chapter 5 the membrane radius was varied between 10-100 μm and the resultant collapse voltage and resonant frequency were calculated. When the results were plotted against the membrane radius, a complicated non-linear relationship was observed. Plotting the results against the modified aspect ratio produced a linear relationship that allowed a designer to determine the correct input parameters for a specific collapse voltage and resonant frequency within a specified accuracy bandwidth. The modified aspect ratio was defined as the thickness divided by the radius squared (t_M/r_M^2).

To develop the operating condition relationships in regards to membrane thickness, the parameter was varied between 0.2-2.0 μm. Plotting the collapse voltage and resonant frequency results with respect to the modified aspect ratio illustrates that the CMUT model will follow the linear relationships within specified accuracy bandwidths. The bandwidths chosen in Chapter 5 were 10% and 20% and the geometric configurations that meet these conditions were tabulated to aid in the CMUT design.

To design for a resonant frequency within 10% accuracy using the modified aspect ratio relationship, the membrane radius should be kept between 10-90 μm, and the membrane thickness should be kept between 0.8-2.0 μm. This will allow for resonant

frequency design between 0.7-47.9 MHz. For a 10% accuracy in collapse voltage the membrane radius and thickness should be maintained between 10-90 μm and 0.6-1.2 μm, respectively. A 20% accuracy bandwidth will have increased radius and thickness ranges.

To design CMUT with varying significant parameters other than the membrane geometric parameters, a set of multiplication factors were developed. These factors were derived from the results of the parametric study and allow the designer to account for the variations they may be faced with during the fabrication process. Significant parameters for which multiplication factors were developed are the membrane's modulus of elasticity, density, and residual stress, the air permittivity, and the metallization factor. The metallization factor accounted for either full metallization patterning or half metallization patterning.

6.4.2 Step-By-Step Modeling for Collapse Voltage and Resonant Frequency

A step-by-step modeling process was created to calculate the membrane radius and thickness of a CMUT element designed for specific collapse voltage or resonant frequency. The process calculates the modified aspect ratio using the aforementioned linear relationships and multiplication factors. With the modified aspect ratio defined the designer selects an appropriate radius and thickness to fall within the proper accuracy bandwidth and the finite element model is created. The modeling results can be compared with the design requirements to verify the process.

A flow chart of the modeling process can be found in Chapter 5, as well as three design examples. The first example required a resonant frequency of 15 MHz and the use

of multiplication factors to account for varied membrane properties. Using the modeling process a CMUT element with an 18.3 μm radius and 1 μm thickness was defined. This produced a resonant frequency of 15.5 MHz which was within the +/-10% specified by the designer.

In the second example, a CMUT was designed for a minimum collapse voltage of 250 V with specific geometric requirements. The process defined an element radius of 45 μm and a thickness of 1.45 μm. This model produces a collapse voltage of 274 V, giving an accuracy of 9.6% and meeting the geometric requirements.

The third and final example illustrated the design of a half metallization CMUT for a resonant frequency of 2.03 MHz +/-10%. A 1.0 μm thick membrane with a radius of 50 μm and a top electrode radius of 25 μm was defined. The model resonated at 2.145 MHz, giving an accuracy of 5.4%.

6.4.3 Mechanical Impedance Modeling with FEA

Calculating the element's mechanical impedance is required to ensure the CMUT can properly transmit and receive ultrasound in a particular medium. For efficient sensing in a gas atmosphere the mechanical impedance of the CMUT should match that of the surrounding medium. For air the mechanical impedance must be very low, therefore CMUTs need to operate at their resonant frequency.

When the reduced order model was used to calculate the mechanical impedance it was able to accurately display the reduced impedance that occurs at the resonant frequency. However, the values at other frequencies differed from the mechanical impedance calculated using the analytical model. While more work is required to verify

the impedance accuracy of the reduced order model, the agreement of results at the resonant frequency verifies the model's usefulness for gas sensing designs.

6.5 Proposed Future Work

This dissertation illustrates how finite element analysis can be used to accurately model capacitive micromachined ultrasonic transducers. The optimum finite element model was verified to accurately calculate the collapse voltage and resonant frequency of CMUT elements when compared with previously reported results. A process was also developed to design CMUTs for specific applications. This research should prove to be very beneficial for future work to enhance the FEA models and illustrate how a CMUT can be designed and fabricated.

One area where further research is required is the modeling of the mechanical impedance with greater accuracy. This is necessary to properly match the impedance of the CMUT designs with the impedance of the sensing medium. A suspected reason for the inaccurate impedances is not properly accounting for the static deflection caused by the bias DC voltage. The static deflection reduces the distance between the electrodes that causes a larger capacitive force than what was used in the impedance calculations. This in turn leads to higher impedances.

Another area of proposed research is how temperature variations affect the CMUT's operation. An assumption taken from the research literature is that CMUTs are better suited than piezoelectric transducers for ultrasound sensing at high operating temperatures. The finite element models presented in this thesis could be used to verify this assumption. To model the temperature effects, accurate thermal properties for the

membrane and electrode materials would be required. This would involve a thorough understanding of how the material properties, such as the modulus of elasticity, are affected by large changes in temperatures. Of particular interest would be the shift in collapse voltage and resonant frequency as a result of the induced thermal stresses.

The final and most important proposal for future work would be the fabrication of a working CMUT to verify the accuracy of the finite element model. Using the design process outlined, an element geometry could be calculated for a given design parameter. This geometry could be used to build the CMUT using the fabrication process outlined in Chapter 2. The model's operating parameters could then be verified using the true operating parameters taken from the fabricated sensor. To perform this task the researcher will require extensive knowledge of microfabrication.

APPENDIX A

MATHEMATICAL MODELING OF CMUTs

The mathematical modeling previously published in the reference material has evolved from simpler membrane equations to more complex diaphragm with tension and stiffness equations. During this transformation the nomenclature for the published papers was not kept constant and in the final published work [2] many typographical errors can be found in the mathematical formulae. Thus in order to properly verify the accuracy of the finite element models the correct mathematical models needed to be established. A thorough derivation of these models starting from Mason's equations and simple electrostatic-structural models can be found in the proceeding Appendix A.

A.1 Mason's Derivation of the Dynamic Response of a CMUT

The dynamic response of a CMUT membrane can be mathematically modeled using the equations presented by Mason for a '*Diaphragm with Tension and Stiffness*' in section 5.5 of "*Electromechanical Transducers and Wave Filters*", pg 181-184. In this section, Mason's equations have been specifically altered for CMUT membranes and the notation has been modified to match the notation presented in this thesis.

The derivation starts with the governing equation of motion satisfied by every point on the surface for a circular diaphragm.

$$\frac{(E_M+\sigma_M)t_M^3}{12(1-\upsilon_M^2)}\nabla^4 x(r)-\sigma_1\nabla^2 x(r)-P_{Cap}+\rho_M t_M\frac{\partial^2(x(r))}{\partial t^2}=0 \qquad \text{(a.1)}$$

Assuming $x(r)$ is a function of time, t, yields the following derivation:

$$x(r)=Xe^{j\omega t} \qquad \text{(a.2)}$$

$$\frac{\partial^2(x(r))}{\partial t^2}=j^2\omega^2 Xe^{j\omega t}=(-1)\omega^2 x(r)=-\omega^2 x(r) \qquad \text{(a.3)}$$

Mason utilized a surface tension in the planar directions equal to the following:

$$\sigma_1=t_M*\sigma_M \qquad \text{(a.4)}$$

Substituting a.3 and a.4 into a.1 results in:

$$\frac{(E_M+\sigma_M)t_M^3}{12(1-\upsilon_M^2)}\nabla^4 x(r)-t_M\sigma_M\nabla^2 x(r)-P_{Cap}-\omega^2\rho_M t_M x(r)=0 \qquad \text{(a.5)}$$

A solution for the membrane's displacement can be derived by combining the homogeneous and particular solutions of a.5. The homogeneous solution is obtained by removing the capacitor pressure and assuming free vibration.

$$\frac{(E_M+\sigma_M)t_M^3}{12(1-\upsilon_M^2)}\nabla^4 x(r)-t_M\sigma_M\nabla^2 x(r)-\omega^2\rho_M t_M x(r)=0 \qquad \text{(a.6)}$$

Using polar coordinates the following derivations can be made:

$$\nabla^2=\frac{1}{r}\frac{\partial}{\partial r}\left(r\frac{\partial}{\partial r}\right)+\frac{1}{r^2}\frac{\partial^2}{\partial\theta^2}+\frac{\partial^2}{\partial z^2}=\left(\frac{\partial^2}{\partial r^2}+\frac{1}{r}\frac{\partial}{\partial r}\right)=(a+b) \qquad \text{(a.7)}$$

Since $x(r)$ is a function of r only, the θ and z terms in a.7 reduce to 0.

$$\nabla^4=\nabla^2\nabla^2=\left(\frac{\partial^2}{\partial r^2}+\frac{1}{r}\frac{\partial}{\partial r}\right)\left(\frac{\partial^2}{\partial r^2}+\frac{1}{r}\frac{\partial}{\partial r}\right)=(a+b)(a+b)=a^2+2ab+b^2 \qquad \text{(a.8)}$$

This yields the following:

$$\left[\frac{(E_M+\sigma_M)t_M^2}{12\rho_M(1-\upsilon_M^2)}(a^2+2ab+b^2)-\frac{\sigma_M}{\rho_M}(a+b)-\omega^2\right]x(r)=0 \qquad \text{(a.9)}$$

Allowing for the following algebraic expressions a.7 can be simplified:

$$c=\frac{(E_M+\sigma_M)t_M^2}{12\rho_M(1-\upsilon_M^2)} \qquad \text{(a.10)} \qquad \text{and} \qquad d=\frac{\sigma_M}{\rho_M} \qquad \text{(a.11)}$$

$$(ca^2+2cab+cb^2-da-db-\omega^2)x(r)=0 \qquad \text{(a.12)}$$

Following Mason's derivation, the homogeneous solution can be expressed as the sum of 2 Bessel functions of the first kind. The Bessel functions of the second kind approach infinity as $r = 0$, therefore those values are inadmissible.

$$x(r)_H = AJ_0(k_1 r)+BJ_0(k'_2 r) \qquad \text{(a.13)} \qquad \text{where} \qquad k'_2 = jk_2 \qquad \text{(a.14)}$$

The solution above can be derived from the following expression:

$$(a+b+k_1^2)(a+b-k_2^2)x(r)=0 \qquad \text{(a.15)}$$

$$(a^2+2ab+b^2+k_1^2a+k_1^2b-k_2^2a-k_2^2b-k_1^2k_2^2)x(r)=0 \qquad \text{(a.16)}$$

k_1 and k_2 can be solved for by subtracting a.12 from a.16:

$$\frac{d}{c}a+\frac{d}{c}b+\frac{\omega^2}{c}=(k_2^2-k_1^2)a+(k_2^2-k_1^2)b+k_1^2k_2^2 \qquad \text{(a.17)}$$

$$k_2^2=k_1^2+\frac{d}{c} \quad \text{(a.18)} \quad \text{and} \quad k_1^2=k_2^2-\frac{d}{c} \quad \text{(a.19)} \quad \text{and} \quad \frac{\omega^2}{c}=k_1^2k_2^2 \quad \text{(a.20)}$$

Substituting a.18 into a.20 will yield:

$$ck_1^4+dk_1^2-\omega^2=0 \qquad \text{(a.21)}$$

Substituting a.19 into a.20 will yield:

$$ck_2^4-dk_2^2-\omega^2=0 \qquad \text{(a.22)}$$

Noting that $k_2 = -jk'_2$, a.22 can be rewritten as:

$$ck'^4_2 + dk'^2_2 - \omega^2 = 0 \qquad \text{(a.23)}$$

Therefore, k_1 and k'_2 must satisfy the following:

$$cy^2 + dy - \omega^2 = 0 \qquad \text{(a.24)} \qquad \text{where} \qquad k_1^2 = k'^2_2 = y \qquad \text{(a.25)}$$

Solving for y using the quadratic formula gives:

$$y = \frac{-d \pm \sqrt{d^2 + 4c\omega^2}}{2c} \qquad \text{(a.26)}$$

Therefore k_1 is equal to:

$$k_1 = \sqrt{\frac{\sqrt{d^2 + 4c\omega^2} - d}{2c}} \qquad \text{(a.27)}$$

And k'_2 is equal to:

$$k'_2 = j\sqrt{\frac{\sqrt{d^2 + 4c\omega^2} + d}{2c}} \qquad \text{(a.28)}$$

This gives the following homogeneous solution:

$$x(r)_H = AJ_0\left(r\sqrt{\frac{\sqrt{d^2 + 4c\omega^2} - d}{2c}}\right) + BJ_0\left(rj\sqrt{\frac{\sqrt{d^2 + 4c\omega^2} + d}{2c}}\right) \qquad \text{(a.29)}$$

For the particular solution, look at equation a.5 and assume the homogeneous solution goes to zero. This yields the following:

$$-P_{Cap} - \omega^2 \rho_M t_M x(r) = 0 \qquad \text{(a.30)}$$

Which gives the following particular solution:

$$x(r)_P = \frac{-P_{Cap}}{\omega^2 \rho_M t_M} \qquad \text{(a.31)}$$

Combining the homogeneous and particular solutions yields the total solution:

$$x(r)_T = AJ_0\left(r\sqrt{\frac{\sqrt{d^2+4c\omega^2}-d}{2c}}\right)+BJ_0\left(rj\sqrt{\frac{\sqrt{d^2+4c\omega^2}+d}{2c}}\right)-\frac{P_{Cap}}{\omega^2\rho_M t_M} \tag{a.32}$$

Which can be further simplified using k_1, k_2, and the modified Bessel function:

$$k_2 = -jk'_2 = (-j)\left(j\sqrt{\frac{\sqrt{d^2+4c\omega^2}+d}{2c}}\right)=\sqrt{\frac{\sqrt{d^2+4c\omega^2}+d}{2c}} \tag{a.33}$$

$$J_0(jk_2r)=I_0(k_2r) \tag{a.34}$$

$$x(r)_T = AJ_0(k_1r)+BI_0(k_2r)-\frac{P_{Cap}}{\omega^2\rho_M t_M} \tag{a.35}$$

The constants A and B can be solved for using the following identities that state the displacement and curvature of the membrane will be 0 at the membrane edge ($r = r_M$):

$$x(r)\big|_{r=r_M} = 0 = AJ_0(k_1r_M)+BI_0(k_2r_M)-\frac{P_{Cap}}{\omega^2\rho_M t_M} \tag{a.36}$$

$$\left.\frac{\partial(x(r))}{\partial r}\right|_{r=r_M} = 0 = -Ak_1J_1(k_1r_M)+Bk_2I_1(k_2r_M) \tag{a.37}$$

From equation a.37 a relationship between A and B can be obtained:

$$A=\frac{k_2I_1(k_2r_M)}{k_1J_1(k_1r_M)}B \tag{a.38}$$

Combining a.38 and a.36 yields the values of the constants:

$$A=\frac{P_{Cap}}{\omega^2\rho_M t_M}\left[\frac{k_2I_1(k_2r_M)}{k_2I_1(k_2r_M)J_0(k_1r_M)+k_1J_1(k_1r_M)I_0(k_2r_M)}\right] \tag{a.39}$$

$$B=\frac{P_{Cap}}{\omega^2\rho_M t_M}\left[\frac{k_1J_1(k_1r_M)}{k_2I_1(k_2r_M)J_0(k_1r_M)+k_1J_1(k_1r_M)I_0(k_2r_M)}\right] \tag{a.40}$$

Putting the constants into equation a.35 yields the equation of motion:

$$x(r)=\frac{P_{Cap}}{\omega^2\rho_M t_M}\left[\frac{k_2 I_1(k_2 r_M)J_0(k_1 r)+k_1 J_1(k_1 r_M)I_0(k_2 r)}{k_2 I_1(k_2 r_M)J_0(k_1 r_M)+k_1 J_1(k_1 r_M)I_0(k_2 r_M)}-1\right] \qquad \text{(a.41)}$$

The velocity of the membrane at any particular point will be the derivative of the displacement with respect to time:

$$v(r)=\frac{\partial(x(r))}{\partial t}=j\omega X e^{j\omega t}=j\omega x(r) \qquad \text{(a.42)}$$

The lumped velocity value is obtained by integrating the product of the velocity times the area with respect to the radius, *r*, for the entire radius range:

$$\begin{aligned} V_{Lump} &= \int_0^{r_M}[j\omega x(r)][2\pi r]\partial r \\ &= j\frac{2\pi P_{Cap}}{\omega\rho_M t_M}\int_0^{r_M}\left(r\left[\frac{k_2 I_1(k_2 r_M)J_0(k_1 r)+k_1 J_1(k_1 r_M)I_0(k_2 r)}{k_2 I_1(k_2 r_M)J_0(k_1 r_M)+k_1 J_1(k_1 r_M)I_0(k_2 r_M)}-1\right]\right)\partial r \qquad \text{(a.42)} \\ &= j\frac{P_{Cap}S}{\omega\rho_M t_M}\left[\frac{\frac{2}{r_M}\left(\frac{k_2}{k_1}+\frac{k_1}{k_2}\right)I_1(k_2 r_M)J_1(k_1 r_M)}{k_2 I_1(k_2 r_M)J_0(k_1 r_M)+k_1 J_1(k_1 r_M)I_0(k_2 r_M)}-1\right] \end{aligned}$$

Where the area of the membrane equals: $S=\pi * r_M^2$ (a.43)

The average velocity can be calculated by dividing the lumped velocity by the area:

$$v_{avg}=\frac{V_{Lump}}{S}=j\frac{P_{Cap}}{\omega\rho_M t_M}\left[\frac{2(k_1^2+k_2^2)I_1(k_2 r_M)J_1(k_1 r_M)}{r_M k_1 k_2(k_2 I_1(k_2 r_M)J_0(k_1 r_M)+k_1 J_1(k_1 r_M)I_0(k_2 r_M))}-1\right] \qquad \text{(a.44)}$$

And finally the membrane's mechanical impedance can be calculated by dividing the applied pressure due to the capacitor force by the average velocity:

$$Z_M=\frac{P_{Cap}}{v_{avg}}=j\omega\rho_M t_M\left[\frac{r_M k_1 k_2(k_2 I_1(k_2 r_M)J_0(k_1 r_M)+k_1 J_1(k_1 r_M)I_0(k_2 r_M))}{r_M k_1 k_2(k_2 I_1(k_2 r_M)J_0(k_1 r_M)+k_1 J_1(k_1 r_M)I_0(k_2 r_M))-2(k_1^2+k_2^2)I_1(k_2 r_M)J_1(k_1 r_M)}\right] \qquad \text{(a.45)}$$

This impedance model can be used to verify the accuracy of the modeling impedance.

A.2 Electrostatic Force Derivation

To calculate the mechanical impedance of a CMUT model the electrostatic force between the top and bottom electrodes needs to be determined. This can also be obtained using a parallel plate approximation and the mathematical model presented below. Figures A.1 and A.2 illustrate the equivalent circuit of the parallel plate CMUT approximation.

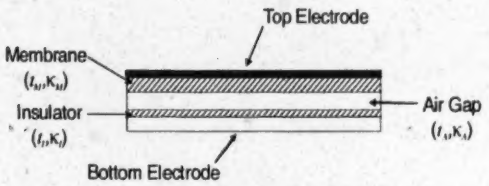

Figure A.1: Parallel Plate Capacitor Design of a CMUT

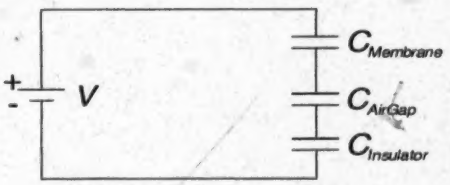

Figure A.2: Circuit Approximation of a Parallel Plate CMUT

The capacitance of the membrane, air gap, and insulator can be written as:

$$C_{Membrane} = \frac{K_M \varepsilon_0 S}{t_M} \qquad \text{(a.46)} \qquad C_{AirGap} = \frac{K_A \varepsilon_0 S}{t_A} \qquad \text{(a.47)}$$

$$C_{Insul} = \frac{K_I \varepsilon_0 S}{t_I} \qquad \text{(a.48)} \qquad \text{Where} \qquad \varepsilon_0 = 8.85x10^{-12}\left[C^2/Nm^2\right]$$

The capacitances are in series and can be added together using the following relationship:

$$\frac{1}{C_{CMUT}} = \frac{1}{C_{Membrane}} + \frac{1}{C_{AirGap}} = \frac{1}{C_{Insulator}} \qquad \text{(a.49)}$$

Which yields:

$$C_{CMUT} = \frac{K_M K_A K_I \varepsilon_0 S}{K_A K_I t_M + K_M K_A t_I + K_M K_I t_A} \qquad \text{(a.50)}$$

Equation a.50 can be reduced by assuming that the membrane and insulator will consist of the same silicon nitride with identical material properties ($\kappa_M=\kappa_I$):

$$C_{CMUT} = \frac{\kappa_M \kappa_A \varepsilon_0 S}{\kappa_A t_M + \kappa_A t_I + \kappa_M t_A} \tag{a.51}$$

The potential energy of the CMUT capacitor can be expressed as:

$$U_{CMUT} = \frac{1}{2} C_{CMUT} V^2 = \frac{(\kappa_M \kappa_A \varepsilon_0 S) V^2}{2(\kappa_A t_M + \kappa_A t_I + \kappa_M t_A)} \tag{a.52}$$

Using the principle of virtual work the force of the capacitor can be derived by calculating the change in potential energy due to a small displacement:

$$F_{Cap} = -\frac{\partial U_{CMUT}}{\partial x} = -\frac{\partial}{\partial x}\left[\frac{(\kappa_M \kappa_A \varepsilon_0 S) V^2}{2(\kappa_A t_M + \kappa_A t_I + \kappa_M t_A)}\right] \tag{a.53}$$

The membrane and insulator thickness' will remain constant but the air gap thickness (t_I) is a function of x and will vary. Therefore the force of the CMUT capacitor is equal to:

$$F_{Cap} = -\frac{\partial}{\partial x}\left[\frac{(\kappa_M \kappa_A \varepsilon_0 S) V^2}{2(\kappa_A t_M + \kappa_A t_I + \kappa_M t_A(x))}\right] = \frac{1}{2} V^2 \frac{\kappa_M^2 \kappa_A \varepsilon_0 S}{(\kappa_A t_M + \kappa_A t_I + \kappa_M t_A)^2} \tag{a.54}$$

The applied voltage, V, is a function of both the bias DC voltage and the driving AC voltage:

$$V = V_{DC} + V_{AC} \sin(\omega t) \tag{a.55}$$

The squared voltage term will be equal to:

$$V^2 = (V_{DC} + V_{AC} \sin(\omega t))(V_{DC} + V_{AC} \sin(\omega t)) = V_{DC}^2 + 2V_{DC}V_{AC} \sin(\omega t) + V_{AC}^2 \sin^2(\omega t) \tag{a.56}$$

By making $V_{DC} >> V_{AC}$, the capacitor force can be split into two terms; one for the static force caused by the DC bias voltage and one for the time varying force caused by both the DC voltage and AC voltage:

$$F_{Cap(Static)} = \frac{1}{2} V_{DC}^2 \frac{\kappa_M^2 \kappa_A \varepsilon_0 S}{\left(\kappa_A t_M + \kappa_A t_I + \kappa_M t_A\right)^2} \tag{a.57}$$

$$F_{Cap(time)} = \frac{\kappa_M^2 \kappa_A \varepsilon_0 S V_{DC} V_{AC}}{\left(\kappa_A t_M + \kappa_A t_I + \kappa_M t_A\right)^2} \tag{a.58}$$

The third force term comprised of the $V_{AC}^2 \sin^2(\omega t)$ function is considered to have a negligible effect due to the small amplitude of the V_{AC} term.

The electrostatic pressure used to calculate the mechanical impedance of a CMUT membrane can be calculated by dividing the time varying force by the area:

$$P_{Cap(time)} = \frac{\kappa_M^2 \kappa_A \varepsilon_0 V_{DC} V_{AC}}{\left(\kappa_A t_M + \kappa_A t_I + \kappa_M t_A\right)^2} \tag{a.59}$$

Dividing the electrostatic pressure calculated using equation a.59 with the average velocity of the finite element membrane (see Section 5.2) will give the mechanical impedance of the CMUT model. This impedance can be compared with the impedance of the analytical model presented in equation a.45. A comparison of the mechanical impedance's obtained from both the analytical model and finite element model can be found in Section 5.2.

APPENDIX B

FINITE ELEMENT MODELING CODE

The following code can be used with ANSYS v.7 (or higher version).

B.1 2D Axisymmetric Model Code

B.1a) 2D CMUT Modeling and ESSOLV Loop

```
/title,2-D Axisymmetric CMUT Using ESSOLV And Do Loop

*do,vltg,800,1500,100

parsav
/clear
parres

/prep7, CMUT deflection from an applied DC voltage

! Create the membrane geometry

ts=1                          ! Substrate thickness
Rm=25                         ! Membrane radius
tm=.6                         ! Membrane thickness
ta=1                          ! Air gap
ti=0                          ! Insulation thickness
rin=0                         ! Inner electrode radius
rout=2                 ! Outer electrode radius
te=0.1                 ! Electrode thickness
de=.6                         ! Electrode distance from bottom of membrane

rectng,0,Rm+2*tm,0,ts
rectng,0,Rm+2*tm,ts,ts+ti+ta+tm
rectng,Rm+tm,Rm+2*tm,ts+tm,ts+ti+ta+tm
asba,2,3
rectng,0,Rm,ts+ti,ts+ti+ta
rectng,rin,rout,ts+ti+ta+de,ts+ti+ta+de+te
aovlap,all

aglue,3,7
aglue,6,7

! Set electrostatic material properties

et,1,121,,,1                 ! Element for silicon nitride region
et,2,121,,,1                 ! Element for substrate region
et,3,121,,,1                  ! Element for electrode
et,4,121,,,1                  ! PLANE121 element for air region

emunit,epzro,8.854e-6        ! Free-space permittivity, μMKSV units
mp,perx,1,20                  ! Relative permittivity for silicon nitride
mp,perx,2,11.8                ! Relative permittivity for silicon substrate
mp,perx,4,1.04               ! Relative permittivity for air
```

```
asel,s,area,,7              ! Area for silicon nitride membrane
aatt,1,,1

asel,s,area,,6               ! Area for substrate
aatt,2,,2

asel,s,area,,3               ! Area for electrode
aatt,3,,3

asel,s,area,,5              ! Area for air elements
cm,air,area                 ! Group air area into component
aatt,4,,4

allsel,all
smrtsiz,1
amesh,3                      ! Mesh electrode
amesh,7                     ! Mesh membrane
amesh,6                      ! Mesh substrate
mshape,1
amesh,5                     ! Mesh air with triangle elements

asel,s,area,,3               ! Apply voltage to electrode
lsla,s
dl,all,,volt,vltg

asel,s,area,,6               ! Apply the ground connection
lsla,s
dl,all,,volt,0

allsel,all
et,3,0                       ! Set electrode to null element type

physics,write,ELECTROS      ! Write electrostatic physics file

physics,clear               ! Clear Physics

et,1,82,,,1                 ! Define membrane element type
et,2,0                       ! Set substrate to null element type
et,3,82,,,1                  ! Define electrode element type
et,4,0                      ! Set air to null element type

mp,ex,1,320e3               ! Set modulus  μN/(μm)**2 for silicon nitride
mp,nuxy,1,0.263              ! Set Poisson's ratio

mp,ex,3,67.6e3               ! Set modulus for electrode (Aluminum)
mp,nuxy,3,0.3555     ! Set Poisson's ratio for elelctrode

dl,22,,ux,0                 ! Apply Membrane constraints
dl,21,,uy,0
dl,24,,ux,0

dl,18,,ux,0                  ! Apply electrode contraints

allsel,all
finish

physics,write,STRUCTURE     ! Write structural physics file

ESSOLV,'ELECTROS','STRUCTURE',2,0,'air',,,,40,,0  ! Solve coupled-field problem

*enddo
```

B.2 3D Solid Model Code

B.2a) 3D CMUT Geometry, Prestress, and Modal Solution

```
/PREP7

/title,3-D Capacitive Micromachined Ultrasonic Transducer

et,1,solid45                ! Select Element Types
et,2,solid95
ele = 3                             ! Element Length

rm = 50                             ! Set Membrane Radius
re = 50                             ! Set Electrode Radius
tm = 1                  ! Set Membrane Thickness
te = 0.2                    ! Set Electrode Thickness
tin = 0                     ! Set Insulator Thickness
gap = 1                             ! Set Air Gap
tranloc = 0                 ! TRANS126 Connection Point

Denm = 3.27e-15                     ! Membrane Density
Em = 320e3                  ! Membrane Modulus of Elasticity
Pm = 0.263                  ! Membrane Poisson's Ratio
Am = 1e-6                   ! Membrane Expansion Coefficient


Dene = 2.7e-15                      ! Electrode Density
Ee = 67.6e3                 ! Electrode Modulus of Elasticity
Pe = 0.3555                 ! Electrode Poisson's Ratio
Ae = 1e-6                   ! Electrode Expansion Coefficient

Etran = 6e5                 ! TRAN126 Modulus of Elasticity
V_in = 30                   ! Set Bottom Electrode Voltage
T = -60                             ! Membrane Tension
step = 10                   ! Number of Substeps

cylind,rm,,0,tm,0,360,              ! Create Membrane Geometry
cylind,re,,tm,tm+te,0,360,          ! Create Electrode Geometry

! Separate Volumes for Mapped Meshing

wpcsys
wprota,,,90
vsbw,all

wprota,,90,
vsbw,all

vglue,all                   ! Attach Membrane and Electrode

! Create Membrane and Electrode Material Model

MPTEMP,,,,,,,,
MPTEMP,1,0
MPDATA,EX,1,,Em
MPDATA,PRXY,1,,Pm
MPTEMP,,,,,,,,
MPTEMP,1,0
MPDATA,DENS,1,,Denm
MPTEMP,,,,,,,,
MPTEMP,1,0
UIMP,1,REFT,,,
MPDE,ALPX,1
MPDE,ALPY,1
MPDE,ALPZ,1
MPDATA,ALPX,1,,Am
```

```
MPTEMP,,,,,,,,
MPTEMP,1,0
MPDATA,EX,2,,Ee
MPDATA,PRXY,2,,Pe
MPTEMP,,,,,,,,
MPTEMP,1,0
MPDATA,DENS,2,,Dene
MPTEMP,,,,,,,,
MPTEMP,1,0
UIMP,2,REFT,,,
MPDE,ALPX,2
MPDE,ALPY,2
MPDE,ALPZ,2
MPDATA,ALPX,2,,Ae

! Set Area Meshing Options

MOPT,EXPND,.5,
MOPT,TRANS,1,
MOPT,SPLIT,2

csys,1                          ! Set Cylindrical Coordinate System

lsel,s,loc,z,tm/2               ! Mesh Density of Membrane
lesize,all,,,2,,1

lsel,s,loc,z,tm+te/2                    ! Mesh Density of Electrode
lesize,all,,,1,,1

vsel,s,loc,z,0,tm               ! Set Element Type and Material Properties for
Membrane
vatt,1,,1,0

vsel,s,loc,z,tm,tm+te                   ! Set Element Type and Material Properties for
Electrode
vatt,2,,2,0

vsel,all                        ! Select Membrane and Electrode for Meshing

esize,ele,0,                    ! Set Element Length

vmesh,all                       ! Mesh Membrane and Electrode

! Constrain Membrane and Electrode Edges

csys,1                          ! Set Cylindrical Coordinate System
asel,s,loc,x,re,rm              ! Select Edge of Membrane and Electrode
da,all,ux,0                     ! Applies 0 Displacement to the Selected Areas
da,all,uy,0

lsel,s,loc,x,rm                         ! Set Vertical Displacement Limits
lsel,r,loc,z,0
dl,all,,uz,0

vsel, all

/SOLU

tref,0
tunif,T*(1-Pm)/(Em*Am)

! Create the TRANS126 Elements

asel,s,loc,z,tranloc,tranloc    ! Select the Area to Connect TRANS126 Elements
nsla,s,1                        ! Select the Nodes
cm,TRANO,node                   ! Create TRANO Component

allsel                          ! Select Everything

emtgen,'TRANO','EMTELM','EMTPNO','UZ',-gap-tin,tin,Etran,0.8854e-5
eplot
```

```
! Apply Bottom Electrode Constraints

/solu
nsel,s,loc,z,-gap-tin            ! Select Nodes at Bottom Electrode
d,all,volt,v_in                  ! Set Bottom Electrode Voltage (final)

ic,all,volt,v_in/step            ! Set Initial Electrode Voltage

d,all,UZ,0                 ! Constain Electrode in Z Direction

! Apply Top Electrode Voltage

cmsel,s,TRANO              ! Select Top Electrode Nodes
d,all,volt,0               ! Set Top Electrode Voltage to Zero

allsel

save

! Static Solution

/solution
autots,on
nsubs,10,500,3
kbc,0

antype,static
eqslv,sparse
!nlgeom,on
solve

/post1
set,last
pldisp,2
/view,1,wp
/replot

! Modal Solution

/solution
allsel
antype,,rest
pstres,on
ematwrite,yes
solve
fini

/prep7
eplot
/view,1,wp
/replot
upcoord,1,on
/replot
fini

/solution
antype,modal
eqslv,sparse
pstres,1
modopt,lanb,5,0,0,,off,,2
mxpand,5,,,1
lumpm,0
psolv,eiglanb
fini
```

B.2b) Harmonic Solution

```
! Harmonic Solution

/solution
cmsel,s,TRANO                ! Select Top Electrode Nodes
d,all,volt,1                 ! Set AC volt to 1

nsel,s,loc,z,-gap-tin              ! Select Nodes at Bottom Electrode
d,all,volt,0                 ! Set AC Volt to 0

allsel

antype,harm
pstres,1
harfrq,2000000,2500000
nsubst,100
kbc,1
outres,all,all
solve
```

B.2c) Graphing the Harmonic Solution

```
! Graphing the Harmonic Response

/post26
nsol,2,4,u,z,                    ! Select Center Node

add,4,1,,,,,1/1000000                  ! Set Graph scale to MHz (Adds New
Frequency Variable)
plcplx,0

! Graphical Options

/axlab,x,Frequency (MHz)         ! Label X-axis
/axlab,y,Displacement                  ! Label Y-axis

/xrange,2,2.5                    ! Set X-axis Range
/yrange,0,5                      ! Set Y-axis Range

/gropt,divx,10                         ! Number of X-Divisions
/gropt,divy,10                         ! Number of Y-Divisions

/gthk,axis,1.5
/gropt,ltype,0
/devdisp,text,1,200              ! Changes Text Size

xvar,4                           ! Plots MHz Frequency
wpstyle,,,,,,,,0                 ! Removes the working plane

plvar,2                                ! Plot Displacement vs. Frequency
prvar,2                                ! Print Displacement vs/. frequency
finish
```

B.3 Reduced Order Model Code

B.3a) Full Metallization Model Mapping

```
/PREP7

/title,3-D Capacitive Micromachined Ultrasonic Transducer Using ROM144

ele = 3                              ! Element Length
step = 10                       ! Number of Substeps

rm = 50                              ! Set Membrane Radius
re = rm                              ! Set Electrode Radius
tm = 1                          ! Set Membrane Thickness
te = 0.2                        ! Set Electrode Thickness
tin = 0                         ! Set Insulator Thickness
gap = 1                              ! Set Air Gap
f = 1                           ! Farfield Above the Electrode

Denm = 3.27e-15                      ! Membrane Density
Em = 320e3                      ! Membrane Modulus of Elasticity
Pm = 0.263                      ! Membrane Poisson's Ratio
Am = 1e-6                       ! Membrane Expansion Coefficient
Perm = 5.7                      ! Membrane Permittivity Constant
T = -60                              ! Membrane Tension

Dene = 2.7e-15                       ! Electrode Density
Ee = 67.6e3                     ! Electrode Modulus of Elasticity
Pe = 0.3555                     ! Electrode Poisson's Ratio

Pera = 1                        ! Air Permittivity Constant
Peri = 5.7                      ! Insulator Permittivity Constant
v_in = 30                       ! Set Bottom Electrode Voltage

ET,1,SOLID45                         ! Membrane Element
ET,2,SOLID95                    ! Electrode Element
ET,3,SOLID122                        ! Air Element

EMUNIT,EPZRO,8.85e-6                 ! Free space permittivity
MP,PERX,3,Pera                          ! Relative permittivity of air

cylind,rm,,0,tin+gap+tm+te+f+tin,0,360  ! Create Air
cylind,rm,,tin+gap,tin+gap+tm,0,360     ! Create Membrane
cylind,re,,tin+gap+tm,tin+gap+tm+te,0,360      ! Create Top electrode

vovlap,all

! Separate Volumes for Mapped Meshing

wpcsys
wprota,,,90
vsbw,all

wprota,,90,
vsbw,all

vsel,s,loc,z,tin+gap,tin+gap+tm+te

vglue,all                       ! Attach Membrane and Electrode

vsel,s,loc,z,0,tin+gap

vglue,all

vsel,s,loc,z,tin+gap+tm+te,tin+gap+tm+te+f+tin
```

```
vglue,all

allsel

/prep7

MOPT,EXPND,.5,
MOPT,TRANS,1,
MOPT,SPLIT,2
esize,ele,0,                ! Set Element Length

csys,1                      ! Set Cylindrical Coordinate System

lsel,s,loc,z,tin+gap+tm/2  ! Mesh Density for Membrane
lesize,all,,,2,,1
lsel,all
vsel,s,loc,z,tin+gap+tm/2
vatt,1,,1
vmesh,all

lsel,s,loc,z,tin+gap+tm+te/2     ! Mesh Density for Electrode
lesize,all,,,1,,1
vsel,s,loc,z,tin+gap+tm+te/2
vatt,2,,2
vmesh,all

lsel,s,loc,x,rm                  ! Mesh Density for Air Gap
lsel,r,loc,z,(gap+tin)/2
lesize,all,,,2,,1
vsel,s,loc,z,(gap+tin)/2
vatt,3,,3
vmesh,all

lsel,s,loc,x,rm                  ! Mesh Density for Air Above Electrode
lsel,r,loc,z,tin+gap+tm+te+(f+tin)/2
lesize,all,,,2,,1
vsel,s,loc,z,tin+gap+tm+te+(f+tin)/2
vatt,3,,3
vmesh,all

asel,s,loc,z,gap+tin             ! Movable Electrode
nsla,s,1
cm,COND1A,area
cm,COND1,node

asel,s,loc,z,0                   ! Ground Electrode
nsla,s,1
cm,COND2A,area
cm,COND2,node

allsel

vsel,u,loc,z,tin+gap+tm/2  ! Region for DVMORPH (Air)
vsel,u,loc,z,tin+gap+tm+te/2
cm,AIR,volu

vsel,all
esel,s,mat,,1
nsle,s,all
nsel,r,loc,z,tin+gap+tm/2
cm,NEUN,node                ! Create Neutral Plane

allsel

et,1,0                      ! Set Structural Elements to Null Elements
et,2,0

physics,write,ELEC          ! Write Electrostatic Physics File
physics,clear

et,1,solid45
et,2,solid95
```

```
et,3,0

! Set Material Properties

MP,DENS,1,Denm                    ! Membrane Properties
MP,EX,1,Em
MP,PRXY,1,Pm
MP,ALPX,1,Am

MP,DENS,2,Dene                    ! Electrode Properties
MP,EX,2,Ee
MP,PRXY,2,Pe

! Constrain Membrane Edges

csys,1                        ! Set Cylindrical Coordinate System

asel,s,loc,x,re,rm
asel,r,loc,z,tin+gap,tin+gap+tm+te
nsla,s,1
cm,FIXA,area
da,all,ux,0
da,all,uy,0
da,all,uz,0

allsel
fini

/solu

tref,0
tunif,T*(1-Pm)/(Em*Am)
fini

physics,write,STRU            ! Write Structural Physics File

/prep7

allsel

et,3,solid122
eplot
fini

save
```

B.3b) Half Metallization Model Mapping

```
/PREP7

/title,3-D Capacitive Micromachined Ultrasonic Transducer Using ROM144

ele = 3                             ! Element Length
step = 10                     ! Number of Substeps

rm = 50                             ! Set Membrane Radius
re = rm/2                           ! Set Electrode Radius
tm = 1                        ! Set Membrane Thickness
te = 0.2                      ! Set Electrode Thickness
tin = 0.4                     ! Set Insulator Thickness
gap = 1                             ! Set Air Gap
f = 1                         ! Farfield Above the Electrode

Denm = 3.27e-15                     ! Membrane Density
Em = 320e3                    ! Membrane Modulus of Elasticity
Pm = 0.263                    ! Membrane Poisson's Ratio
Am = 1e-6                     ! Membrane Expansion Coefficient
Perm = 7.6                    ! Membrane Permittivity Constant
T = -60                             ! Membrane Tension
```

```
Dene = 2.7e-15                    ! Electrode Density
Ee = 67.6e3                  ! Electrode Modulus of Elasticity
Pe = 0.3555                  ! Electrode Poisson's Ratio

Pera = 1                     ! Air Permittivity Constant
Peri = 5.7                   ! Insulator Permittivity Constant
v_in = 30                    ! Set Bottom Electrode Voltage

ET,1,SOLID45                      ! Membrane Element
ET,2,SOLID95                 ! Electrode Element
ET,3,SOLID122                     ! Air Element

EMUNIT,EPZRO,8.85e-6              ! Free space permittivity
MP,PERX,3,Pera                       ! Relative permittivity of air

cylind,re,,0,tin+gap+tm+te+f+tin,0,360  ! Create Air
cylind,rm,re,0,tin+gap+tm+te+f+tin,0,360
cylind,rm,re,tin+gap+tm,tin+gap+tm+te,0,360

cylind,re,,tin+gap,tin+gap+tm,0,360     ! Create Membrane
cylind,rm,re,tin+gap,tin+gap+tm,0,360

cylind,re,,tin+gap+tm,tin+gap+tm+te,0,360      ! Create Top electrode

vovlap,all

! Separate Volumes for Mapped Meshing

wpcsys
wprota,,,90
vsbw,all

wprota,,90,
vsbw,all

csys,1                       ! Set Cylindrical Coordinate System

vsel,s,loc,z,tin+gap,tin+gap+tm
cm,membrane,volu

vsel,s,loc,z,tin+gap+tm,tin+gap+tm+te
vsel,r,volu,,27,30
cm,electrode,volu

cmsel,s,membrane,volu
cmsel,a,electrode,volu

vglue,all                    ! Attach Membrane and Electrode

vsel,s,loc,z,0,tin+gap

vglue,all

vsel,s,loc,z,tin+gap+tm,tin+gap+tm+te+f+tin
cmsel,u,electrode,volu

vglue,all

allsel

MOPT,EXPND,.5,
MOPT,TRANS,1,
MOPT,SPLIT,2
esize,ele,0,                 ! Set Element Length

lsel,s,loc,z,tin+gap+tm/2  ! Mesh Density for Membrane
lesize,all,,,2,,1
lsel,all
cmsel,s,membrane,volu
vatt,1,,1
vmesh,all
```

```
lsel,s,loc,z,tin+gap+tm+te/2      ! Mesh Density for Electrode
lesize,all,,,1,,1
cmsel,s,electrode,volu
vatt,2,,2
vmesh,all

lsel,s,loc,x,rm                   ! Mesh Density for Air Gap
lsel,r,loc,z,(gap+tin)/2
lesize,all,,,2,,1
vsel,s,loc,z,0,tin+gap
vatt,3,,3
vmesh,all

lsel,s,loc,z,tin+gap+tm+te+(f+tin)/2          ! Mesh Density for Air Above
Electrode
lesize,all,,,2,,1
vsel,s,loc,z,tin+gap+tm,tin+gap+tm+te+f+tin
cmsel,u,electrode,volu
vatt,3,,3
vmesh,all

asel,s,loc,z,gap+tin              ! Movable Electrode
asel,u,area,,100,110
nsla,s,1
cm,COND1A,area
cm,COND1,node

asel,s,loc,z,0                    ! Ground Electrode
nsla,s,1
cm,COND2A,area
cm,COND2,node

allsel

cmsel,u,membrane,volu             ! Region for DVMORPH (Air)
cmsel,u,electrode,volu
cm,AIR,volu

vsel,all
esel,s,mat,,1
nsle,s,all
nsel,r,loc,z,tin+gap+tm/2
cm,NEUN,node                 ! Create Neutral Plane

allsel

et,1,0                      ! Set Structural Elements to Null Elements
et,2,0

physics,write,ELEC          ! Write Electrostatic Physics File
physics,clear

et,1,solid45
et,2,solid95
et,3,0

! Set Material Properties

MP,DENS,1,Denm                    ! Membrane Properties
MP,EX,1,Em
MP,PRXY,1,Pm
MP,ALPX,1,Am

MP,DENS,2,Dene                    ! Electrode Properties
MP,EX,2,Ee
MP,PRXY,2,Pe

! Constrain Membrane Edges

csys,1                      ! Set Cylindrical Coordinate System
```

```
asel,s,loc,x,rm
asel,r,loc,z,tin+gap,tin+gap+tm
nsla,s,1
cm,FIXA,area
da,all,ux,0
da,all,uy,0

lsel,s,loc,x,rm
lsel,r,loc,z,tin+gap
nsll,s,1
cm,FIXB,line
dl,all,,uz,0

allsel
fini

/solu

tref,0
tunif,T*(1-Pm)/(Em*Am)
fini

physics,write,STRU          ! Write Structural Physics File

/prep7

allsel

et,3,solid122
eplot
fini

save
```

B.3c) Reduced Order Model Generation Pass

```
/filnam,gener                    ! Jobname for the Generation Pass

rmanl,cmut,db,,3,z               ! Assign model database, dimensionality, oper.
direction
resume,cmut,db                   ! Resume model database

rmcap,cap12,1,2                  ! Define capacitance
rmclist                          ! List capacitances

! Define master nodes

rmaster,3                   ! R=0
rmaster,63                  ! R=5.36
rmaster,66                  ! R=10.71
rmaster,71                  ! R=19.64
rmaster,77                  ! R=30.36
rmaster,82                  ! R=39.29
rmaster,33                  ! R=50
rmaster,79                  ! Average Disp, R=33.93

rmalist
                            ! Apply element loads
physics,clear
physics,read,STRU

/solu
antype,static
nlgeom,on
acel,,,9.81e6               ! Acceleration in Z-direction 9.81e6 m/s**2
lswrite,1
acel,0,0,0
esel,s,type,,1
```

```
nsle,s,1
nsel,r,loc,z,gap+tin
sf,all,pres,0.1            ! 100 kPa
allsel
lswrite,2
lssolve,1,2
fini

/post1                              ! Extract neutral plane displacements
set,1                               ! due to element loads
rmndisp,'eload','write'
set,2
rmndisp,'eload','append'
fini

physics,clear
physics,read,STRU
                                    ! Perform prestressed modal analysis
/solu
nlgeom,off
pstress,on                  ! Include Pstress Membrane (Due to Temp.)
solve
fini

/solu
antype,modal
modopt,lanb,9
mxpand,9
pstress,on
solve
fini

/post1                              ! Extract modal displacements at neutral
rmnevec                             ! plane nodes
fini

rmmselect,3,'nmod',-1,1    ! Automated mode selection

rmmlist                    ! List selected mode parameters

rmmrange,2,'UNUSED'                 ! do not use unsymmetric mode for ROM

rmsave,cmut,rom            ! Save ROM database

rmsmple,1                           ! nlgeom,on
rmporder,6,,2                       ! Set polynomial orders for modes 1 and 3
rmroption,sene,lagrange,0  ! Specify response surface parameter
rmroption,cap12,lagrange,1

rmrgenerate   ! Generate response surface

rmrstatus,sene    ! Print status of response surface
rmrstatus,cap12

rmrplot,sene,func  ! Plot response surface
rmrplot,cap12,func

rmsave,cmut,rom               ! Save ROM database

rmlvscale,2,0,0               ! Necessary to consider element loads
                              ! in a VHDl-AMS model
rmxport                       ! Extract model input files for system simulation
```

B.3d) Pull-in (Collapse) Voltage Use Pass

```
! *** Voltage displacement function up to pull in
! *** A voltage sweep is applied in COND2
```

```
/clear
/filnam,use1

rmresu,cmut,rom                 ! Resume ROM database

/PREP7
ET,1,144,1                      ! Define ROM element type

*do,i,1,30                      ! Define 30 nodes
n,i
*enddo

rmuse,on                        ! Activate ROM use pass
e,1,2,3,4,5,6,7,8               ! Define node connectivity
emore,9,10,11,12,13,14,15,16
emore,17,18,19,20,21,22,23,24
emore,25,26,27,28,29,30
FINISH

/gst,off

! Compute voltage sweep up to pull-in,
! Sweep conductor is COND2
! Start an equidistant voltage sweep up to 'PI' by a voltage increment of 10 V
! Increase voltage beyond 'PI' up to pull-in with accuracy of 1 Volt
! Create gap elements to converge at pull-in

DCVSWP,'pi',1,2,200,10,1

DCVSWP,'gv',1,2,264,10,,1

/post26
/axlab,x,Voltage
/axlab,y,Modal amplitudes
nsol,2,1,emf,,mode1             ! Torsion mode
nsol,3,2,emf,,mode3             ! Transversal mode
nsol,4,12,volt,,voltage         ! Applied voltage
xvar,4
plvar,2,3                       ! Modal displacements

/axlab,y,Nodal displacements
nsol,6,21,ux,,center            ! Membrane Center
nsol,7,22,ux,,
nsol,8,23,ux,,
plvar,6

fini
```

B.3e) Harmonic Excitation Use Pass

```
! *** Prestressed harmonic analysis

/clear
/filname,use2
rmresu,cmut,rom

/PREP7
ET,1,144,1

*do,i,1,30
n,i
*enddo

rmuse,on
e,1,2,3,4,5,6,7,8
emore,9,10,11,12,13,14,15,16
emore,17,18,19,20,21,22,23,24
emore,25,26,27,28,29,30
```

```
FINISH

/gst,off

/solu
antyp,static
outres,all,all
cnvtol,curt,1.0d-6,,2
pstress,on
d,11,volt,0
d,12,volt,30
solve
fini

/solu
antype,harmonic
pstress,on
harfrq,1000000,5000000
nsubst,100
kbc,1
d,11,volt,1e-6
d,12,volt,0
solve
fini

/post26
/axlab,x,Frequency
/axlab,y,Modal Amplitude
nsol,2,1,emf,,mode1
plvar,2

/axlab,y,Nodal amplitude
nsol,3,21,ux,,R=0
nsol,4,22,ux,,R=5.36
nsol,5,23,ux,,R=10.71
nsol,6,24,ux,,R=19.64
nsol,7,25,ux,,R=30.36
nsol,8,26,ux,,R=39.29
nsol,9,27,ux,,R=50
nsol,10,28,ux,,R=33.93
plvar,3,4,5,6,7,8,9,10

prvar,2
prvar,10

fini
```

APPENDIX C

CALCULATING AVERAGE MEMBRANE DISPLACEMENT

Following are the steps taken to obtain the average membrane displacement and radial distance at which this displacement occurs for all CMUT circular geometries.

1. The average membrane displacement is calculated by first obtaining the nodal displacement for numerous points throughout the CMUT membrane's geometry. In the reduced order model these points are specified by the master nodes.
2. The displacement of the master nodes is plotted with respect to their radial distances to illustrate membrane deflection and curvature. Plotting the values for varying frequencies will highlight the increase in displacement and curvature as the frequency approaches resonance.
3. Next the CMUT's geometry is split into radial areas, numbering one for every master node not located on the membrane's outer edge. Radial areas consist of concentric rings with inner and outer diameters defined by the halfway point between adjacent master nodes. The innermost radial area will have a inner diameter of 0, while the outermost radial area will have a outer diameter equal to the total diameter of the membrane.
4. Each master node displacement is then multiplied by the corresponding radial area and the products are summed together.
5. The sum of the displacement-area calculations is divided by the total area to obtain the average membrane displacement. For many applications the CMUT is

approximated as a piston type ultrasound sensor with deflection in only one direction. For this approximation the impedance is calculated using the average displacement and velocity.

6. Once the average displacement is calculated the radial distance at which this occurs can be obtained graphically. This radial distance can be expressed as a percentage of the total radial distance. Future models will utilize a master node at the radial distance that will generate the average displacement so that the results can be used in further analysis.

Figure C.1 and Table C.1 demonstrate the aforementioned process of obtaining the average displacement and radial distance.

Table C.1: Average Displacement Calculated Using Master Nodes and Radial Areas

Master Node	Radial Position (μm)	Disp. @ Varying Frequency (Microns)			Radial Area	Inner Diameter	Outer Diameter	Area (μm^2)
		4.74 MHz	4.68 MHz	4.50 MHz				
1	0.00	3.27E-02	7.16E-03	2.18E-03	R1	0.00	2.57	20.7
2	5.14	2.96E-02	6.50E-03	1.98E-03	R2	2.57	7.71	166.0
3	10.28	2.17E-02	4.75E-03	1.45E-03	R3	7.71	12.86	332.4
4	15.43	1.15E-02	2.53E-03	7.70E-04	R4	12.86	18.00	498.7
5	20.57	3.05E-03	6.69E-04	2.04E-04	R5	18.00	24.00	791.7
6	24.00	1.82E-04	4.00E-05	1.22E-05	Total Area	0.00	24.00	1809.6

Avg Disp. @ Frequency = sum(master node disp. x radial area) / total area =	4.74 MHz	4.68 MHz	4.50 MHz
	1.16E-02	2.54E-03	7.74E-04

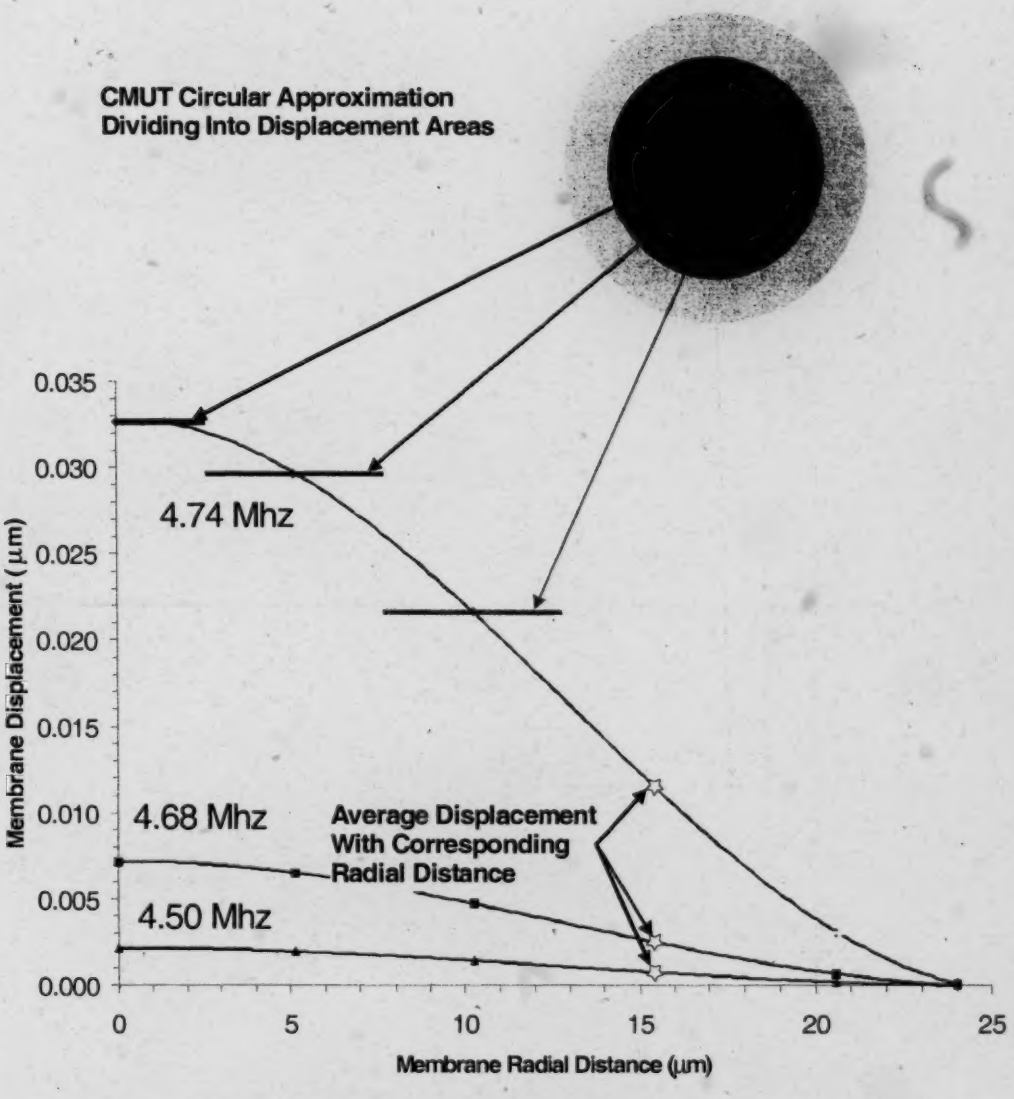

Figure C.1: Calculating Average Displacement Radial Distances

From Figure C.1 it can be observed that the average displacement takes place at a radial distance of 15.3 μm. This equates to 64% of the total membrane radial distance of 24 μm.

This process was carried out for 6 different test cases with displacements observed at 3 frequencies for each test case. The results were then averaged to obtain a radial percentage for a master node location that can calculate the average membrane displacement for any circular CMUT membrane. Table C.2 shows the radial percentage results form the test cases and their corresponding average. The test case involved both full and half metallization CMUTs.

Table C.2: Radial Percentage Averaging

Test No.	Membrane Radius (mm)	Avg. Disp. Radial Distance (mm)	Radial Percentage	Metallization
1	24.0	15.3	64%	FM
2	24.0	15.3	64%	HM
3	48.0	34.0	71%	FM
4	50.0	35.0	70%	FM
5	50.0	34.0	68%	FM
6	50.0	34.5	69%	HM
Average Radial Percentage =			**68%**	

The average radial percentage obtained was 68%. All reduced order models should implement a master node at a radial distance of 68% of the membrane radius. This master node can be utilized to calculate the average displacement, which is a requirement for impedance modeling as illustrated in Chapter 5.

APPENDIX D

CMUT DESIGN EXAMPLES

D.1 Design Example #1

Design Problem

Design a CMUT with a resonant frequency of 15 MHz +/- 10%. The silicon nitride from which the membrane will be fabricated has a modulus of elasticity and density of 310 GPa and 3000 kg/m^3, respectively. During fabrication a residual stress of 150 MPa will be induced in the membrane. All other material parameters are assumed to be similar to those found in Table 5.1. The fabrication shop is set up to etch 1.0 μm thick silicon nitride membranes and 0.1 μm thick full metallization aluminum electrodes.

Solution

Step 1: $RF_1 = 15$ MHz

$E_M = 310$ GPa

$\rho_M = 3000$ kg/m^3

$\sigma_M = 150$ MPa

Step 2: $$ME_{RF} = 1 + \frac{310 - 320}{320} x0.314 = 0.990$$

$$MD_{RF} = 1 + \frac{3000 - 3270}{3270} x0.426 = 0.965$$

$$RS_{RF} = 1 + \frac{150 - 100}{100} x0.155 = 1.078$$

$$MF_{RF} = 1 \rightarrow (FM)$$

Step 3: $$RF_0 = \frac{15MHz}{0.990 * 0.965 * 1.078 * 1.000} = 14.565MHz$$

Step 4: $$AR_{Mod} = \frac{14.565 - 0.35}{4750} = 0.00299$$

Step 5: $t_M = 1.0$ μm From Table 5.2 accuracy falls within user defined +/-10%

Step 6: $$r_M = \sqrt{\frac{t_M}{AR_{Mod}}} = \sqrt{\frac{1.0}{0.00299}} = 18.3\mu m$$ Table 4.2 accuracy +/-10%

Step 7: CMUT created using reduced order FEA model

Step 8: Harmonic analysis yielded a resonant frequency of 15.5 MHz which is 3.33% greater than the design resonant frequency but well within the +/-10% tolerance.

Step 9: The above process allowed for the accurate design of a CMUT with a resonant frequency of 15 MHz +/-10%. The chosen design utilizes a membrane with a thickness and radius of 1.0 μm and 18.3 μm, respectively. This design met all fabrication requirements and will result in a resonant frequency of 15.5 MHz.

D.2 Design Example #2

Design Problem

Design a CMUT with a collapse voltage greater than 250 V. The air gap will consist of a gas with a dielectric constant of 1.03. During fabrication a residual stress of 80 MPa will be induced in the membrane. The top electrode will be fabricated with full metallization. All other model parameters are assumed to be similar to those found in Table 5.1. The CMUT elements will be fabricated in an array with a minimum of 40 elements resting upon a $1mm^2$ silicon substrate. The spacing between element edges must not exceed 40 μm.

Solution

Step 1: $CV_1 > 250$ V

$\kappa_A = 1.03$

$\sigma_M = 80$ MPa

Step 2: $ME_{CV} = 1.00$

$$AP_{CV} = 1 + \frac{1.03 - 1.00}{1.00} x(-0.451) = 0.986$$

$$RS_{CV} = 1 + \frac{80 - 100}{100} x0.131 = 0.974$$

$$MF_{CV} = 1 \rightarrow (FM)$$

Step 3: $$CV_0 = \frac{250V}{1.000 * 0.986 * 0.974 * 1.000} = 260.3MHz$$

Step 4: $AR_{Mod} = \frac{260.3 - 30}{322000} = 0.000715$

Step 5: Due to the array constraints, a 7x7 matrix configuration was chosen that allows for 49 elements. With a 40 μm minimum spacing between element edges, the diameter of each element cannot exceed 97.1 μm. An element membrane radius of 45 μm is selected. From Table 5.2 the accuracy falls within the user defined bandwidth +/-20%

Step 6: $t_M = AR_{Mod} * r_M^2 = 0.000715 * (45)^2 = 1.45 \mu m$ Table 5.2 accuracy +/-20%

Step 7: CMUT created using reduced order FEA model

Step 8: The model produced a collapse voltage of 274 V, which was 10% greater than the designer specified collapse voltage.

Step 9: A 10% increase falls within the chosen 20% accuracy range and meets the CV > 250 V design criteria. The model was able to meet the required geometric constraints. Figure 5.7 illustrates the CMUT array configuration.

D.3 Design Example #3

Design Problem

Design a CMUT with a resonant frequency of 2.03 MHz. During fabrication a residual stress of 60 MPa will be induced in the membrane. The top electrode will be fabricated with half metallization and will be 0.2 μm thick. All other model parameters are assumed to be similar to those found in Table 5.1.

Solution

Step 1: $RF_1 = 15$ MHz

$E_M = 310$ GPa

$\rho_M = 3000$ kg/m^3

$\sigma_M = 150$ MPa

Step 2: $$ME_{RF} = 1 + \frac{310 - 320}{320} x0.314 = 0.990$$

$$MD_{RF} = 1 + \frac{3000 - 3270}{3270} x0.426 = 0.965$$

$$RS_{RF} = 1 + \frac{150 - 100}{100} x0.155 = 1.078$$

$$MF_{RF} = 1 \rightarrow (FM)$$

Step 3: $$RF_0 = \frac{15MHz}{0.990 * 0.965 * 1.078 * 1.000} = 14.565MHz$$

Step 4: $$AR_{Mod} = \frac{14.565 - 0.35}{4750} = 0.00299$$

Step 5: $t_M = 1.0$ μm From Table 5.2 accuracy falls within user defined +/-10%

Step 6: $r_M = \sqrt{\frac{t_M}{AR_{Mod}}} = \sqrt{\frac{1.0}{0.00299}} = 18.3\mu m$ Table 4.2 accuracy +/-10%

Step 7: CMUT created using reduced order FEA model

Step 8: Harmonic analysis yielded a resonant frequency of 15.5 MHz which is 3.33% greater than the design resonant frequency but well within the +/-10% tolerance.

Step 9: The above process allowed for the accurate design of a CMUT with a resonant frequency of 15 MHz +/-10%. The chosen design utilizes a membrane with a thickness and radius of 1.0 μm and 18.3 μm, respectively. This design met all fabrication requirements and will result in a resonant frequency of 15.5 MHz.

REFERENCES

[1] W. P. Mason, *Electromechanical Transducers and Wave Filters.* New York, NY: Van Nostrand, 1942.

[2] I. Ladabaum, X. C. Jin, H. T. Soh, A. Atalar, and B. T. khuri-Yakub, "Surface micromachined capacitive ultrasonic transducers," *IEEE Trans. Ultrason., Ferroelect., Freq. Contr.*, vol. 45, no. 3, pp. 678-690, 1998.

[3] A. Bozkurt, I. Ladabaum, A. Atalar, B. T. Khuri-Yakub, "Theory and analysis of electrode size optimization for capacitive microfabricated ultrasonic transducers," *IEEE Trans. Ultrason., Ferroelect., Freq. Contr.*, vol. 46, no. 6, pp. 1364-1374, 1999.

[4] B. Bayram, G. G. Yaralioglu, A. S. Ergun, B. T. Khuri-Yakub, "Influence of the electrode size and location on the performance of a CMUT", Edward L. Ginzton Laboratory, Stanford University, Stanford, CA 94305-4085.

[5] I. Ladabaum, D. Spoliansky, "Micromachined ultrasonic transducers: 11.4 MHz transmission in air and more," *American Institute of Physics, Appl. Phys. Lett. 68 (1),*1996.

[6] X. Jin, I. Ladabaum, B. T. Khuri-Yakub, "The microfabrication of capacitive ultrasonic transducers," *IEEE Journal of Microelectromechanical Systems,* vol. 7, no. 3, pp. 295-302, 1998.

[7] X. Jin, I. Ladabaum, F. L. Degertekin, S. Calmes, B. T. Khuri-Yakub, "Fabrication and characterization of surface micromachined capacitive ultrasonic immersion transducers," *IEEE Journal of Microelectromechanical Systems,* vol. 8, no. 1, pp. 100-114, 1999

[8] D. Schindel, D. Hutchins, L. Zou, S. Sayer, "The design and characterization of air-coupled capacitance transducers," *IEEE Trans. Ultrason., Ferroelect., Freq. Contr.,* vol. 42, no. 1, pp. 42-50, 1995.

[9] H. T. Soh, I. Ladabaum, A. Atalar, C. F. Quate, B. T. Khuri-Yakub, "Silicon micromachined ultrasonic immersion transducers," *American Institute of Physics, Appl. Phys. Lett. 69 (24),*1996.

[10] M. I. Haller, B. T. Khuri-Yakub, "A surface micromachined electrostatic ultrasonic air transducer," *IEEE Trans. Ultrason., Ferroelect., Freq. Contr.,* vol. 43, no. 1, pp. 1-6, 1996.

[11] Y. Roh, B. T. Khuri-Yakub, "Finite element analysis of underwater capacitor micromachined ultrasonic transducers," *IEEE Trans. Ultrason., Ferroelect., Freq. Contr.*, vol. 49, no. 3, pp. 293-298, 2002.

[12] A. S. Ergun, A. Atalar, B. Temelkuran, E. Ozbay, "A sensitive detection method for capacitive ultrasonic transducers," *American Institute of Physics, Appl. Phys. Lett. 72 (23),*1998.

[13] R. A. Serway, *Physics for Scientists and Engineers*, 4th ed. Saunders College Publishing, 1996.

[14] J. A Pelesko, D. H. Bernstein, *Modeling MEMS and NEMS*. Chapman & Hall/CRC, 2003.

[15] W. T. Thomson, M. D. Dahleh, *Theory of Vibration with Applications*, 5th ed. Upper Saddle River, NJ: Prentice Hall, 1998.

[16] S. Timoshenko, D. H. Young, *Vibration Problems in Engineering*, 3rd ed. Princeton, NJ: Van Nostrand, 1955.

[17] S. Timoshenko, J. N. Goodier, *Theory of Elasticity*, 2nd ed. McGraw-Hill Book Company, 1951.

[18] Y. Huang, A. S. Ergun, E. Haeggstrom, M. H. Badi, B. T. Khuri-Yakub, "Fabricating capacitive micromachined ultrasonic transducers with wafer-bonding technology," Edward L. Ginzton Laboratory, Stanford University, Stanford, CA 94305-4085.

[19] Z.-H. Jin, R. C. Batra, "Thermal fracture of ceramics with temperature-dependent properties," *Journal of Thermal Stresses,* vol. 21, pp. 157-176, 1998.

[20] D. C. Pressey, "Temperature-stable, capacitance pressure gauges," *Journal of Scientific Instruments,* vol. 30, pp. 20-24, 1953.